

5-2021

Increased oxidative phosphorylation in an iPSC- derived model of Rothmund-Thomson syndrome associated osteosarcomagenesis

Brittany Jewell

Follow this and additional works at: https://digitalcommons.library.tmc.edu/utgsbs_dissertations



Part of the [Medicine and Health Sciences Commons](#)

Recommended Citation

Jewell, Brittany, "Increased oxidative phosphorylation in an iPSC- derived model of Rothmund-Thomson syndrome associated osteosarcomagenesis" (2021). *The University of Texas MD Anderson Cancer Center UTHealth Graduate School of Biomedical Sciences Dissertations and Theses (Open Access)*. 1069.

https://digitalcommons.library.tmc.edu/utgsbs_dissertations/1069

This Dissertation (PhD) is brought to you for free and open access by the The University of Texas MD Anderson Cancer Center UTHealth Graduate School of Biomedical Sciences at DigitalCommons@TMC. It has been accepted for inclusion in The University of Texas MD Anderson Cancer Center UTHealth Graduate School of Biomedical Sciences Dissertations and Theses (Open Access) by an authorized administrator of DigitalCommons@TMC. For more information, please contact digitalcommons@library.tmc.edu.

Increased oxidative phosphorylation in an iPSC- derived model of Rothmund-Thomson
syndrome associated osteosarcomagenesis

By

Brittany Ellis Jewell, BS

APPROVED:

Dung-Fang Lee, Ph.D.
Advisory Professor

Jeffrey T. Chang, Ph.D.

Jeffrey A. Frost, Ph.D.

John F. Hancock, M.B., B.Chir. , Ph.D.

Guang Peng, M.D., Ph.D.

Lisa L. Wang, M.D.

Dean, The University of Texas
MD Anderson UTHealth Graduate School of Biomedical Sciences

Increased oxidative phosphorylation in an iPSC- derived model of Rothmund-Thomson
syndrome associated osteosarcomagenesis

A

Dissertation

Presented to the Faculty of

The University of Texas

MD Anderson UTHealth

Graduate School of Biomedical Sciences

in Partial Fulfillment

of the Requirements

for the Degree of

Doctor of Philosophy

by

Brittany Ellis Jewell, BS

Houston, Texas

May 2021

Copyright

As the author of these published Elsevier articles, I have retained the right to use them for publication in my dissertation:

Generation of an induced pluripotent stem cell line from an individual with a heterozygous RECQL4 mutation

Author: Brittany E. Jewell, Mo Liu, Linchao Lu, Ruoji Zhou, Jian Tu, Dandan Zhu, Zijun Huo, An Xu, Donghui Wang, Helen Mata, Weidong Jin, Weiya Xia, Pulivarthi H. Rao, Ruiying Zhao, Mien-Chie Hung, Lisa L. Wang, Dung-Fang Lee

Publication: Stem Cell Research

Publisher: Elsevier

Date: December 2018

© 2018 The Authors. Published by Elsevier B.V.

Osteosarcoma: Molecular Pathogenesis and iPSC Modeling

Author: Yu-Hsuan Lin*, Brittany E. Jewell*, Julian Gingold, Linchao Lu, Ruiying Zhao, Lisa L. Wang, Dung-Fang Lee

Publication: Trends in Molecular Medicine

Publisher: Elsevier

Date: August 2017

© 2017 Elsevier Ltd. All rights reserved.

Dedication

To my Mom – you are the best. You enabled me to follow my dreams and never- not once- discouraged my pursuit of science or the use of my mind.

To my late husband – you were the best. You supported my dreams to be a wife, mother, and scientist, and believed in my ability to do all three well when I was scared. The world is a better place because you loved me.

To my small girl – you will grow and be the best. You are so patient, smart, brave, and kind. Thank you for being all of these things while I pursued my goals.

Acknowledgments

I would like to thank my advisor, Dr. Dung-Fang Lee, for his support of this project and my career development. Dr. Lee has provided an environment where cutting edge science meets caring people. During my time in his lab, I faced incredible challenges, which he handled with patience, kindness, and encouragement. I am thankful for the effort and dedicated time during this pandemic to make sure that I was able to finish this project. Integral to the lab is Dr. Ruying Zhao, who in addition to her own trainees, made time to train me and improve my technical expertise, my critical thinking, and presentation skills. I particularly appreciate her presenting me with my ceremonial lab coat. I also want to express my sincerest and most heartfelt appreciation to my lab-mates, beginning with Dr. Mo Liu. Mo's mentorship was critical in my development as a critical thinker and scientist. She taught me how to read with a careful eye, extend my thinking, and take my oral presentations to the next level. Her work ethic is second-to-none and her tenacity in support of my education has changed my life. Next, Dr. An Xu, has been the best lab-mate anyone could ask for. Thank you for your patience when I was a new grad student, for carrying my project when Alan passed away, and for talking soccer. Dr. Dandan Zhu: thank you so much for your kindness and encouragement. Your warmth and responsiveness, even after a twelve-hour day, made doing science better. Our lab manager, Ying Liu, held my hand through the simplest of tasks without ire and I appreciate your willingness to share snacks with Penelope and me. To Dr. Donghui Wang, Yu-Hsuan Lin, Alaa Tamim, Dr. Zijun Huo, and Dr. Jian Tu: I couldn't have asked for a better group of trainees to start the Lee lab with. I am so thankful for the hours we worked side-by-side, for the input on my project, for the discussions regarding your projects, and for the conversation.

Next, I would like to thank our collaborator and my advisory committee member, Dr. Lisa Wang. Dr. Wang provided resources, valuable intellectual conversation, mentorship, and clinical expertise that enabled this project to launch. With Dr. Wang and her lab,

including Weidong Jin, Ta-Tara Rideau, and Dr. Linchao Lu, we were able to conduct this study in a patient-centered manner. Special thanks to Dr. Lu for his valuable input, willingness to answer all of my many questions, and his expertise on all things RTS.

I especially would like to thank collaborators on this work: Dr. Erica Underwood, Dr. Junhyoung Park, Dr. Benny Kaiparettu, and Dr. Pramond Dash. Your expertise has been an invaluable resource and allowed me to follow the data without hindrance. I was able to answer the important questions because of your help and mentorship. Special thanks to Dr. Christopher Vellano, Dr. Phillip Jones, and the IACS group at MD Anderson for the use of their compound and for technical advice on this project.

I would like to specifically acknowledge my committee members. Dr. Jeffrey Frost, Dr. Jeffrey Chang, and Dr. John Hancock. Thank you for teaching me through rotations and continuing to do so throughout graduate school. Each of you provided input that shaped the way I thought about my project and every paper that I read. Dr. Peng, thank you for offering your expertise on helicases and DNA repair. I have learned much from our discussions and particularly appreciate your encouragement to present at my first scientific conference. Thank you all for offering your expertise and time.

I would not be where I am without fantastic mentors. Although many acknowledged here are mentors, I had the privilege to learn about biomedical science in action from Dr. Robert B. Couch and Diane Niño. Thank you for your belief in me as a young scientist and for your support. Special thanks also to Dr. Pedro (Tony) Piedra, who will always be like family. Thank you to Dr. Robert Atmar for showing me what a clinical trial looks like and how molecular biomedicine can impact patient care. Also, I am incredibly grateful to Dr. Anthony Flores. Thank you for being one of the best teachers I have ever had and for providing opportunities to grow and learn.

This work and my training were supported by the John J. and Charlene Kopchick Fellowships at the MD Anderson UTHealth GSBS, the Gulf Coast Consortia, Training Interdisciplinary Pharmacology Scientists (TIPS) Program (NIH Grant No. T32GM120011)

and the UTHealth Innovation for Cancer Prevention Research Training Program Pre-Doctoral Fellowship (Cancer Prevention and Research Institute of Texas grant # RP160015). Additionally, I would like to acknowledge the AACR Minority in Cancer Research Scholarship and the Tzu Chi Foundation. I am so thankful to each of these organizations for their support of my graduate studies.

During my time as a Ph.D. student, I had the great honor to serve the State of Texas and the University of Texas System on the Board of Regents. I want to express my deep gratitude to each of the Board members with whom I served: Kevin Eltife, R. Steven Hicks, Sarah Martinez Tucker, Jeffrey Hildebrand, Paul Foster, Ernest Aliseda, Janiece Longoria, Rad Weaver, David Beck, Dr. Nolan Perez, Kelcy Warren, Christina Melton-Crain, and Jodie Jiles. Special thanks also to Student Regents Ben Dower, Dr. Kyle Kalkwarf, Dr. Karim Meijer, Max Richards, Dr. Ashely Perguson, Dr. Varun Joseph, Jaciel Castro, Daniel Dominguez, and Patrick O. Ojeaga II. Each of these individuals volunteered their time to improve the higher education of Texans and dedicated many hours in service to the University of Texas System. Thank you for undertaking this monumental responsibility and keeping watch over my education and that of the other 240,000 students in the UT System. In the midst of this pandemic, I also am incredibly thankful for your dedication to the health of the people of Texas. I particularly am grateful for the mentorship and advice of Chancellors J.B. Milliken and Larry Faulkner. Your leadership, skill in mentoring, and life-long quest for knowledge are unmatched and I am a better scientist for it. Special thanks also to Vice Chancellors Dr. Wanda Mercer, Dr. Randa Safady, Dr. David Daniel, Dr. Raymond Greenberg, Dr. David Lakey, Dr. Scott Kelley, and Dr. Steven Leslie for your willingness to teach me, conversations which sharpened my critical thinking skills, and for sharing your vast experience. I must thank Pam Smith and Elaine Moore for their support of my pursuit of science while serving on the Board. Each extra minute of planning and consideration allowed me to further an experiment or read another paper. This work would

not be what it is without you. Finally, thank you to Francie Frederick, whose perspective is peerless and whose counsel is invaluable.

I also am very grateful for the mentorship and leadership of Dr. Peter Pisters, President of MD Anderson Cancer Center and Dr. Giuseppe Colasurdo, President of UTHealth. Special thanks to the Deans of the Graduate School, Dr. Michelle Barton and Dr. Michael Blackburn, for your mentorship, the time you spent dedicated to all GSBS students, and the effort you put forth to ensure that I was able to meet my goals. I would not have met these goals without the consistent and experienced efforts of Brenda Gaughan and Cheryl Spitzenberger. Through all of the many life changes and ebbs and flows of graduate school, you both were steadfast, creative, and so supportive. This work would not be what it is without you.

I would like to thank the faculty, postdoctoral fellows, staff, and students of the Department of Integrative Biology and Pharmacology for your presence at student seminars, your feedback on retreats, and your support to get the science done. In particular, I would like to acknowledge Dr. Carmen Dessauer, Departmental Vice-Chair, Dr. Shane Cunha, and Dr. Kartik Venkatachalam for your mentorship, advice, and input on my project throughout its development. My appreciation to Deborah Brougher for your encouragement and support. Special thanks to Catrina Stevens and Diana Pecina, who, in addition to being fantastic friends, supported my travel, helped me with applications for scholarships and fellowships, and assisted me in navigating the world of UTHealth with so much patience. I don't know where I would be without you.

I would like to thank the faculty and students of the Biochemistry and Cell Biology Program, especially Dr. Rebecca Berdeaux and Dr. Darren Boehnning. Your leadership of the program and our many conversations helped me establish my own style of leadership, taught me how to deal with the adversities that science brings, ushered me through a pandemic, and helped me grow. Thanks to all of the BCB students for creating a welcoming and intellectually challenging environment that I consider myself lucky to be a part of. I am

grateful, especially, to Nathaniel Berg for the many discussions and for your help with this project.

I would like to express my gratitude to my UTHHealthCares family, Rigoberto Gutierrez, Neelesh Mutyala, Mary Esmeralda Fuentes, Margaret Wang, Honey Ghirmay, and Dr. Latanya Love. Thank you for your selfless dedication to our shared goals and for always being there.

I am incredibly grateful to my lifelong friends, Tylere Kelly, Dr. Meagan Sovine, and Lauren Morstead, for your unwavering support. I think back to high school when I had dreams of studying childhood cancer and I am eternally grateful for your friendship and love along the way. To my college friends, Jenny Casey, Dr. Sarah Morris, Dr. Lindsey Cortes, and Stefanie Sturman. Thank you for the late nights studying and for being there every step of the way. To Chandni Valson and the entire Joseph family, Morgan Lindsey and the Lindsey family, Dr. Priyanka Kachroo, and the St. Paul's Moms: thank you for your friendship, support, and encouragement. I am forever thankful for the group of friends I found in graduate school. Thank you, Dr. Kelsey Maxwell-Acosta, for your support, love, friendship, advice, encouragement, for the fun times and for being there in the very hard times. Graduate school began with your expertise and, thankfully, your scientific mind has been at my side all along. Similarly, I forever am grateful to Rachel Gellenbeck and Ashabari Sprenger for the joy you bring to my life and for being there for everything, from the pursuit of scientific questions to brunch. To my dear friends: Jiexi Li, Fatma Yasar, Walaa Kattan, Alexis Mobely, Elia Lopez, Dr. Alexandria Cogdill, Dr. Autumn Marsden, Dr. Samantha Berkey, and Dr. Tanya Baldwin: thank you for your support, the many fun times, and for being steadfast in your friendship. I am so lucky to have a group of supportive individuals who made the pursuit of my Ph.D. possible and who make my life richer.

Finally, and most importantly, I am eternally grateful for my large and loving family who constantly tell me that I am worthy of being a scientist, in addition to the other things that I am. Thank you to Penelope. I could not ask for a better daughter. Your constant

encouragement is a testament to your kind heart and your love of science is inspiring.

Thank you to my late husband, Alan, who was a fantastic scientist in his own right. Your curiosity for the most important questions combined with the tenacity that you possessed for your family and me is something I strive towards every day. Your leadership in putting God first has kept me grounded in faith and in constant awe of the creation which I study. Thank you for always believing that this is what I am meant to do. I am so thankful for my parents, Brian and Alice Ellis, who, throughout my life, told me that I can be whatever I want to be, if I work hard. This has been the hardest work of my life and I could not be prouder of what I accomplished with your support. Thank you for being fantastic grandparents to Penelope, allowing me to work and travel with peace of mind and a work ethic I learned from you both. Mom and Dad, I love you. To my brother, Brian: thank you for your love and support. It has been a pleasure to grow up with you and strive for new accomplishments with your hands on my back. Thank you to my sister, Laura, for your sprinkles of encouragement along the way. To my grandparents who always remind me that I am capable of great things: thank you for making sure that when things failed, I didn't feel like a failure. Thank you for your wisdom and care. To my many aunts, uncles, nephews and cousins: your love and laughter has helped me keep perspective in life and in science. Jocelyn Villarreal and Alyssa Perez: thank you for consistently supporting me in all aspects of life, for always being there for Penelope, and for being fantastic friends. To my whole family: thanks for listening to lab stories, for the singing, dancing, and the great food. Thank you for your love, your presence in my life, and your support of my goal to be a scientist.

Increased oxidative phosphorylation in an iPSC- derived model of Rothmund-Thomson
syndrome associated osteosarcomagenesis

Brittany Ellis Jewell, BS

Advisory Professor: Dung-Fang Lee, Ph.D.

Osteosarcoma is the most common bone malignancy in children and adolescents worldwide. Patients with Type II Rothmund-Thomson Syndrome (RTS) are highly predisposed to develop osteosarcoma, with 30% of patients in the largest cohort study developing osteosarcoma. Patients with Type II RTS have biallelic mutations in the DNA helicase RECQL4, which has been shown to have mitochondrial functions that include DNA replication and repair.

We describe the generation of 12 induced pluripotent stem cell lines (iPSCs) from two paired RTS patient/ parental control (Family) sets. These iPSCs were validated, then differentiated to the bone precursor, mesenchymal stem cells (MSCs). After verification of the MSCs, we differentiated the MSCs to osteoblasts, which are thought to be the cells that form osteosarcoma. We hypothesized that transcriptional changes that occur during differentiation may be important during osteosarcomagenesis. During differentiation, increased oxidative phosphorylation related genes, specifically transcription of genes which encode complex I of the electron transport chain, were upregulated. We next demonstrated that the observed transcriptional changes led to phenotypic changes in enzyme activity. We then explored the nature of oxidative phosphorylation and glycolysis in RTS osteoblasts and found that maximal respiration and ATP production increased compared to Family osteoblasts. We then sought to explore inhibitors of oxidative phosphorylation that might reverse the phenotype of ATP production preferentially through the electron transport chain.

We utilized the specific inhibitor of complex I, IACS-010759, and examined the nature of oxidative phosphorylation after treatment. We found significantly decreased maximal respiration and cell proliferation after treatment at physiological doses. Transcriptional changes that occurred after treatment demonstrated a decrease in cell cycling and tumor-promoting pathways and a restoration of normal cellular processes, including upregulation in genes that may prevent tumor formation. This study helps shed light on the long-understudied molecular pathogenesis of osteosarcoma and provides new insights for a more specific and clinically relevant therapeutic.

Table of Contents

COPYRIGHT	III
DEDICATION	IV
ACKNOWLEDGMENTS	V
LIST OF ILLUSTRATIONS	XV
LIST OF TABLES	XVII
ABBREVIATIONS.....	XVIII
CHAPTER ONE: INTRODUCTION	1
1.1 OSTEOSARCOMA	3
1.2 ROTHMUND-THOMSON SYNDROME	6
1.3 RECQL4	6
1.4 ROTHMUND-THOMSON SYNDROME MODELS	10
1.5 EXISTING MODELS OF OSTEOSARCOMA	12
1.6 INDUCED PLURIPOTENT STEM CELLS	13
CHAPTER TWO: ESTABLISHING ROTHMUND-THOMSON SYNDROME INDUCED PLURIPOTENT STEM CELLS	15
2.1 INTRODUCTION	16
2.2 CULTURING RTS FIBROBLASTS	16
2.3 ESTABLISHING FAMILIAL INDUCED PLURIPOTENT STEM CELLS: <i>RECQL4</i> ^{MUT/WT} CONTROLS	18
2.4 ESTABLISHING <i>RECQL4</i> ^{MUT/MUT} TYPE II RTS OSTEOSARCOMA PATIENT – DERIVED INDUCED PLURIPOTENT STEM CELLS	25
.....	33
2.5 GENERATION OF MESENCHYMAL STEM CELLS AND THEIR DERIVED OSTEOBLASTS	34
CHAPTER THREE: TRANSCRIPTIONAL CHANGES DURING OSTEOBLAST DIFFERENTIATION REVEAL INCREASED OXIDATIVE PHOSPHORYLATION IN TYPE II RTS PATIENT – DERIVED CELLS	37
3.1 INTRODUCTION	38
3.2 ALTERED MITOCHONDRIAL RESPIRATORY GENE SIGNATURE IN RTS OSTEOBLASTS	38
.....	46
.....	47
.....	48
3.3 CHARACTERIZATION OF MITOCHONDRIAL COMPLEX I, II, III, AND IV ACTIVITIES IN RTS OSTEOBLASTS	49
3.4 CHARACTERIZATION OF OXIDATIVE PHOSPHORYLATION IN RTS OSTEOBLASTS	51
CHAPTER FOUR: TARGETING COMPLEX I TO REVERSE INCREASED RELIANCE ON OXIDATIVE PHOSPHORYLATION IN OSTEOBLASTS.....	57
4.1 INTRODUCTION	58
4.2 INHIBITION OF OXIDATIVE PHOSPHORYLATION VIA COMPLEX I	58
4.3 TRANSCRIPTIONAL CHANGES AFTER COMPLEX I INHIBITION	62
CHAPTER FIVE: DISCUSSION	66
5.1 MODELING RTS ASSOCIATED BONE MALIGNANCIES USING iPSC-DERIVED OSTEOBLASTS	67
5.2 INCREASED ATP PRODUCTION VIA OXIDATIVE PHOSPHORYLATION	68
5.3 TARGETING COMPLEX I UPREGULATION WITH IACS-010759	70
5.4 IMPLICATIONS OF THIS STUDY	70
CHAPTER SIX: METHODS	72
6.1 CULTURE OF RTS AND FAMILY FIBROBLASTS	73

6.2 REPROGRAMMING FIBROBLASTS TO iPSCs	73
6.3 DIFFERENTIATING MESENCHYMAL STEM CELLS	74
6.4 DIFFERENTIATING OSTEOBLASTS	74
6.5 SENDAI VIRUS PCR.....	75
6.6 qRT-PCR	75
6.7 IMMUNOFLUORESCENT STAINING	78
6.8 ALKALINE PHOSPHATASE STAINING	78
6.9 ALIZARIN RED STAINING.....	78
6.10 KARYOTYPING.....	79
6.11 TERATOMA	79
6.12 RNASEQ	79
6.13 CELL PROLIFERATION ASSAYS	80
6.14 ENZYMATIC ASSAYS	80
6.15 SEAHORSE ASSAYS.....	80
BIBLIOGRAPHY	82
VITA.....	95

List of Illustrations

FIGURE 1: CHARACTERISTICS OF ROTHMUND- THOMSON SYNDROME.....	7
FIGURE 2: RECQL4 FUNCTIONS IN RESOLVING R-LOOPS.....	11
FIGURE 3: RECQL4 MUTATIONS ASSOCIATED WITH ROTHMUND-THOMSON SYNDROME...	17
FIGURE 4: REPROGRAMMING FIBROBLASTS TO ESTABLISH IPSCS.....	19
FIGURE 5: VERIFICATION OF FAMILY B2 INDUCED PLURIPOTENT STEM CELLS.....	20
FIGURE 6: IMMUNOFLUORESCENCE OF FAMILY B2 IPSCS.....	22
FIGURE 7: CHARACTERIZING FAMILY B2 IPSCS.....	23
FIGURE 8: FAMILY B2 TERATOMA.....	24
FIGURE 9: IMMUNOFLUORESCENCE OF PATIENT AND FAMILY IPSCS.....	29
FIGURE 10: QRT-PCR OF IPSCS.....	30
FIGURE 11: TERATOMA ASSAY.....	31
FIGURE 12: ZERO-FOOTPRINT IPSC GENERATION.....	32
FIGURE 13: G-BAND KARYOTYPING OF IPSCS.....	33
FIGURE 14: DIFFERENTIATION OF MESENCHYMAL STEM CELLS.....	35
FIGURE 15: DIFFERENTIATION OF OSTEOBLASTS.....	36
FIGURE 16: GSEA ANALYSES IDENTIFIED ENRICHED GENE ONTOLOGY BIOLOGICAL PROCESSES (GO_BP) IN RTS AND FAMILY OSTEOBLASTS.....	40-41
FIGURE 17: KEGG PATHWAY ANALYSES REVEAL ENRICHED PATHWAYS IN RTS AND FAMILY OSTEOBLASTS.....	42
FIGURE 18: REACTOME ANALYSIS CONFIRMS RTS INCREASED METABOLISM VIA ELECTRON TRANSPORT IN MITOCHONDRIA.....	43
FIGURE 19: CREA ANALYSIS DEMONSTRATES CHROMOSOMAL SIGNATURE PREDISPOSED TO OSTEOSARCOMA IN DAY 24 OSTEOBLASTS.....	45
FIGURE 20: ADDITIONAL PATHWAY ANALYSES PROVIDE PATHWAYS THAT MAY CONTRIBUTE TO TUMORIGENIC POTENTIAL.....	46
FIGURE 21: COMPLEX I GENES ARE SIGNIFICANTLY UPREGULATED IN RTS PATIENT DAY 24 OSTEOBLASTS COMPARED TO FAMILY CONTROLS.....	47

FIGURE 22: GO-BP ANALYSIS SHOWS UPREGULATION IN SPORADIC OSTEOSARCOMA COMPARED TO HEALTHY BONE.....	48
FIGURE 23: RTS PATIENT OSTEOBLASTS HAVE INCREASED ENZYME ACTIVITY THROUGH COMPLEX I.....	50
FIGURE 24: SEAHORSE ASSAYS SHOW INCREASED OXYGEN CONSUMPTION RATE IN RTS PATIENTS.....	49
FIGURE 25: SEAHORSE ASSAYS REVEAL INCREASE IN MITOCHONDRIAL RESPIRATION IN RTS PATIENT A.....	53
FIGURE 26: SEAHORSE ASSAYS REVEAL INCREASE IN MITOCHONDRIAL RESPIRATION IN RTS PATIENT B.....	54
FIGURE 27: SEAHORSE ASSAYS DEMONSTRATE LESS RELIANCE ON GLYCOLYSIS IN RTS PATIENTS THAN FAMILY OSTEOBLASTS.....	56
FIGURE 28: TREATMENT WITH COMPLEX I INHIBITOR IACS-010759 DECREASES OXIDATIVE PHOSPHORYLATION IN RTS PATIENTS.....	58
FIGURE 29: IACS-010759 IS SPECIFICALLY INHIBITS RTS PATIENT OSTEOBLASTS.....	61
FIGURE 30: TRANSCRIPTIONAL CHANGES AFTER IACS-010759 IMPLICATE IMPORTANT OSTEOSARCOMA-RELATED GENES.....	63
FIGURE 31: IACS-010759 CAUSES TRANSCRIPTIONAL CHANGES THAT PROMOTE HEALTHY CELLULAR FUNCTION.....	64
FIGURE 32: IACS-010759 CAUSES TRANSCRIPTIONAL CHANGES THAT INDICATE REVERSAL OF TUMOR PROMOTING PATHWAYS ASSOCIATED WITH RTS OSTEOBLASTS.....	65

List of Tables

TABLE 1: STR ANALYSIS.....21

TABLE 2: PATIENT SAMPLES FOR IPSC REPROGRAMMING.....27

TABLE 3: PRIMERS.....77

Abbreviations

AIG: anchorage independent growth

ASC: adipocyte stem cells

ATP: adenosine triphosphate

BER: base excision repair

BM-MSCs: bone marrow-derived MSCs

DSBR: (DNA) double strand break repair

ESC: embryonic stem cell

GO_BP: gene ontology biological pathway

GSEA: gene set enrichment analysis

hESC: human embryonic stem cell

HR: homologous recombination

iPSC: induced pluripotent stem cell

KEGG: Kyoto Encyclopedia of Genes and Genomes

LFS: Li-Fraumeni Syndrome

MSC: mesenchymal stem cells

mtDNA: mitochondrial DNA

NER: nucleotide excision repair

NHEJ: non-homologous end joining

PSC: pluripotent stem cell

RTS: Rothmund-Thomson Syndrome

SEM: standard error of the mean

TCA: Tricarboxylic acid (cycle)

TFT: transcription factor target (as in pathway analysis)

UV: ultraviolet

XPA: xeroderma pigmentosum group

Chapter One: Introduction

Figures and text are partially reprinted from Lin, Y.H.* , Jewell, B.E.* , Gingold, J., Lu, L., Zhao, R., Wang, L.L., and Lee, D.F. (2017). Osteosarcoma: Molecular Pathogenesis and iPSC Modeling. Trends Mol Med 23, 737-755. *co-first authors

Osteosarcoma is one of the most frequent primary malignant tumors in childhood and adolescence. A poorly defined molecular mechanism and insufficient models have resulted in very few therapeutic options for this potentially lethal disease. The osteosarcoma survival rate has not changed in 40 years (Mirabello et al., 2009b), demonstrating the need for improved models and detailed molecular studies. In this study, we describe a novel model of Type II Rothmund-Thomson Syndrome (RTS) associated osteosarcoma that will allow us to address the current gap in knowledge regarding the molecular mechanisms of osteosarcoma initiation and progression. The model makes use of induced pluripotent stem cells (iPSCs) derived from dermal fibroblasts of patients with RTS.

Modeling human disease using patient-derived iPSCs is at the forefront of personalized medicine, as it allows for the production of somatic cells with complete genetic fidelity to the patients from which they are derived. In short, patient dermal fibroblasts are cultured and reprogrammed, yielding iPSCs, which then can differentiate into osteoblasts—the precursors of osteosarcoma. The monogenetic nature of RTS associated osteosarcoma makes an iPSC approach especially advantageous. It provides an infinite source of non-immortalized cells suitable for inquiry into the molecular pathophysiology of this disease and ultimately provides a platform for further study of therapeutic approaches.

Type II RTS is a rare genetic disorder with an osteosarcoma predisposition in which all patients share mutations in *RECQL4*, which encodes one of five human RecQ DNA helicases (Chu and Hickson, 2009). Type II RTS patients are highly predisposed to developing osteosarcoma, making them an ideal cohort to better understand the molecular mechanisms underlying this malignancy (Lu et al., 2020). We hypothesized that RTS patient-derived iPSCs can be used to model osteosarcomagenesis caused by the dysregulation of pathways that are altered in *RECQL4* mutated osteoblasts, which could attribute to osteosarcoma development. Furthermore, we hypothesized that these altered

cellular pathways would shed light on a targetable molecule that could be taken advantage of in the hopes of a new potential treatment for osteosarcoma.

1.1 Osteosarcoma

Osteosarcoma is the most common pediatric bone malignancy, affecting about 4 per million children per year, worldwide (Mirabello et al., 2009a). Despite the prevalence, osteosarcoma survival rates have remained unchanged for over three decades.

Osteosarcoma survival rates continue to hover around 70%, while survival after metastasis is about 30% (Lin et al., 2017b). This is largely due to the lack of new treatments, limited by the identification of suitable targets for treatment (Zhao et al., 2020). Such targets can be identified by a more thorough understanding of the molecular mechanism of osteosarcomagenesis. Osteosarcoma is a bone forming tumor that presents as increased opacity upon radiographic imaging via X-ray. It has been shown that many clonal origins exist and can propagate simultaneously (Gambera et al., 2018).

There are two primary competing hypotheses regarding the cellular origin of osteosarcoma, the mesenchymal stem cell (MSC) origin hypothesis and the osteoblast origin hypothesis (Lee et al., 2015; Rodriguez et al., 2012; Tataria et al., 2006; Xiao et al., 2013). The MSC hypothesis proposes that a mutation-carrying MSC will give rise to osteosarcoma (Rodriguez et al., 2012; Xiao et al., 2013). A high frequency of pathogenic variants in the *TP53* and *RB1* tumor suppressor genes and the *c-MYC* and *RAS* oncogenes is found in genomic studies of human osteosarcoma (Chen et al., 2014; Kansara et al., 2014). Moreover, transformed human MSCs engineered to deplete *RB1* and overexpress *c-MYC* -- a combination observed in patients with poor survival-- acquire malignant osteosarcoma-like properties. These MSCs express osteosarcoma markers CD99, ALP, osteonectin, and osteocalcin (also known as bone gamma-carboxyglutamic acid-containing protein (BGLAP)). They form lung and liver metastases in immunocompromised mice, suggesting that MSCs constitute the cellular origin of osteosarcomas (Wang et al., 2017).

In contrast, the osteoblast origin hypothesis suggests that osteosarcoma arises from defective differentiation of osteoblast-committed cells. This hypothesis stems from studies of MSCs derived from *Trp53*-mutant mice. These studies show that a *Trp53* mutation might result in early osteogenesis. However, a *Trp53* mutation impedes final maturation from osteoblast precursors into mature osteoblasts. This is evaluated by the expression of the early and intermediate osteogenic marker, osteopontin, rather than the terminal osteogenic marker, osteocalcin (Tataria et al., 2006). Moreover, during osteogenic differentiation, depletion of *Trp53* or both *Trp53* and *Rb1* in murine bone marrow-derived MSCs (BM-MSCs) - but not adipose-derived MSCs (ASCs) - induces the formation of osteosarcoma-like tumors (Rubio et al., 2013). Both undifferentiated BM-MSCs and ASCs develop leiomyosarcoma-like tumors but not osteosarcoma. This finding emphasizes the importance of osteogenic differentiation of MSCs for osteosarcoma development (Rubio et al., 2013).

Induced pluripotent stem cell (iPSC)-derived osteoblasts, but not MSCs, obtained from LFS patients maintained *in vitro* and *in vivo* tumorigenesis, as demonstrated by an anchorage-independent growth (AIG) assay and xenotransplantation in immunocompromised nude mice, respectively (Lee et al., 2015). This suggests that osteoblasts, rather than MSCs, are the cells of origin for osteosarcoma. Supporting this notion, RUNX2 and WNT signaling pathways are disrupted in human osteosarcoma samples. These pathways are essential for osteogenic differentiation. The loss of RUNX2 transcriptional activity and the nuclear accumulation of β -Catenin suggest that osteosarcoma development might entail differentiation defects (Haydon et al., 2002; Thomas et al., 2004). In addition, activation of the intracellular domain of Notch1 in transgenic mice promotes immature osteoblast proliferation and inhibits its maturation. This process is sufficient to induce osteosarcomagenesis (Tao et al., 2014).

These hypotheses might be reconciled partially if the mutation-carrying MSCs indirectly result in osteosarcoma by potentiating the generation of osteoblasts with defective

differentiation. Alternatively, given the variability across osteosarcoma tumor samples, both MSCs and osteoblasts might contribute to osteosarcomagenesis. *TP53* and *RB1* conditionally-disrupted MSCs, pre-osteoblasts, and mature osteoblasts are all reported to develop in osteosarcoma (Quist et al., 2015). Finally, osteosarcoma may arise from mature osteoblasts and osteocytes. For instance, the osteocyte marker, dentin matrix acidic phosphoprotein 1 (DMP1), is increased in patient osteosarcoma samples. Additionally, SV40-immortalized mouse osteocyte cell lines can engraft as a tumor in mice by either subcutaneous or intratibial injection (Sottnik et al., 2014). Therefore, osteocytes could possibly constitute an osteosarcoma progenitor cell type. Although there is still a debate regarding the cellular origins of osteosarcoma, taken together, specific genetic alterations may represent key factors in driving the development of osteosarcoma across cell types.

Despite the unclear molecular mechanism of osteosarcoma and the uncertain cell-of-origin, one common characteristic of sporadic osteosarcoma is chromosomal alterations. Kataegis, localized areas of hypermutations, was reported in 50% of osteosarcoma cases (Chen et al., 2014). Evidence of this phenomenon is supported by other studies (Perry et al., 2014) and also by studies that find increased incidence of chromothripsis, or increased chromosomal breakage throughout the chromosomes resulting in rearrangements, in 30% of osteosarcoma cases (Behjati et al., 2017).

The current standard of care for osteosarcoma treatment is methotrexate, doxorubicin, and cisplatin. Doxorubicin functions by inducing autophagy and inhibiting stemness in osteosarcoma cells (Wang et al., 2018). This is accomplished by LncRNA Sox2OT-V7 via mir-142/ mir-22 (Zhu et al., 2020). It is noted further that epigallocatechin (EGCG), a polyphenol in green tea, has been shown to synergistically combine with Doxorubicin to increase autophagy (Wang et al., 2018).

1.2 Rothmund-Thomson Syndrome

Type II Rothmund-Thomson Syndrome (RTS) is a rare autosomal recessive genetic disorder associated with a 30% prevalence of childhood osteosarcoma. All Type II RTS patients have biallelic *RECQL4* mutations (Wang et al., 2003). *RECQL4* is essential for DNA repair and replication, two processes known to be dysregulated in cancer (Lu et al., 2014). Because of the high incidence of RTS associated osteosarcoma, we hypothesized that mutation of *RECQL4* plays a significant role in osteosarcomagenesis. Type II RTS patients with osteosarcoma and sporadic osteosarcoma patients share defining characteristics including outcomes, histology, primary location, and treatment (Hicks et al., 2007). Unlike other rare genetic disorders with an osteosarcoma predisposition, Type II RTS is associated with osteosarcoma largely exclusive of other malignancies (Lu et al., 2020). This makes Type II RTS patients the ideal cohort in which to study osteosarcomagenesis. Insights from this study have the potential to provide significant insight into cellular processes important for sporadic osteosarcoma.

1.3 RECQL4

RTS was described first by Dr. Auguste Rothmund in the late 1800s, who reported the characteristic rash and cataracts. In the early 1900s, Dr. Sydney Thomson observed the same rash, in addition to bone abnormalities (Taylor, 1957). Despite the heterogeneity of osteosarcoma genetic background, 30% of patients in the largest surveillance study of Type II RTS were diagnosed with osteosarcoma (Lu et al., 2014).

Patients with RTS are diagnosed before two years of age, after presenting with poikiloderma, shortened stature, sparse hair or eyelashes, and/ or radial ray defects (Wang et al., 2003; Wang and Plon, 1993) (Figure 1). After diagnosis, directed sequencing is performed to examine if patients have mutations in *ANAPC1* (Ajeawung et al., 2019) or *RECQL4* (Wang et al., 2003), which are associated with Type I and Type II RTS,

respectively. Type I RTS patients have bilateral juvenile cataracts, but do not have an association with osteosarcoma. Type II RTS patients have biallelic mutations in the *RECQL4* gene, which encodes the RECQL4 DNA helicase (Lu et al., 2020).

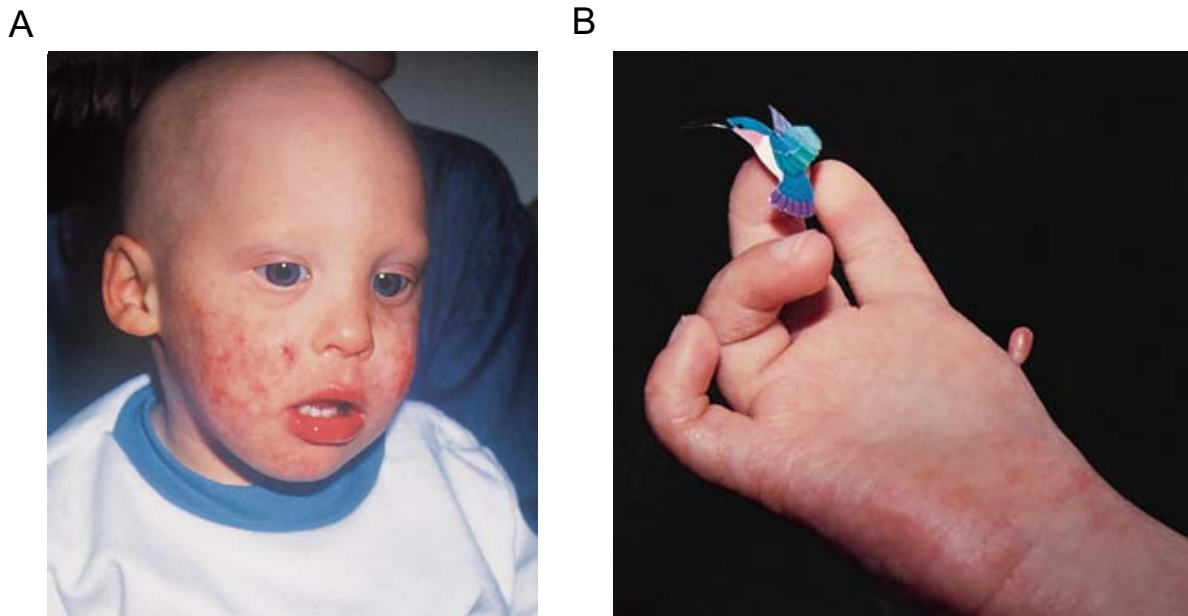


Figure 1: Characteristics of Rothmund- Thomson Syndrome

Rothmund-Thomson Syndrome is characterized by A) sparse hair and eyelashes, poikiloderma (red erythema on the cheeks) and B) radial ray defects, in this case resulting in a missing digit.

Images courtesy of Lisa L. Wang, 2016, and are used with permission.

RECQL4 is one of five human ATP-dependent helicases, all of which are associated with a predisposition to cancer (Brosh, 2013; Peng et al., 2019). Like other RECQ DNA helicases, RECQL4 is thought to aid in firing at the origin of replication (Croteau et al., 2014). Indeed, it has been demonstrated that a depletion of RECQL4 in cells reduces the frequency of firing at the origin of replication (Thangavel et al., 2010), pointing to replication as a critical function. RECQL4 also has been shown to function in non-homologous end joining as a means of double strand break repair (Shamanna et al., 2014). We will build upon the foundational principle that osteosarcoma can be caused by aberrant DNA replication and incomplete repair resulting from mutations in *RECQL4* by exploring dysregulated transcriptional pathways in the presence of *RECQL4* mutations,

RECQL4 is one member of the RecQ DNA helicase family, with several functions that are described, below. RECQL4 has been demonstrated to function in the initiation of DNA replication, DNA damage repair, and maintenance of the integrity of telomere and mitochondrial DNA (Lu et al., 2017). The N-terminus (1~200 aa) of human RECQL4 shares homology with the yeast Sld2 protein, which is important for the initiation of DNA replication (Matsuno et al., 2006; Sangrithi et al., 2005). Human RECQL4 interacts with the DNA replication licensing factor, MCM10, to mediate the formation of the CMG (Cdc45; Mcm2-7; GINS) replication complex (Im et al., 2009; Kliszczak et al., 2015; Xu et al., 2009). Since replication stress causes chromosomal instability in human cells (Lamm et al., 2016), mutations in *RECQL4* could cause replication stress leading to genome instability. RECQL4 also functions in unwinding DNA, making it critical for DNA replication (Brosh, 2013; Chen et al., 2009). In addition, RECQL4 directly participates in DNA damage repair, including nucleotide excision repair (NER) for UV DNA damage, base excision repair (BER) for oxidative DNA damage, and DNA double strand break repair (DSBR) through homologous recombination (HR) and non-homologous end joining (NHEJ) pathways (Lu et al., 2017). RECQL4 co-localizes and interacts with the xeroderma pigmentosum group A (XPA) protein which is required for NER, and UV damage to H1299 and HeLa cells and has been shown

to result in increased co-immunoprecipitation intensity and co-localization between RECQL4 and XPA (Fan and Luo, 2008). In response to H₂O₂ induced oxidative stress, RECQL4 is demonstrated to co-localize with, and stimulate the biochemical activities of apurinic/apyrimidinic endodeoxyribonuclease 1 (APE1), DNA polymerase β , and flap structure-specific endonuclease 1 (FEN1). These are several key factors in the BER pathway, indicating that RECQL4 plays a role in BER in mammalian cells (Schurman et al., 2009). RECQL4 has also been shown to play a role in NHEJ-dependent DSB by interacting with and stimulating the activity of the Ku heterodimer, an important member of the NHEJ pathway (Shamanna et al., 2014). RECQL4 interacts with p53 and masks the p53 nuclear localization signal, which in turn facilitates p53 mitochondrial localization in untreated normal human fibroblasts (De et al., 2012), providing a new regulatory mechanism of p53 activity. In addition, RECQL4 can be recruited to laser-induced double strand breaks (DSB) by the MRE11 nuclease in the human osteosarcoma U2OS cell line, and is required for 5' end resection of DSB, the initial step of HR-dependent DSB (Lu et al., 2016). In mammalian cells, RECQL4 also associates with RAD51, a key protein involved in homologous recombination; thus, a defect in RECQL4 function is expected to result in defective HR associated genomic instability (Petkovic et al., 2005). Supporting this idea, karyotype analyses in cells from *Recql4*-deficient mice show increased aneuploidy and premature centromere separation (Mann et al., 2005).

RECQL4 is shown to localize in the nucleus during S phase and in the cytoplasm during G2/M phase (De et al., 2012). In mitochondrial nucleoids, the RECQL4-p53 complex physically interacts with mitochondrial DNA polymerase (PolyA/B2) in human fibroblasts. It potentiates its binding to the mitochondrial DNA (mtDNA) control region as demonstrated by the electrophoretic mobility shift assay (Gupta et al., 2014). Recent studies demonstrate that RECQL4 is essential for the resolution of DNA: RNA hybrids during replication (Chang et al., 2020). Also called R-loops, these DNA: RNA hybrids are formed during transcription and resolve when a wild type RECQL4 associates with the TWINKLE complex. In contrast,

when RECQL4 is mutated, as is the case in Type II RTS, there is no association with the TWINKLE complex, the R loops remain, and mtDNA replication is halted (Figure 2). This is of particular importance because RECQL4 function in mtDNA replication is found to be essential to prevent cellular transformation in fibroblasts (Kumari et al., 2016). Interestingly, loss of RECQL4 in the mitochondria of RTS fibroblasts results in decreased mitochondrial membrane potential and complex V activity, which leads to aerobic glycolysis and cell invasion (Kumari et al., 2016). However, it is still ambiguous if dysregulation of mitochondrial integrity by loss of RECQL4 contributes to Type II RTS patient-associated bone malignancies.

1.4 Rothmund-Thomson Syndrome Models

Historically, Type II RTS associated osteosarcoma has been difficult to study due to the essential nature of *RECQL4* and the rarity of this disease. In mouse models, global knockouts of *Recql4* are embryonic lethal, whereas attempts at knockouts of the helicase domain do not develop osteosarcoma (Hoki et al., 2003; Mann et al., 2005). While global knockout of mouse *Recql4* targeting exon 5 to 8 causes embryonic lethality (Ichikawa et al., 2002), inactivation of *Recql4* in skeletal tissues has recapitulated some features of RTS, including skeletal abnormalities and small stature (Lu et al., 2015). Cells from these *Recql4* conditional mutant mice display elevated p53 activity (De et al., 2012; Lu et al., 2015), and the skeletal phenotypes in these mice can be partially rescued by p53 inactivation (Lu et al., 2015). Conditional *Recql4* knockout mice were created and further revealed the essential role of RECQL4 in bone development and in the genetic interaction between RECQL4 and p53 in osteogenesis (Lu et al., 2015).

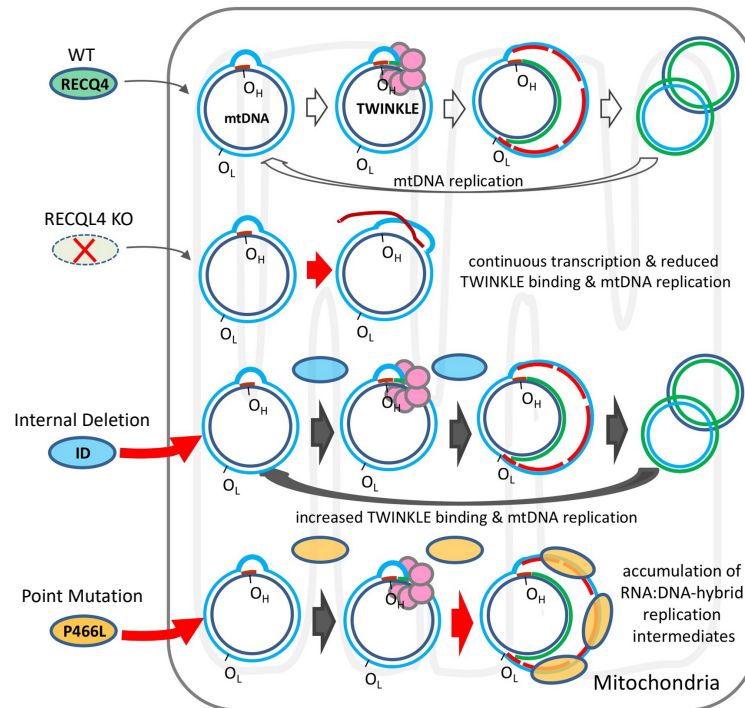


Figure 2: RECQL4 functions in resolving R-loops

A) Wild type RECQL4 associates with the TWINKLE complex in the mitochondria to resolve R-loops, thereby promoting continued mtDNA replication. B) In the absence of RECQL4, mitochondrial R loops persist, leading to persistent transcription, but less mtDNA replication. C) Internal deletion of RECQL4, often associated with RAPADALLINO but not RTS, results in increased TWINKLE binding resulting in an abundance of mtDNA replication. D) Point mutations in RECQL4, often associated with RTS result in less TWINKLE binding and an accumulation of R-loops. We hypothesize that the increased stress caused by R-loops might trigger increased transcription of genes that promote ATP production via oxidative phosphorylation, thereby promoting cell proliferation and survival.

Figure adapted from Chang et al., Scientific Reports, 2020.

While RECQL4 is necessary for osteoblast development, it is not necessary for bone homeostasis (Ng et al., 2015). Furthermore, mice that lack *Recql4* in osteoblast progenitor cells demonstrate a decrease in mineral apposition rate and bone formation rate (Ng et al., 2015), but no increase in osteosarcoma. These results imply that osteosarcoma susceptibility is most likely triggered by mutant, not null, alleles of *RECQL4* in RTS patients. Taken together, current understanding of RECQL4 allows for the possibility that defective HR-induced genomic instability might contribute to initiating osteosarcoma development in RTS patients with *RECQL4* mutations. Furthermore, genomic instability, combined with aberrant mtDNA replication, provides a compelling line of inquiry. Indeed, although the molecular mechanism of osteosarcomagenesis in RTS remains unclear, genomic instability due to mutations in *RECQL4* is implicated in disease development. Murine models have been helpful in understanding RTS, but have not been shown to replicate osteosarcoma (Lu et al., 2020), suggesting another model is necessary to study Type II RTS associated bone malignancies.

1.5 Existing Models of Osteosarcoma

Despite the relative prevalence of osteosarcoma, models to study the pathophysiology of disease are not abundant. Several cancer-derived cell lines are currently used to study osteosarcoma, including U2OS, G292, SJSA, OHS, SAOS-2, MG-63 and TE85 (Schott et al., 2020). Over time, it became apparent that in order to make inroads towards new therapeutic options, new models were necessary. In 2015, orthotopic patient-derived osteosarcoma xenografts were described as a method to examine the diversity of the disease and to study recurrent osteosarcoma (Blattmann et al., 2015). Current efforts by the Children's Oncology Group and others are underway to continue building the available osteosarcoma xenograft models, but the conclusions from these studies rely on a robust

cohort to replicate the genetic diversity observed in the patient population (Roberts et al., 2019).

Recent discussions indicate that more models of osteosarcoma are critical to better understand the pathophysiology of osteosarcoma (Schott et al., 2020). Genetically engineered mouse models with conditional and tissue specific P53 and RB knockouts show promise in recapitulating disease and metastasis in some cases (Guijarro et al., 2014), but these models do not capture the heterogenous nature of osteosarcoma, nor do they allow for investigation of RTS associated osteosarcoma. Previously reported models of Li-Fraumeni syndrome (LFS) associated osteosarcomagenesis (Kim et al., 2018; Lee et al., 2015; Zhou et al., 2017) demonstrate that patient-derived induced pluripotent stem cells (iPSCs) are an appropriate model to study the pathological mechanisms in LFS patients genetically predisposed to osteosarcoma. Therefore, we sought to establish an induced pluripotent stem cells (iPSC) model of RTS to address the current need for more varied models of osteosarcomagenesis,

1.6 Induced Pluripotent Stem Cells

One of the major challenges of studying RTS associated osteosarcomagenesis is the lack of a model that recapitulates the disease (Lin et al., 2017b). Several attempts at producing *Recq14* deficient mice (Lu et al., 2015; Ng et al., 2015) and other organisms like drosophila and zebrafish (2017; Wu et al., 2008) fail to recapitulate the osteosarcoma phenotype and, by nature of the models, are unable to address early transcriptional changes that lead to osteosarcoma. For example, whole body knockout of *Recq14* is embryonic lethal (Ichikawa et al., 2002) and conditional knockouts of the helicase coding region of *Recq14* do not result in osteosarcoma (Lu et al., 2015; Ng et al., 2015). In this study, we address these issues by working with induced pluripotent stem cells (iPSC), which were subsequently differentiated to recapitulate osteosarcoma.

Landmark studies (Takahashi and Yamanaka, 2006) paved the way for this investigation by demonstrating how reprogramming somatic cells results in stem cells, called iPSCs. They described a method to transduce four transcription factors to confer pluripotency. These factors are added to cultured primary fibroblasts and, over time, de-differentiated stem cells survive and proliferate. Furthermore, *in vitro* modeling of human disease has become possible with these iPSC methodologies (Takahashi et al., 2007) . Additionally, numerous laboratories demonstrate that PSCs (ESCs and iPSCs) overcome many limitations found in other model systems and can serve as a relevant model system to study the etiologies of cancer, including osteosarcoma (in LFS (Lee et al., 2015), Werner's Syndrome (Cheung et al., 2014; Shimamoto et al., 2014), Diamond Blackfan Anemia (Doulatov et al., 2017; Garcon et al., 2013) and Retinoblastoma (Zeng et al., 2016)) (Figure 3B), brain tumors (Duan et al., 2015; Funato et al., 2014), and leukemia (Mulero-Navarro et al., 2015).

Chapter Two: Establishing Rothmund-Thomson Syndrome Induced Pluripotent Stem Cells

Figures and text are partially reprinted from Jewell BE, Liu M, Lu L, Zhou R, Tu J, Zhu D, Huo Z, Xu A, Wang D, Mata H, Jin W, Xia W, Rao, P, Zhao R, Hung MC, Wang LL, Lee DF. Generation of an induced pluripotent stem cell line from an individual with a heterozygous RECQL4 mutation. Stem Cell Res. 2018 October 9; 33: 36-40.

2.1 Introduction

RECQL4, one of five human RecQ DNA helicases, is known as a guardian of the genome due to its function in multiple DNA metabolic processes, including DNA replication, recombination, and repair (L. Van Maldergem, 2016; Lin et al., 2017a). Biallelic mutations in the *RECQL4* gene are responsible for the majority of cases of Rothmund-Thomson syndrome (RTS), an autosomal recessive disorder characterized by multiple clinical features, including a poikilodermatous skin rash, small stature, skeletal dysplasias, and a striking risk for developing osteosarcoma (L. Van Maldergem, 2016; Lin et al., 2017a).

We first reprogrammed fibroblasts from an RTS heterozygous carrier of the *RECQL4* mutation c.1878+32_1878+55del24, a 24 base pair deletion in intron 11 of the *RECQL4* gene (Figure 3). This mutation results in a shortened intron and is shown to cause aberrant splicing leading to exon skipping (Colombo et al., 2018; Wang et al., 2002). The iPSCs we describe here will be useful in characterizing the role of RECQL4 in DNA damage repair and replication. They also provide the framework for reprogramming iPSCs, which have biallelic *RECQL4* mutations and were derived from patients with osteosarcoma. Furthermore, the control cell lines described in this chapter are the parent of a patient with Type II RTS and associated osteosarcoma. The background genetic similarity to the patient is theoretically 50%, providing an ideal control for future experiments.

2.2 Culturing RTS Fibroblasts

Fibroblasts were isolated from a punch biopsy taken from the arm of an individual with a heterozygous *RECQL4* (c.1878+32_1878+55del24) mutation (The Molecular Basis of Familial Cancer Predisposition Syndromes (IRB# H-7207) Baylor College of Medicine). These fibroblasts were cultured using high glucose media for less than 10 passages. Then, they were preserved very carefully after proliferation by dissociating one 10cm dish of confluent fibroblasts gently with a minimum amount of trypsin (400 μ L), then subsequently

freezing in 1ml of Cryopreservation media. It is important to note that these cells were not immortalized or changed in any manner that might have altered their cell signaling prior to reprogramming.

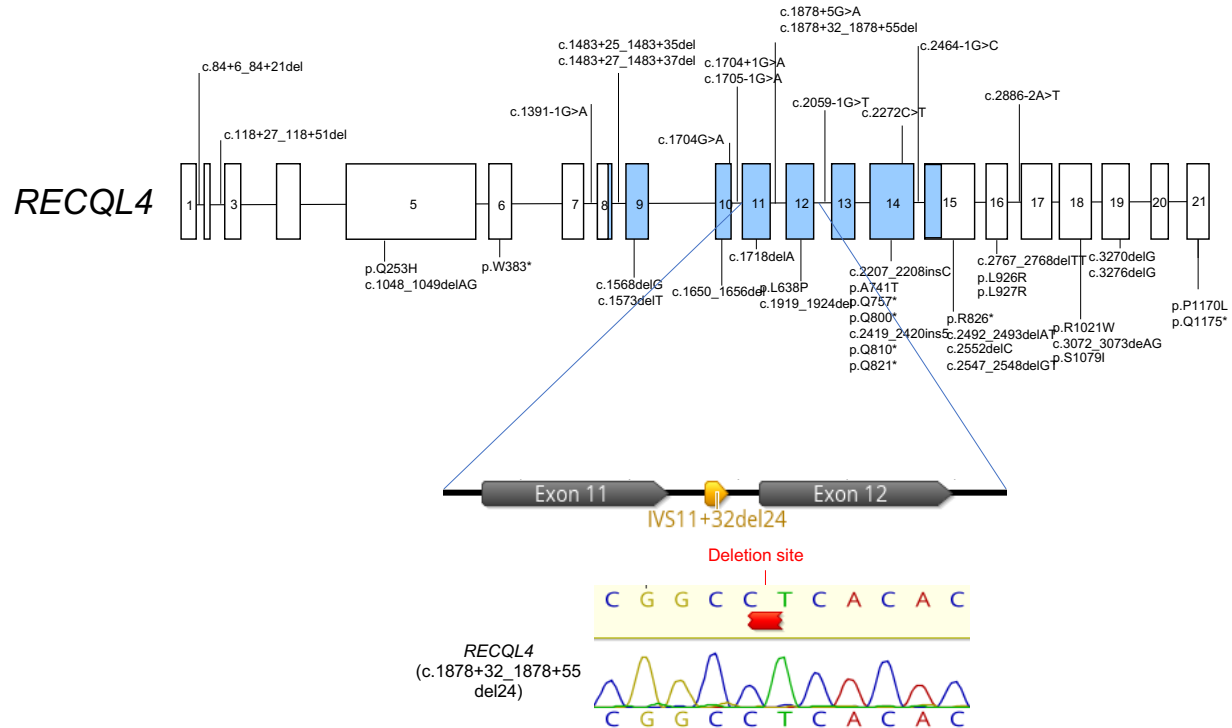


Figure 3: *RECQL4* mutations associated with Rothmund-Thomson Syndrome

The *RECQL4* gene is represented, with the 21 exons marked as boxes and the helicase region highlighted in blue. Mutations occur across the entire gene and are located in both introns and exons. The lower inset depicts the heterozygous mutation described, in the intron 11. This mutation was verified in the Family B2 induced pluripotent stem cells by Sanger sequencing.

The upper portion of this figure was adapted from Van Maldergem et al., *Epstein's Inborn Errors of Development*, 2016.

2.3 Establishing Familial Induced Pluripotent Stem Cells: *RECQL4*^{mut/wt} controls

Primary fibroblasts were reprogrammed by the Yamanaka four factors, OCT4, SOX2, KLF4 and MYC, using the CytoTune-iPS Sendai Reprogramming kit. The emerged iPS clones were picked and cultured on mouse embryonic fibroblasts (MEF) for approximately 11-15 passages (Figure 4). The iPS clone Family B2 exhibited hESC morphology, which was evident by cell clusters with a dense, domed center and well-defined borders (Figure 5) Scale bar, 250 μ m). PCR detection of exogenous *OCT4*, *SOX2*, *KLF4* and *MYC* in Family B2 iPSC line verified loss of the Sendai virus and transgenes (Figure 5.B). PCR-based mycoplasma detection assay further validated that the FCP351G iPSCs were free of mycoplasma (Figure 5.C).

Short tandem repeat (STR) profiling was performed to determine the cell of origin for the clonal Family B2 iPSCs. The STR profile of Family B2 clones were identical to that of Family B2 fibroblasts from which they were derived (Table 1). Immunofluorescence staining of Family B2 iPSCs demonstrated ubiquitous expression of the pluripotency transcription factor NANOG and hESC surface markers, SSEA-4 and TRA-1-81 (Figure 6). In addition to the immunofluorescent staining, Family B2 iPSCs exhibited consistent alkaline phosphatase surface staining among all colonies, which is indicative of stemness (Figure 5.A).

Examination of pluripotent gene expression by qRT-PCR showed that FCP351G iPSCs expressed pluripotency genes *NANOG*, *OCT4*, *SOX2*, *DPPA4*, *REX1* and *TERT* at a level equal to or greater than H1 hESCs. In contrast, Family B2 fibroblasts, the cells from which the iPSCs were reprogrammed, did not express these genes (Figure 7). G-band karyotyping is usually done when reprogramming iPSCs to examine for any chromosomal

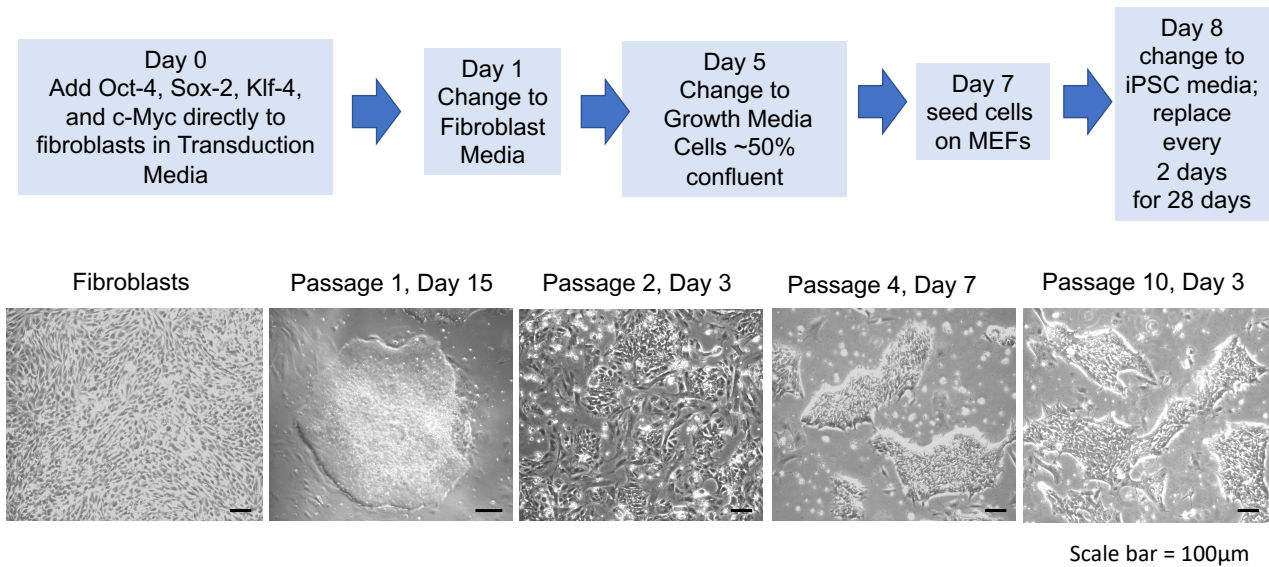


Figure 4: Reprogramming fibroblasts to establish iPSCs

The upper panel summarizes the initial steps in reprogramming, from the starting point of fibroblast through the generation of initial clones. The bottom panel shows phase microscopy of Family B2 fibroblasts, then shows the first passage of an emerged clone. It then depicts the passages at which morphological changes occur until passage 10, at which point stemness was evaluated.

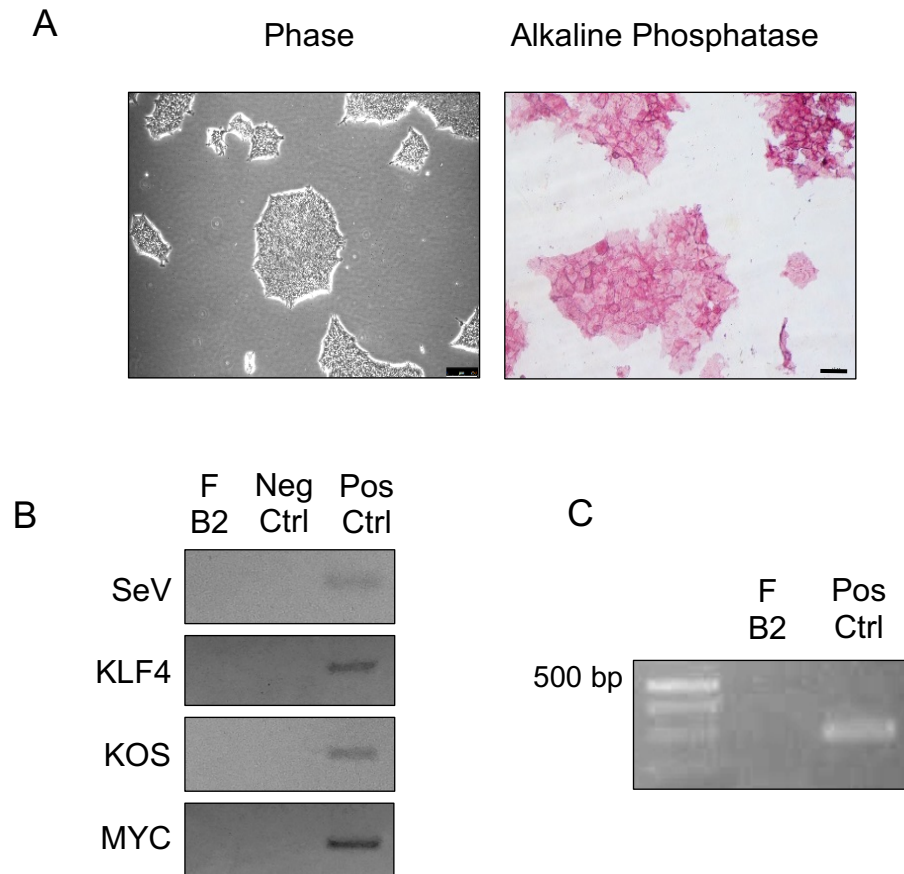


Figure 5: Verification of Family B2 induced Pluripotent Stem Cells

A) Phase microscopy and alkaline phosphatase staining depict stem cell morphology and surface staining indicative of stem cells. B) PCR to test for the Sendai virus delivery vector and Yamanaka factors demonstrated zero footprint iPSCs. C) Mycoplasma testing shows the iPSCs are free of the contaminant.

Table 1: STR analysis

Marker site	Family B2	Family B Fibroblasts
AMEL	X	X
CSF1PO	10,12	10,12
D13S317	11,12	11,12
D16S539	9,12	9,12
D18S51	12,19	12,19
D21S11	31.2,32.2	31.2,32.2
D3S1358	15, 16	15, 16
D5S818	10,12	10,12
D7S820	9,12	9,12
D8S1179	13,14	13,14
FGA	19,23	19,23
TH01	6, 9.3	6, 9.3
TPOX	8,11	8,11
vWA	17,18	17,18
Match each other		

Short tandem repeat analysis of Family B2 induced pluripotent stem cells and Family B fibroblasts, from which the iPSCs were derived, indicate that the iPSCs originate from the fibroblasts, validating our method of reprogramming.

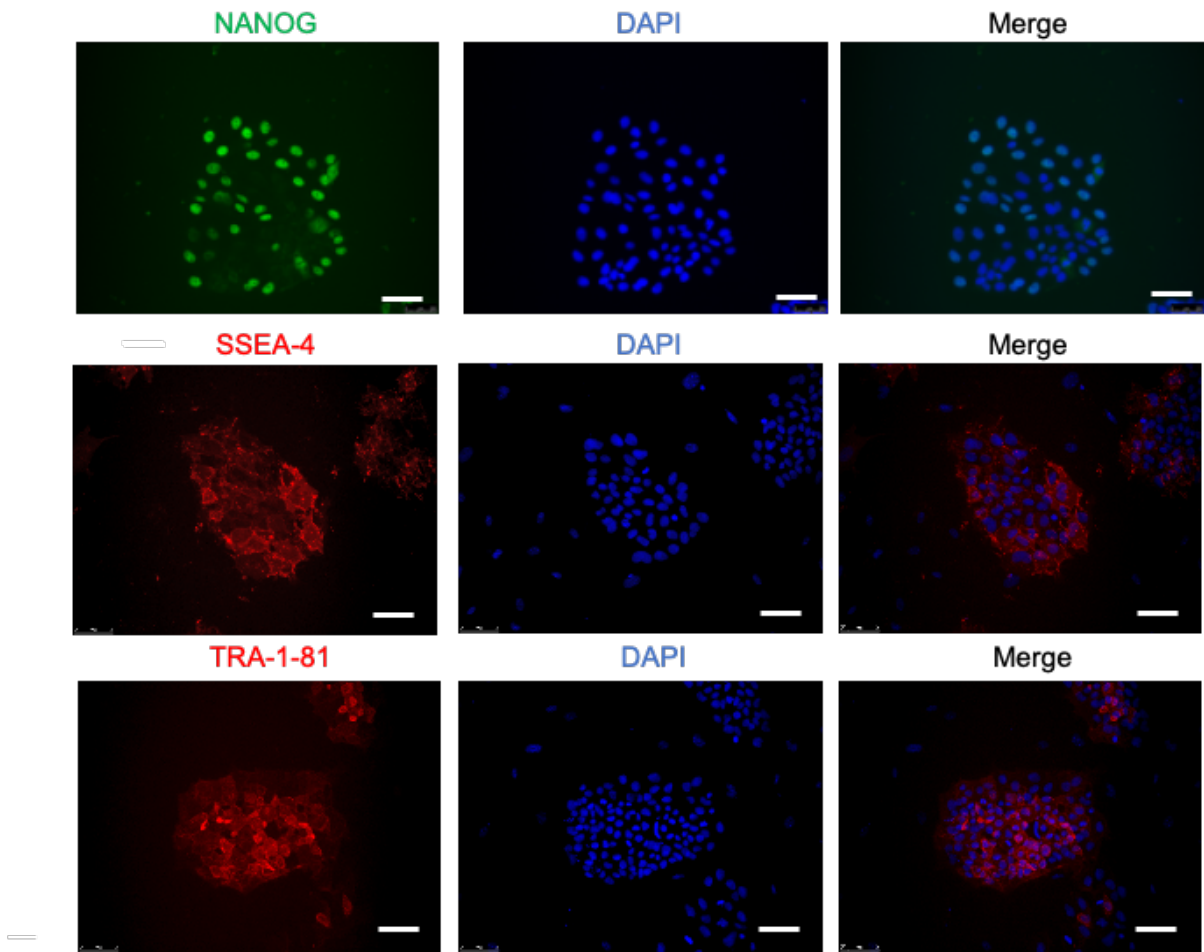
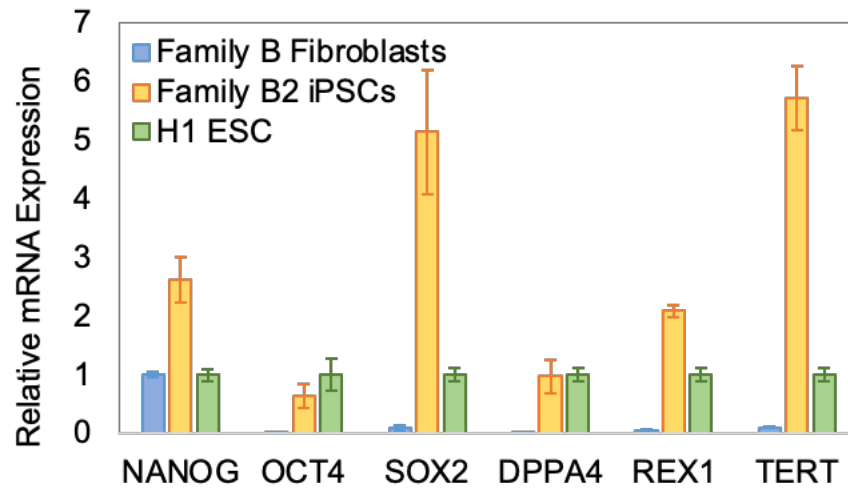


Figure 6: Immunofluorescence of Family B2 iPSCs

Staining of individual clones exhibited ubiquitous expression of the pluripotency markers Nanog, TRA-1-81, and SSEA-4. When merged with the nuclear stain DAPI, very high reprogramming efficiency can be observed.

A



B

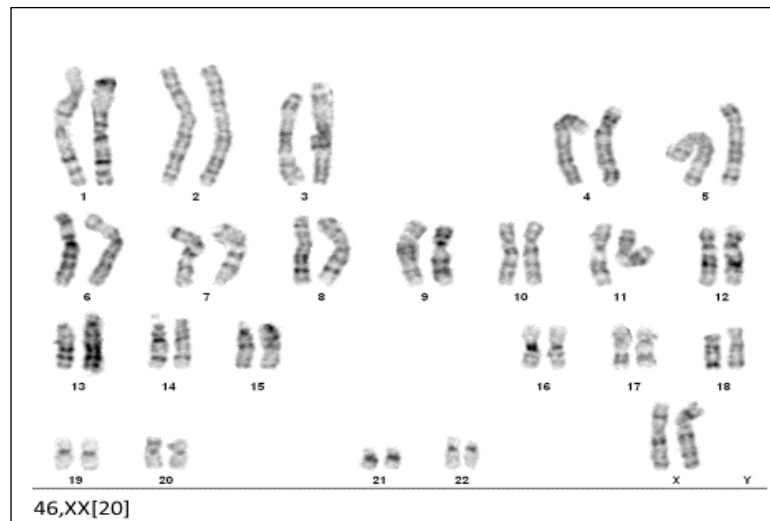
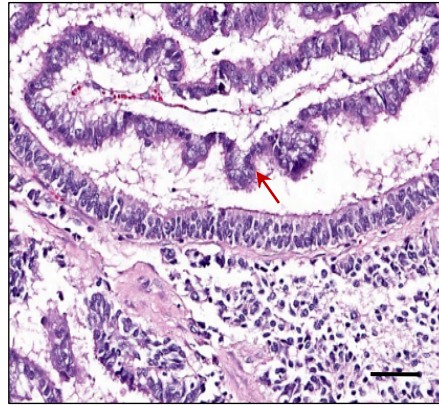


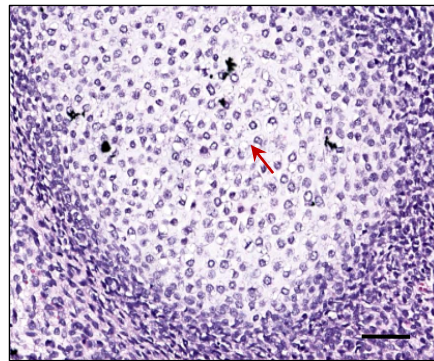
Figure 7: Characterizing Family B2 iPSCs

A) qRT-PCR shows expression of each of the pluripotency markers at approximately the same level of hESCs, but significantly different than the fibroblasts from which they were reprogrammed. B) G-band karyotyping shows a normal chromosomal spread.

Endoderm/Epithelium



Mesoderm/Cartilage



Ectoderm/Melanin

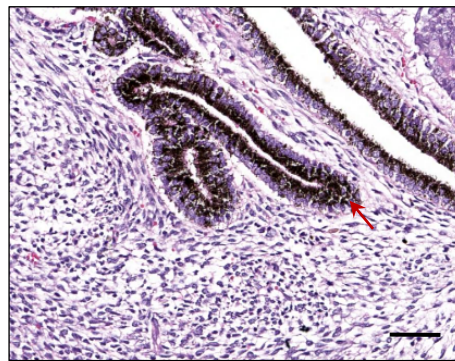


Figure 8: Family B2 teratoma

H&E staining of teratoma formed after subcutaneous injection of iPSCs demonstrate Family B2 iPSCs possess the ability to spontaneously differentiate into all three germ layers, verifying their stemness.

abnormalities that may have occurred during reprogramming. Karyotype analysis confirmed the normal karyotype of the Family B2 iPSCs (Fig 7.B). Teratoma assays then were used, as they are the gold standard of pluripotency. In this assay, iPSCs were injected subcutaneously into nude mice without extraneous growth factors to test their ability to spontaneously differentiate into all three germ layers. Teratoma formation indicated that Family B2 iPSCs were capable of differentiation into three germ layers, including epithelium (endoderm), cartilage (mesoderm), and melanin (ectoderm) (Figure 8), confirming their pluripotency.

2.4 Establishing *RECQL4*^{mut/mut} Type II RTS Osteosarcoma Patient – Derived Induced Pluripotent Stem Cells

After establishing iPSCs from Family (control) *RECQL4*^{mut/wt} cells, we were encouraged that *RECQL4*^{mut/mut} fibroblasts from Type II RTS patients could be reprogrammed, despite the known essential function of *RECQL4*. Because the available current models for studying Type II RTS with osteosarcoma are limited, we aimed to establish a Type II RTS iPSC model in order to contribute to the current body of knowledge of RTS and *RECQL4* mutations. This model is critical for elucidating molecular pathophysiology due to the specificity of the *RECQL4* mutation in osteosarcomagenesis. First, we describe reprogramming of RTS osteosarcoma patient cells to iPSCs and subsequent differentiation to osteoblasts, thereby generating a model to study RTS associated osteosarcoma tumorigenesis.

To dissect the pathological processes of osteosarcomagenesis in Type II RTS, we sought to develop a Type II RTS induced pluripotent stem cell (iPSC) model that could be complementary to current mouse and tissue culture models for investigating how *RECQL4* mutations contribute to Type II RTS patients' bone malignancies. We first chose 4 Type II RTS families in which patients were diagnosed with osteosarcoma. Their corresponding healthy parents were used as controls (Table 2). These Type II RTS patients possessed

biallelic mutations in the DNA helicase *RECQL4* and developed osteosarcoma at different ages. Their parents, referred to as Family, had one heterozygous *RECQL4* mutation and remained healthy. These Type II RTS patients possess biallelic mutations in the DNA helicase *RECQL4* and develop osteosarcoma at different ages, whereas their parents, referred to as Family, with one heterozygous *RECQL4* mutation remain healthy.

Table 2: Patient Samples for iPSC Reprogramming

Fibroblasts	iPSCs	Relationship	Clinical description	RECQL4 gene status
FCP-402	F-A1,2,3	Family1-Father	Normal	c.2719C>T/WT
RTS-120	RTS-A1,2,3	Family1-Proband	Osteosarcoma (10.6y)	c.2719C>T/c.2719C>T
FCP-351	F-B1,2,3	Family2-Mother	Normal	c.1878+32_1878+55del24/WT
RTS-112	RTS-B1,2,3	Family2-Proband	Osteosarcoma (10.8y)	c.1878+32_1878+55del24/c.1573delT
FCP-154	No visible clone	Family3-Mother	Normal	c.1391-1G>A (IVS7)/WT
FCP-153	No visible clone	Family3-Proband	Osteosarcoma (33.3y)	c.1391-1G>A (IVS7)/c.1573delT
FCP-131	No visible clone	Family4-Mother	Normal	c.2269C>T/WT
FCP-129	No visible clone	Family4-Proband	Osteosarcoma (4.3y)	c.2269C>T/c.1573delT

Listed in this table are both RTS osteosarcoma patients, who possess biallelic RECQL4 mutations, and Family (F) controls, who are parents with a heterozygous RECQL4 mutation, but do not develop osteosarcoma or other RTS symptoms. Used in this study are set A and set B, resulting in 12 total iPSC lines.

Type II RTS and control Family fibroblasts were transduced with the Yamanaka four factors (NANOG, OCT4, SOX2 and MYC) (Fusaki et al., 2009; Takahashi and Yamanaka, 2006) via the Sendai virus vector as described previously. After cellular reprogramming and clone selection, two out of four sets successfully generated paired RTS patient/ Family control iPSCs. The low reprogramming efficiency in RTS and their Family iPSCs implied the potential role of RECQL4 in cellular reprogramming. These RTS and Family iPSCs exhibited human embryonic stem cell (hESC) clonal morphology and ubiquitously expressed the pluripotency transcription factors NANOG and OCT4, as well as the hESC surface antigens, TRA1-81 and SSEA4 (Figure 9). Consistently, quantitative reverse transcription PCR (qRT-qPCR) confirmed the similar expression of *NANOG*, *SOX2*, and *OCT4* as compared to the hESC H1 cells (Figure 10). To test the ability of these cell lines to differentiate into all three germ layers *in vivo*, teratoma formation assay, again, was performed. Examination via H&E stained teratoma revealed both RTS and Family iPSCs were capable of differentiating into ectodermal, endodermal, and mesodermal lineages (Figure 11), confirming their pluripotency. We further verified the loss of exogenous *SeV-OCT4*, *SOX2*, *KLF4* and *MYC* transgenes by genomic PCR detection and confirmed no detectable SeV transgenes (Figure 12). This suggested that these RTS and Family iPSCs were zero-genetic footprint.

As RECQ family DNA helicases play a critical role in maintaining genome integrity (Gupta and Schmidt, 2020), the deficiency of these proteins has been associated with genomic instability, several features of cancer predisposition, and a premature aging phenotype (Lu et al., 2017; Mohaghegh and Hickson, 2002). To examine the genomic integrity of these cells, G-band karyotyping was performed in both RTS and Family iPSCs (Figure 13). Chromosome analyses indicated RTS-A and Family-A iPSCs possessed chromosomal abnormalities. Both RTS-B and Family-B iPSCs presented as normal karyotypes. Despite these differences, the phenotype of RTS associated osteosarcoma and no known familial malignancy held true. We suspect that the abnormal chromosome deletions in RTS-A and Family-A iPSCs may have occurred from either original fibroblasts or

the reprogramming process. In addition, lower efficiency in the generation of RTS and Family iPSCs imply an essential role of RECQL4 in cellular reprogramming. All together, we generated six RTS and six Family iPSC cell lines, which exhibited chromosomal and sex diversity, allowing for robust further study.

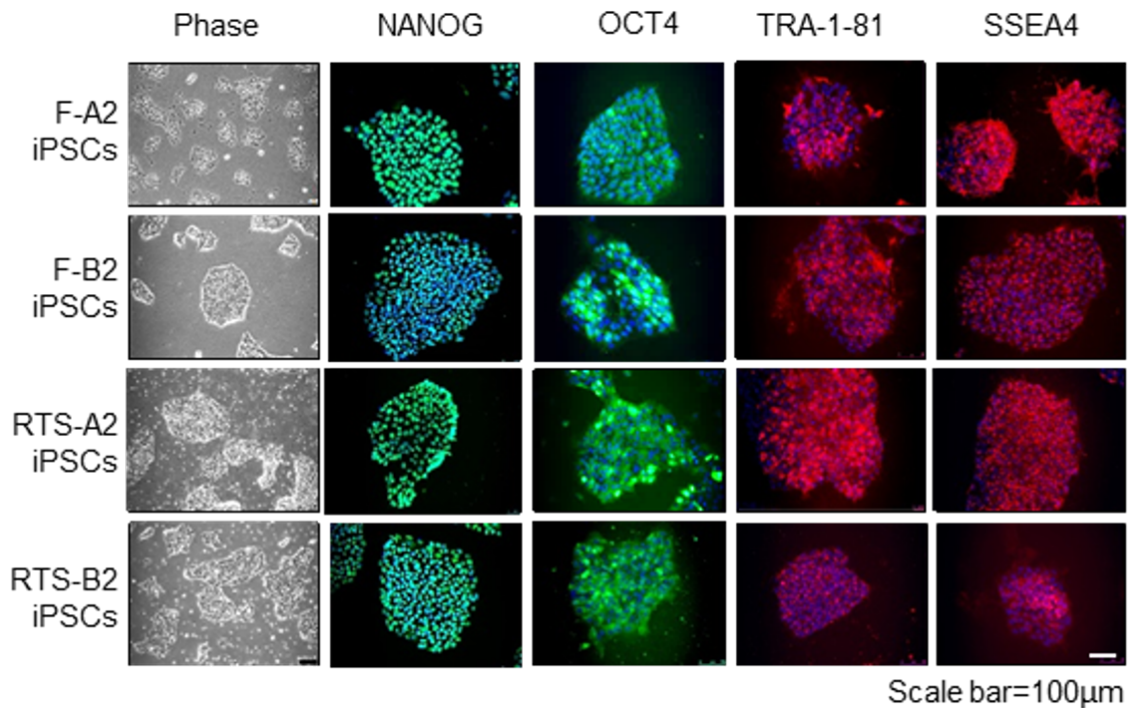


Figure 9: Immunofluorescence of Patient and Family iPSCs

Phase microscopy of individual clones from representative cell lines exhibited clonal morphology, defined borders, and dense centers, indicative of stemness. Immunofluorescent staining using the pluripotency markers Nanog and Oct-4 and the surface markers TRA-1-81, and SSEA-4, co-stained with DAPI. Each of the immunofluorescence microscopy showed ubiquitous expression of each of the pluripotency markers, further indicating stemness and high reprogramming efficiency.

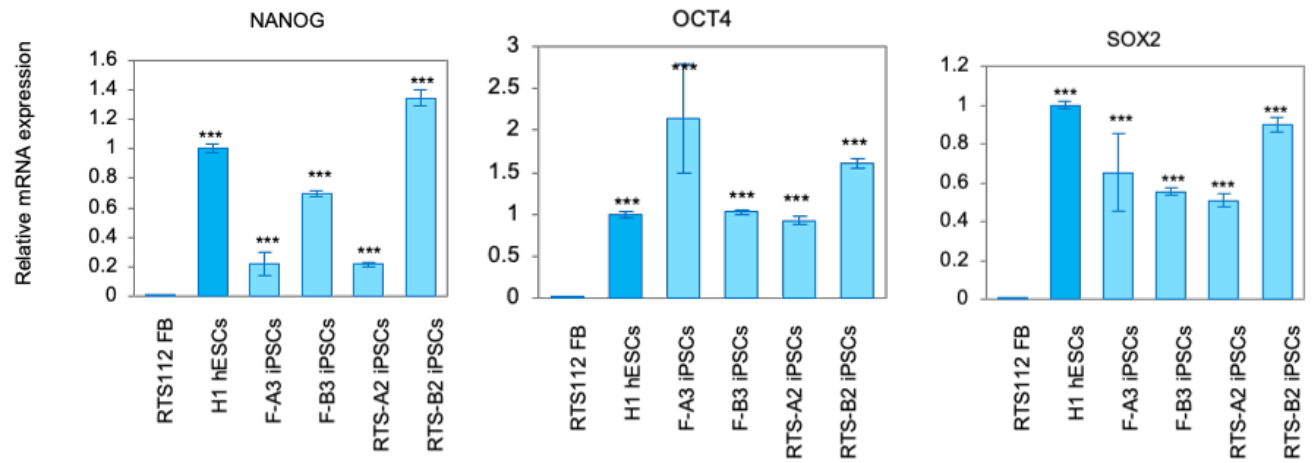


Figure 10: qRT-PCR of iPSCs

qRT-PCR assay for pluripotency genes NANOG, OCT4, and SOX2 in RTS and Family (F) iPSCs. Error bars indicate SEM of triplicates. n=3 biological replicates; error bars represent \pm SEM; statistical significance was determined using one-way ANOVA followed by Student's t test (Tukey's multiple comparison test); ***p < 0.001.

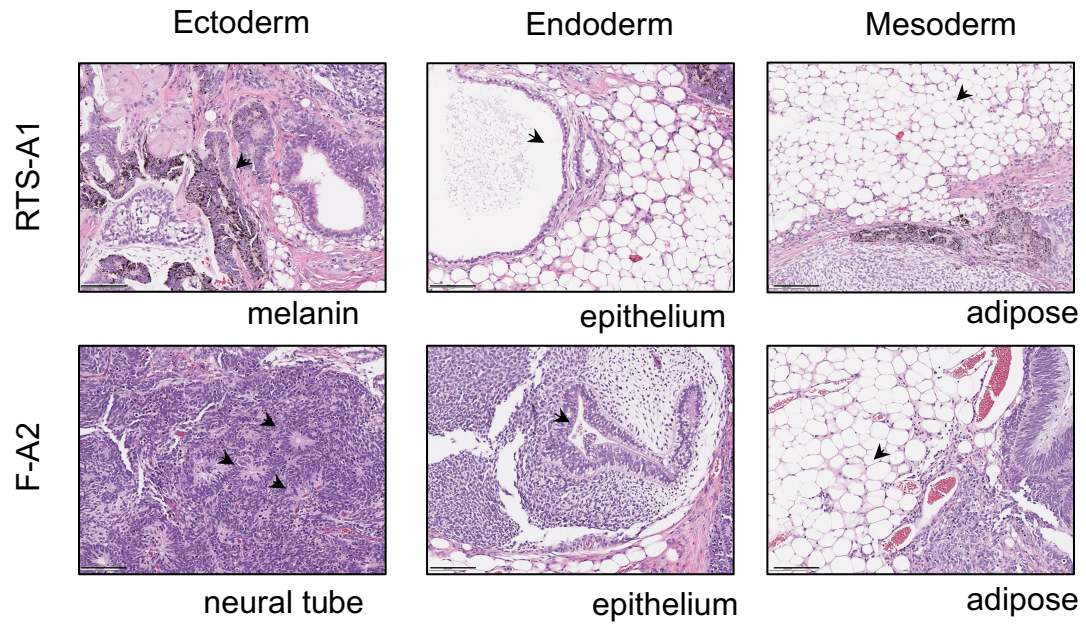


Figure 11: Teratoma assay

In vivo teratoma formation assay demonstrated RTS and Family iPSCs were capable of differentiation into all three germ layers, confirming pluripotency. Scale bar, 200 μ m.

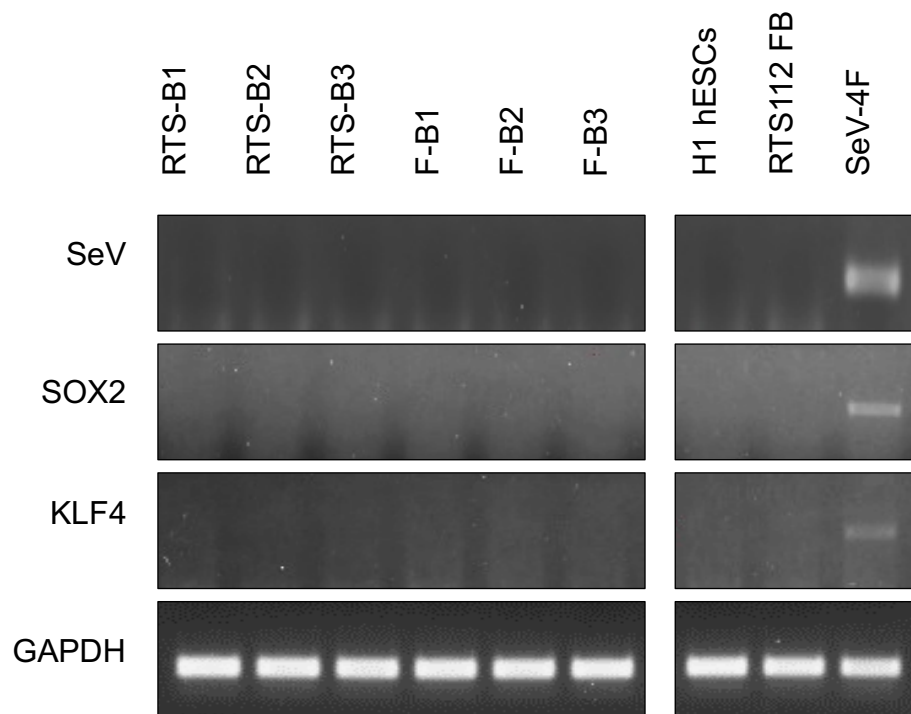
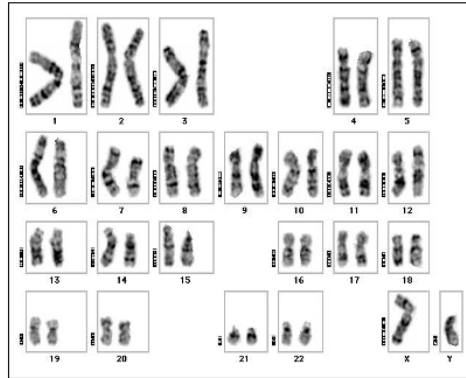


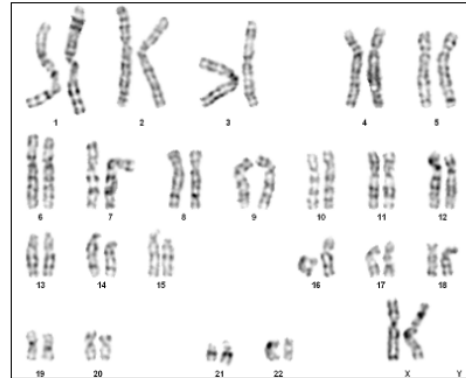
Figure 12: Zero-footprint iPSC generation

PCR detection of SeV genome and transgenes indicated RTS and Family iPSCs are footprint-free.

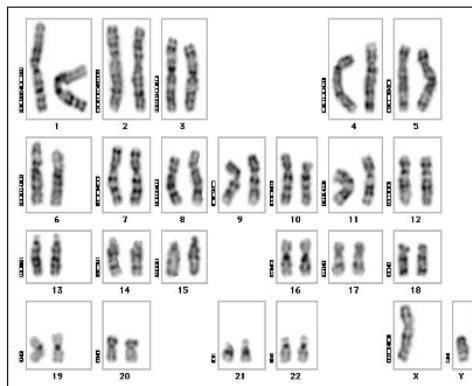
F-A2
46,XY,del(7)(q22)



F-B2
46XX



RTS-A2
46,XY,del(10)(p11.2p13)



RTS-B1
46XX

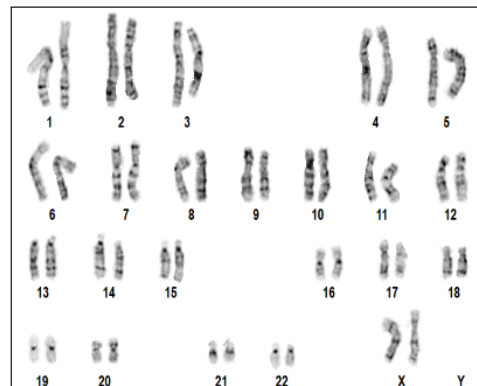


Figure 13: G-band karyotyping of iPSCs

G-band karyotyping of RTS and Family (F) iPSCs showed that set A possess chromosomal abnormalities, while set B possess normal karyotypes.

2.5 Generation of Mesenchymal Stem Cells and Their Derived Osteoblasts

After establishing these RTS and Family iPSC lines, we next sought to utilize these iPSCs to investigate the pathological mechanisms involved in RTS patients associated bone malignancies. We first differentiated these iPSCs to mesenchymal stem cells (MSCs) by a SB-431542 and 7.5% CO₂ induced MSC differentiation method (Leyendecker Junior, 2018). After 60 days of differentiation, cells exhibited the change from clonal morphology to the elongated and swirling pattern typical of MSCs, shown in the phase microscopy (Figure 14). These iPSC-derived MSCs were then examined for the presence of typical MSC surface markers, CD73, CCD44, and CD105. Immunostaining showing high efficiency of CD73, CCD44, and CD105 expression in SB-431542 and 7.5% CO₂ induced MSCs confirmed the successful differentiation of iPSCs to MSCs.

These well-defined MSCs were further differentiated to osteoblasts, a potential osteosarcoma cell-of-origin, by a defined osteogenic differentiation method (Lee et al., 2015). As osteogenic differentiation progressed, MSC morphology shifted from elongated and swirling to a cobblestone appearance, characteristic of osteoblasts (Figure14). Mature osteoblasts are capable of forming the bone by depositing minerals and cellular matrix formation (Capulli et al., 2014). After 24 days of osteoblastic differentiation, positive alizarin red staining (ARS) of RTS and Family MSC-differentiated osteoblasts indicated successful osteogenic differentiation (Figure 15). Taken together, each step, from cellular reprogramming through lineage differentiation, illustrated a model of iPSC-derived osteoblasts suitable for investigating RTS patient associated bone malignancies.

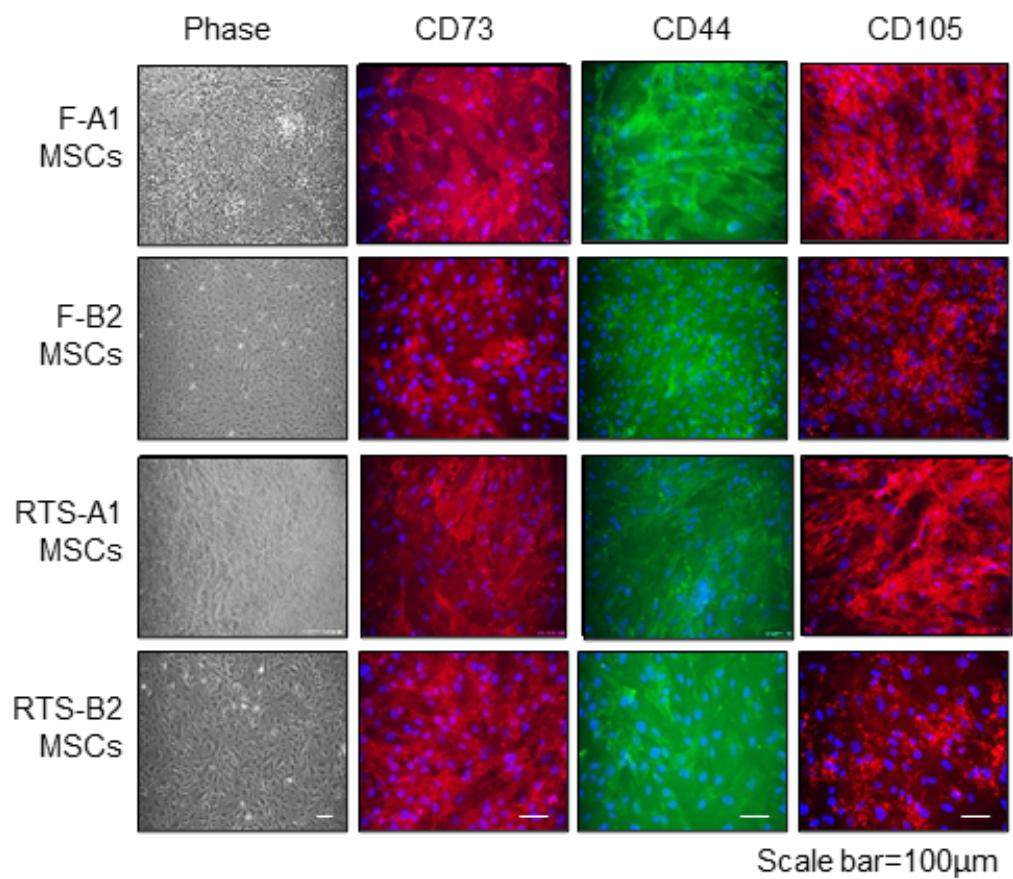


Figure 14: Differentiation of Mesenchymal Stem Cells

Immunostaining demonstrated that iPSC-derived MSCs exhibited swirling morphology (phase) and expressed MSC surface markers CD73, CD44, and CD105. Scale bar, 100 μm.

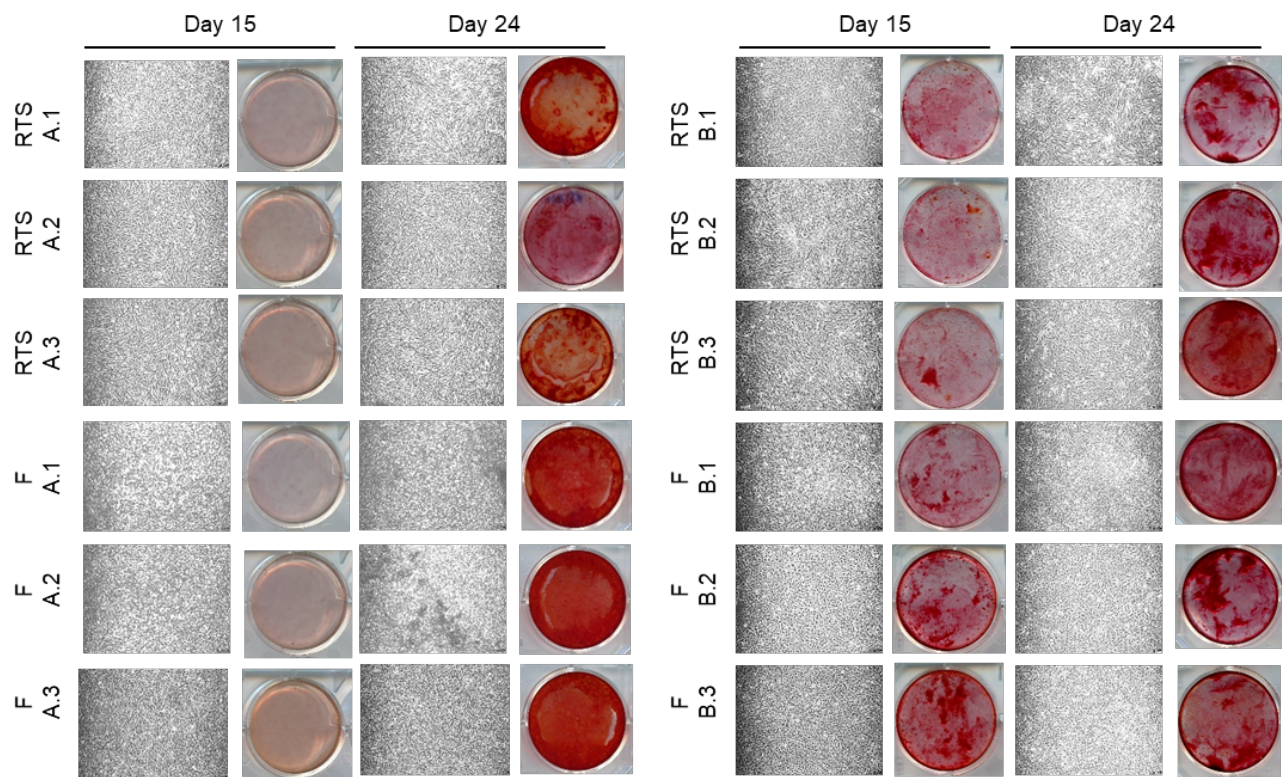


Figure 15: Differentiation of osteoblasts

RTS and Family MSC-derived osteoblasts at early osteoblast stage (Day 15) and Late osteoblast stage (Day 24) exhibited cobblestone morphology, typical of osteoblasts. Alizarin red staining (ARS) demonstrated the ability of differentiated osteoblasts to deposit minerals. Scale bar, 100 μm .

Chapter Three: Transcriptional Changes During Osteoblast Differentiation Reveal Increased Oxidative Phosphorylation in Type II RTS Patient – Derived Cells

3.1 Introduction

Oxidative phosphorylation as a target for treatment has been a topic of particular interest with respect to cancer treatment for several years (Ashton et al., 2018). Metabolic reprogramming has long been understood as a hallmark of cancer, but traditionally the focus has been on glycolytic upregulation (Hanahan and Weinberg, 2000). More recently, the importance of oxidative phosphorylation has become apparent in many cancer types, ranging from solid tumor to hematological malignancies (Ashton et al., 2018). Recent discussions underscore the need for more in-depth investigation into the role of oxidative phosphorylation in cancer development and progression (Zu and Guppy, 2004). Recently, metabolic reprogramming has been shown to be critical to tumorigenesis in other cancers (Bonnay et al., 2020). Interestingly, metastatic osteosarcoma has been shown to be inhibited by Metformin, mediated by PTEN (Li et al., 2018), emphasizing that the dysregulation of mitochondrial functions plays a role in osteosarcomagenesis. Although there is a strong link among oxidative phosphorylation, metabolic reprogramming, and tumorigenesis, it has largely gone unexplored with regard to osteosarcoma.

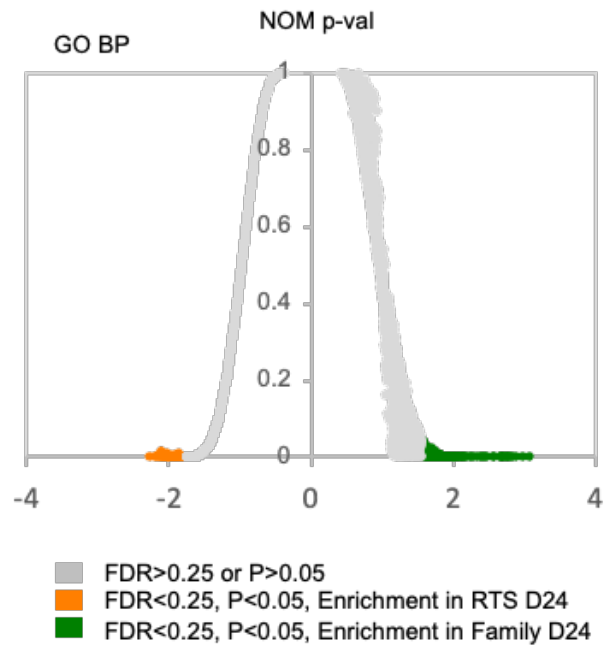
3.2 Altered mitochondrial respiratory gene signature in RTS osteoblasts

RTS and Family iPSC-derived cell samples were collected at three different differentiation stages for RNA-seq analyses in order to gain insight into the underlying pathological mechanisms involved in RTS associated osteosarcomagenesis. These stages were: MSCs (day 0), pre-osteoblasts (day 15) and mature osteoblasts (day24). Transcriptional profiling comparing the RTS and Family cell lines at different differentiation stages allowed us to interrogate the molecular dysregulation leading to osteosarcomagenesis in RTS patients. We first used gene set enrichment analysis (GSEA) to identify enriched Gene Ontology biological processes (GO_BP) in both RTS and Family samples. This was done in order to determine the nature of these discrete transcriptional

profiles (Figure 16.A). The heatmap of summarized enrichment GO_BP demonstrated that many mitochondrial energy production functions were enriched in RTS osteoblasts. These pathways included ATP synthesis coupled electron transport, mitochondrial respiratory chain complex assembly, NADH dehydrogenase complex assembly, and oxidative phosphorylation (Figures 16.B). Interestingly, these pathways were increasingly enriched as differentiation progressed, indicating that the alteration of transcriptome profiling related to ATP production occurred in osteoblast lineages. In contrast, GO_BP analyses revealed significantly decreased enrichment of skeletal development pathways (e.g., bone morphogenesis, bone development, cell matrix adhesion, extracellular matrix assembly, etc.) in the RTS patients (Figure 16.B). This supports the clinical observation that RTS patients show small stature and skeletal abnormalities.

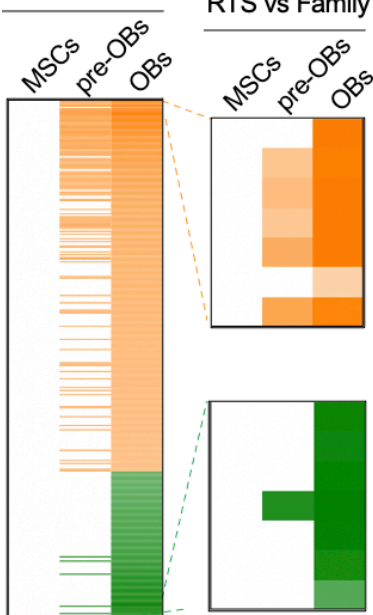
Complementary KEGG pathway analyses also were performed. As a result, it became clear that oxidative phosphorylation is a compelling pathway for further interrogation as an important regulator of increased energy that may contribute to RTS patient associated bone malignancies (Figure 17). Interestingly, the TCA cycle pathway also was upregulated in RTS osteoblasts, providing a potential substrate for an increase in electron transport chain (ETC) activity (Figure 17.B). These findings were validated further by Reactome biologic pathways and process analysis showing elevated transcription in genes related to respiratory electron transport and respiratory electron transport ATP synthesis by chemiosmotic coupling and heat production by uncoupling proteins (Figure 18). In addition to impaired skeletal development pathways found in RTS osteoblasts, KEGG pathway and Reactome analyses also revealed that reduced TGF β , NOTCH3 integrin signaling pathways as well as WNT, a key bone morphogenesis regulator pathway, were impaired in RTS osteoblasts (Figure 18). A decrease in skeletal development pathways was observed consistently in the osteoblast transcriptional signatures in the osteosarcoma-prone genetic disorder, LFS (Lee et al., 2015).

A



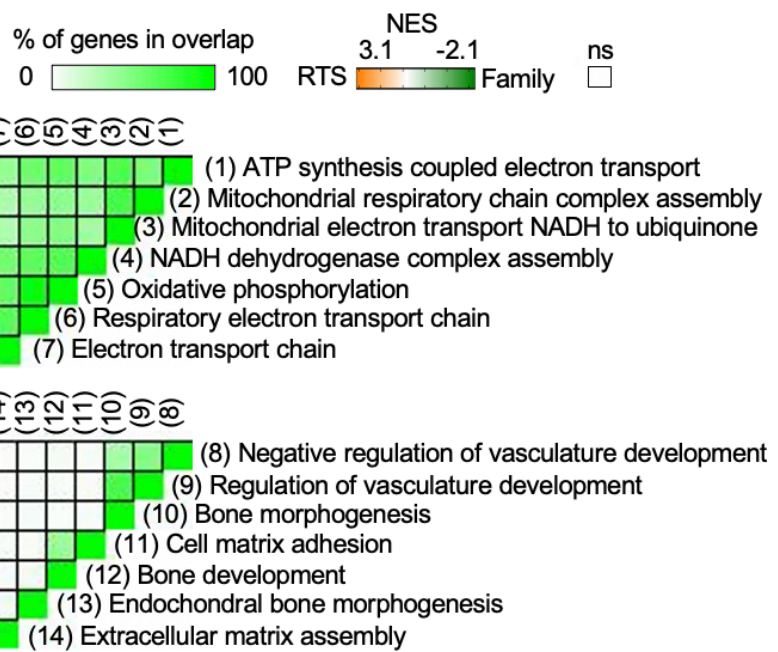
B

RTS vs Family



C

RTS vs Family



D

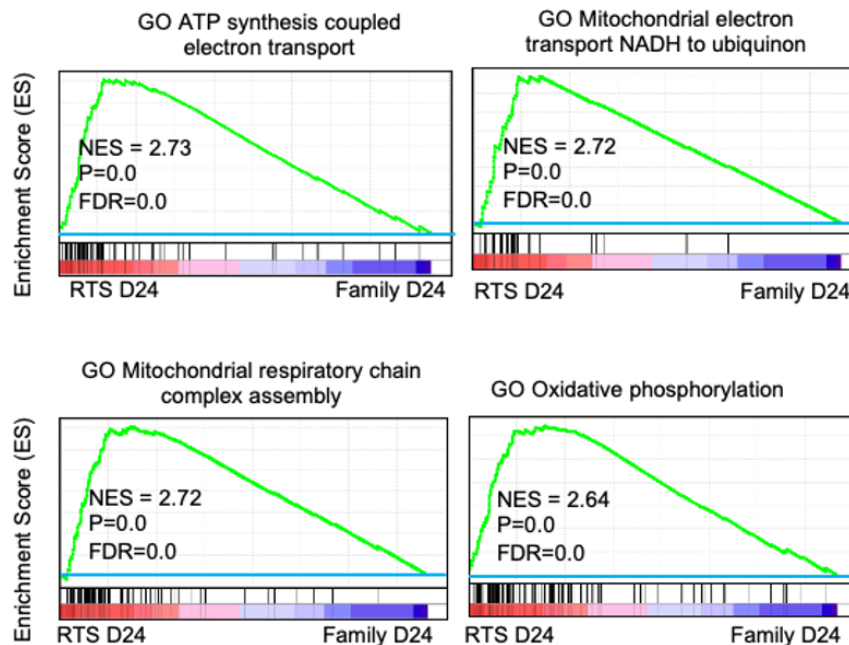


Figure 16: GSEA analyses identify enriched gene ontology biological processes (GO_BP) in RTS and Family osteoblasts.

A) 7525 gene sets were used in GO_BP analysis. A positive NES (green) represents GO_BP gene sets enriched in the transcriptome of Family osteoblasts; in contrast, a negative NES (orange) represents GO_BP gene sets enriched in the transcriptome of RTS osteoblasts. Enriched gene sets were selected based on statistical significance (normalized p-value < 0.05 and FDR q-value < 0.25). B) Heat maps depict the significantly altered GO_BP found in RTS MSCs, pre-osteoblasts, and osteoblasts as compared to Family counterparts. C) GSEA leading edge analysis shows the overlapping enriched gene sets in RTS and Family osteoblasts. D) Mitochondrial ATP production related GSEA GO_BP results showed upregulated ATP synthesis coupled electron transport, mitochondrial electron transport NADH to ubiquinon, mitochondrial respiratory chain complex assembly, and oxidative phosphorylation) in RTS mature osteoblasts.

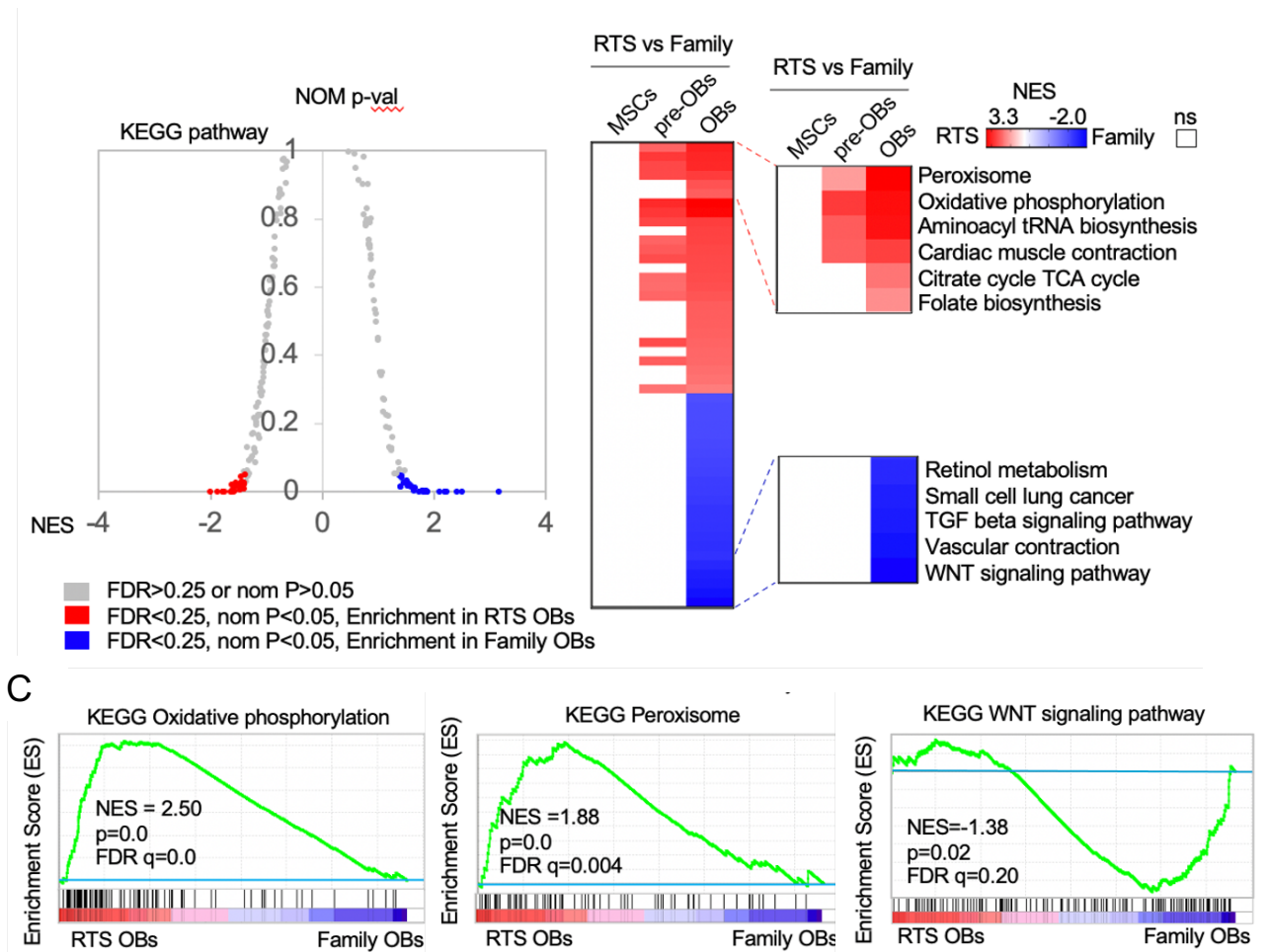


Figure 17: KEGG pathway analyses reveal enriched pathways in RTS and Family osteoblasts

A) 183 pathways were used in KEGG pathway analysis. Positive NES (blue) represents pathways enriched in the transcriptome of Family osteoblasts; negative NES (red) represents pathway enriched in the transcriptome of RTS osteoblasts. Enriched pathways were selected based on statistical significance (normalized p-value < 0.05 and FDR q-value < 0.25). B) Right heat map shows the significantly altered pathways found in RTS MSCs, pre-osteoblasts, and osteoblasts as compared to Family. C) The representative enriched KEGG pathways, including oxidative phosphorylation, peroxisome, and WNT signaling pathways enriched in RTS or Family osteoblasts are shown.

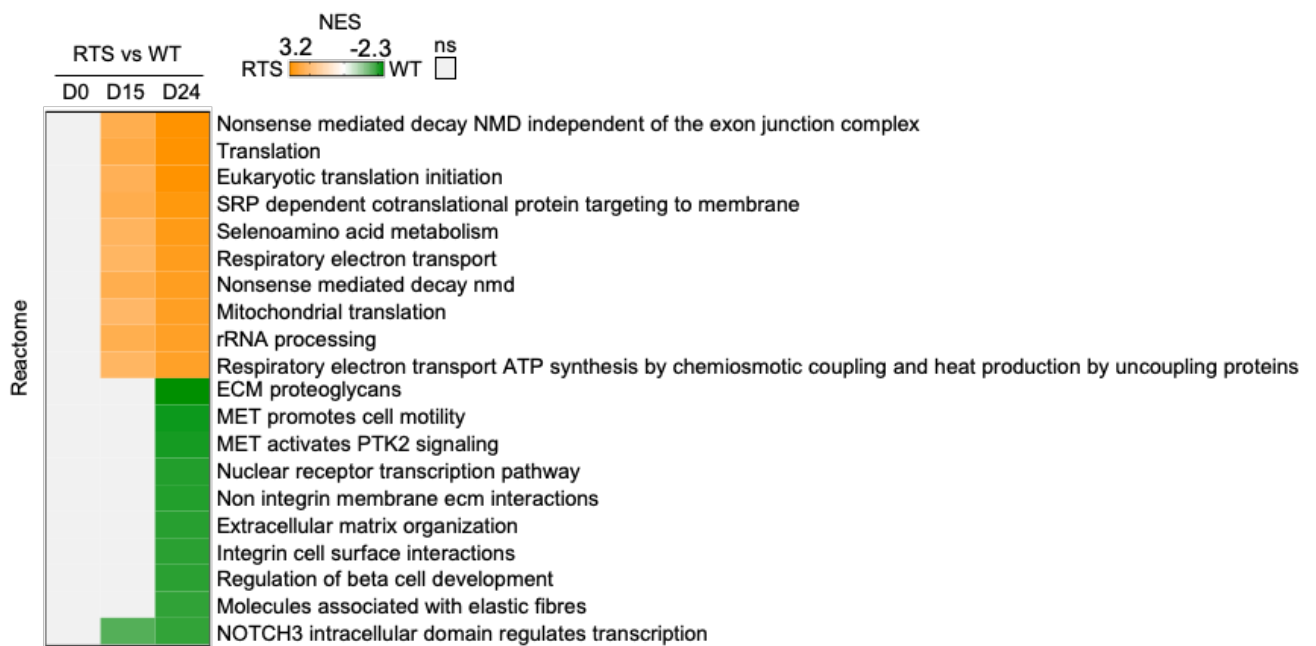


Figure 18: Reactome analysis confirms RTS increased metabolism via electron transport in mitochondria.

Reactome analysis demonstrated that multiple canonical pathways were enriched in RTS and Family MSCs, pre-osteoblasts and osteoblasts, respectively.

In addition to pathway analysis, we also sought to explore the nature of chromosomal predisposition to osteosarcoma. Alterations of the genome in osteosarcoma patients is well understood (Lindsey et al., 2017). Alterations identified by Cytogenetic Region Enrichment Analysis (CREA) (Walkley et al., 2008) reveals that in RTS patients, several cytogenetic regions, which are indicated as important for osteosarcoma-promoting cytogenetic rearrangement, are highly upregulated in RTS day 24 osteoblasts in comparison to Family (Figure 19). To further explore the potential cancer-related pathways contributing to osteosarcomagenesis in RTS patients, we examined the altered oncogenic signatures in RTS osteoblasts in order to further explore the potential cancer-related pathways contributing to osteosarcomagenesis in RTS patients. We discovered that neoplastic pathways involving MYC (Chen et al., 2018) and EIF4E (Qi et al., 2019) were upregulated, while the p53 tumor suppressor pathway was downregulated (Figure 19.A). Furthermore, we analyzed the enrichment of transcription factor targets (TFT) to explore the potential RTS-associated gene signature triggered by transcription factors. We observed upregulated AP1, NRF2, ELK1, prognostic of prostate cancer disease reoccurrence (Pardy et al., 2020). We also found NRF2 targets but downregulated FOXO1, a potential tumor suppressor regulating gluconeogenesis (Gross et al., 2008) targets in RTS osteoblasts (Figure 19.B). Taken together, our transcriptome analyses of RTS osteoblasts emphasized that the elevation of mitochondrial energy production and oncogenic signature, as well as a decrease in tumor suppression pathways, may contribute to osteosarcomagenesis in RTS patients.

We next validated the upregulation of oxidative phosphorylation genes in RTS osteoblasts. We found that *NDUF7*, *NDUFB1*, *NDUFB2*, and *NDUFS8*, which are thought to be involved in both the accessory and catalytic subunits of mitochondrial respiratory complex I (Formosa et al., 2018), were upregulated in RTS osteoblasts as compared to the Family osteoblasts in both paired sets (Figure 20). Importantly, mitochondrial ATP production pathways (e.g., oxidative phosphorylation, respiratory electron transport chain,

TCA cycle, and mitochondrial respiratory complex assembly) were activated significantly in sporadic osteosarcoma as compared to normal osteoblasts and bone tissues (Figure 21). As a result of these observations, our methodic transcriptome analyses led us to hypothesize that the elevated complex I enzymatic activity of RTS osteoblasts may play a critical role in osteosarcomagenesis in RTS patients.

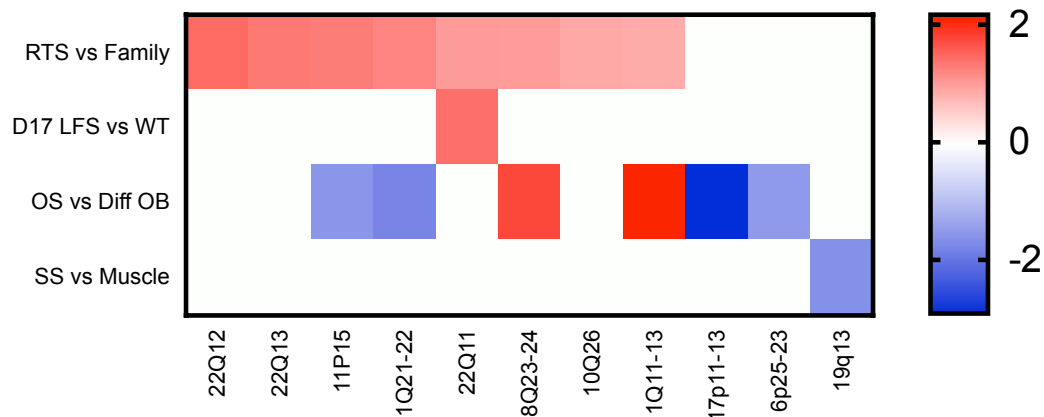


Figure 19: CREA analysis demonstrates chromosomal signature predisposed to osteosarcoma in Day 24 osteoblasts

Cytogenetic analysis of day 24 RTS osteoblasts compared to Family control osteoblasts, Day 17 Li Fraumeni Syndrome (LFS) iPSC derived osteoblasts compared to wild type (WT) osteoblasts, human osteosarcoma (OS) versus differentiated healthy osteoblasts (OB), synovial sarcoma (SS) and muscle demonstrate a pattern of genomic rearrangements that is most pronounced in RTS osteoblasts.

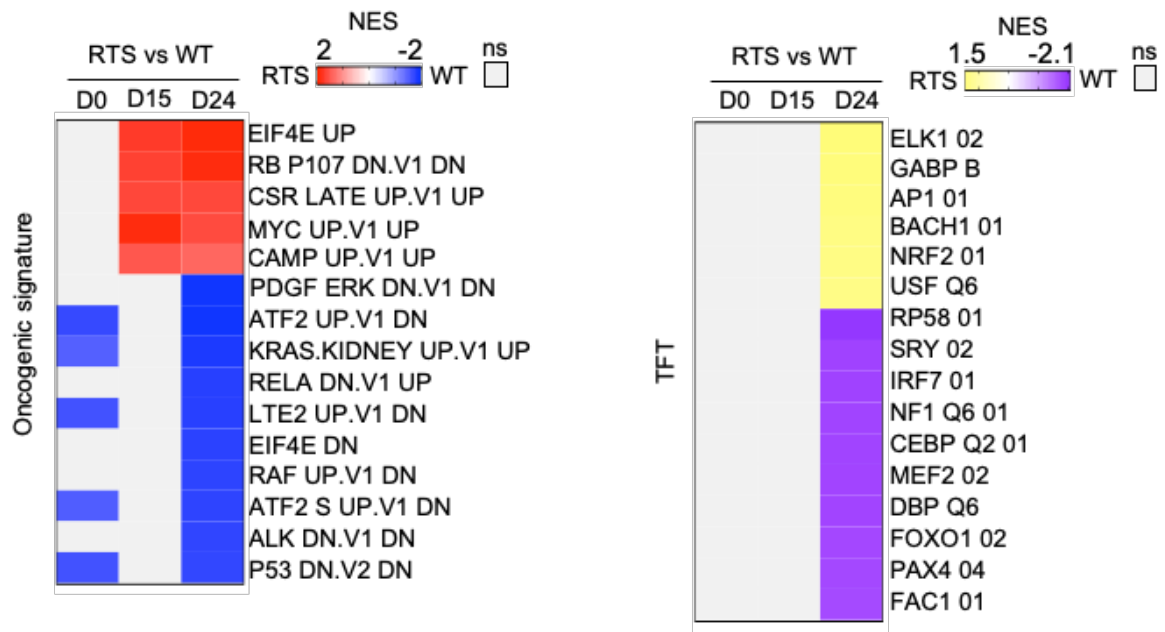


Figure 20: Additional pathway analyses provide pathways that may contribute to tumorigenic potential.

A) Oncogenic signature revealed specific gene-disturbed transcriptome signatures were enriched in either RTS or Family MSCs, pre-osteoblasts and osteoblasts. B) Transcription factor target (TFT) analysis of the regulatory target gene sets revealed potential dysregulated transcription factors in both RTS and Family MSCs, pre-osteoblasts and osteoblasts.

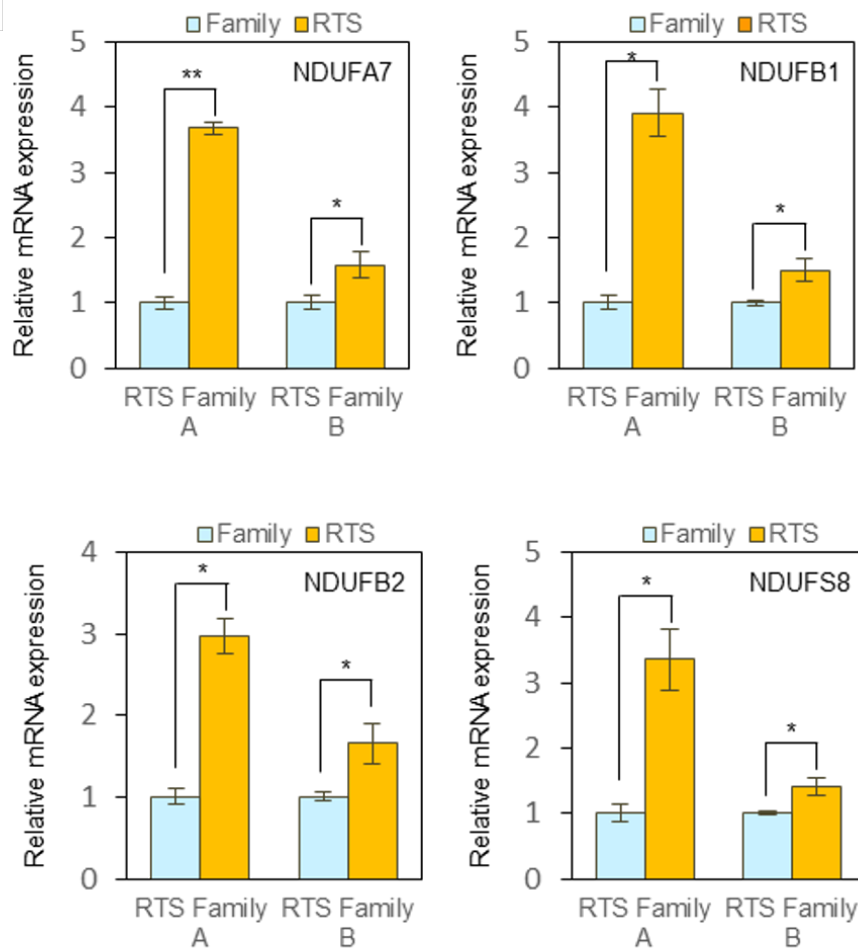
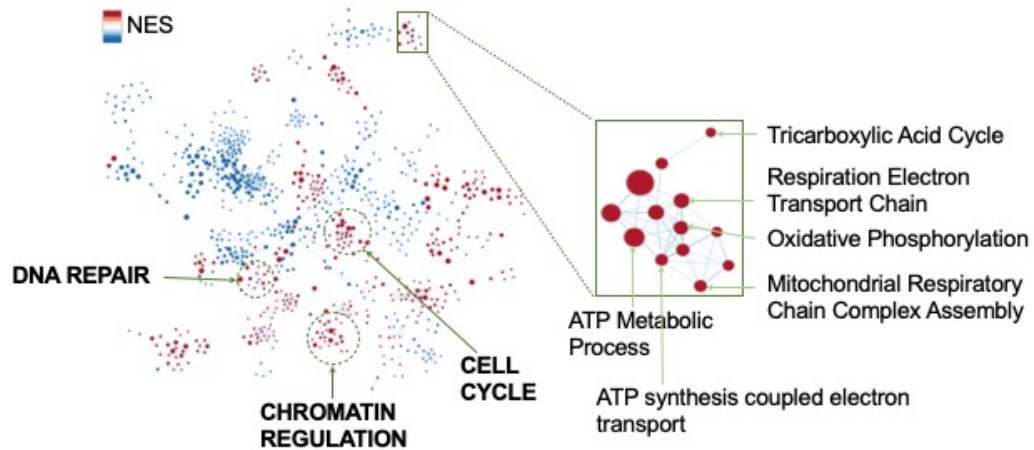


Figure 21: Complex I genes are significantly upregulated in RTS patient day 24 osteoblasts compared to Family controls

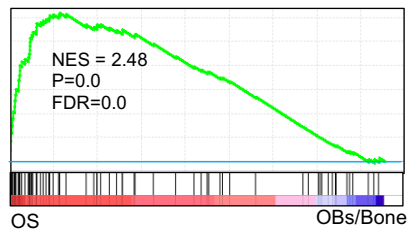
Individual genes (*NDUFA7*, *NDUFB1*, *NDUFB2*, and *NDUFS8*) that compose complex I of the electron transport chain were upregulated significantly in RTS osteoblasts. n=3 biological replicates; error bars represent \pm SEM; statistical significance, which was determined using one-way ANOVA followed by Student's t test (Tukey's multiple comparison test); *p < 0.05; **p < 0.01.

A



B

ATP synthesis coupled electron transport



Respiration electron transport

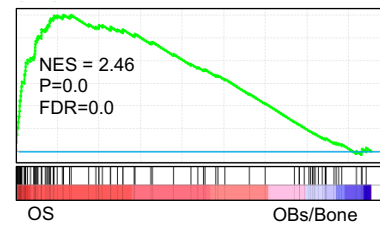


Figure 22: GO-BP analysis shows upregulation in sporadic osteosarcoma compared to healthy bone

A) Network visualization of gene sets enriched in osteosarcoma compared with normal bone and osteoblasts (p value <0.05 , FDR q value <0.1) indicates that GO_BP involved in DNA repair, chromatin regulation, cell cycle, and mitochondrial ATP production and repair were enriched in osteosarcoma. The number of enriched genes in each GO is displayed as node size, with closer distance between nodes representing increased overlap between genes in ontologies. Enriched gene sets in osteosarcoma are displayed in red and enriched gene sets in bone and osteoblasts in blue. B) Representative enriched gene sets (ATP synthesis coupled electron transport and respiration electron transport chain) involved in mitochondrial ATP production were consistent with those observed in RTS osteoblasts.

3.3 Characterization of Mitochondrial Complex I, II, III, and IV activities in RTS Osteoblasts

We systematically examined enzymatic activity through mitochondrial complexes, including complex I, complex I and III, complex II, complex II and III, complex V, and citrate synthase enzyme activity to explore the biochemical activity of the electron transport chain (Figure 22). We found that RTS osteoblasts significantly increased the mitochondrial complex I activity, but not that of complex II, III, or IV. Mitochondrial complex I is of particular importance as it is the first in the electron transport chain, establishing the electrochemical gradient necessary for ATP production (Brandt, 2006). In agreement with mitochondrial enzymatic activity assays, transcriptome results showed significant increase in mitochondrial complex I *NDUFA7A*, *NDUFB1*, *NDUFB2*, *NDUFS8* mRNA expression (Figure 20). These findings led us to conclude that increased activity through mitochondrial complex I was the result of the increased transcription of complex I genes.

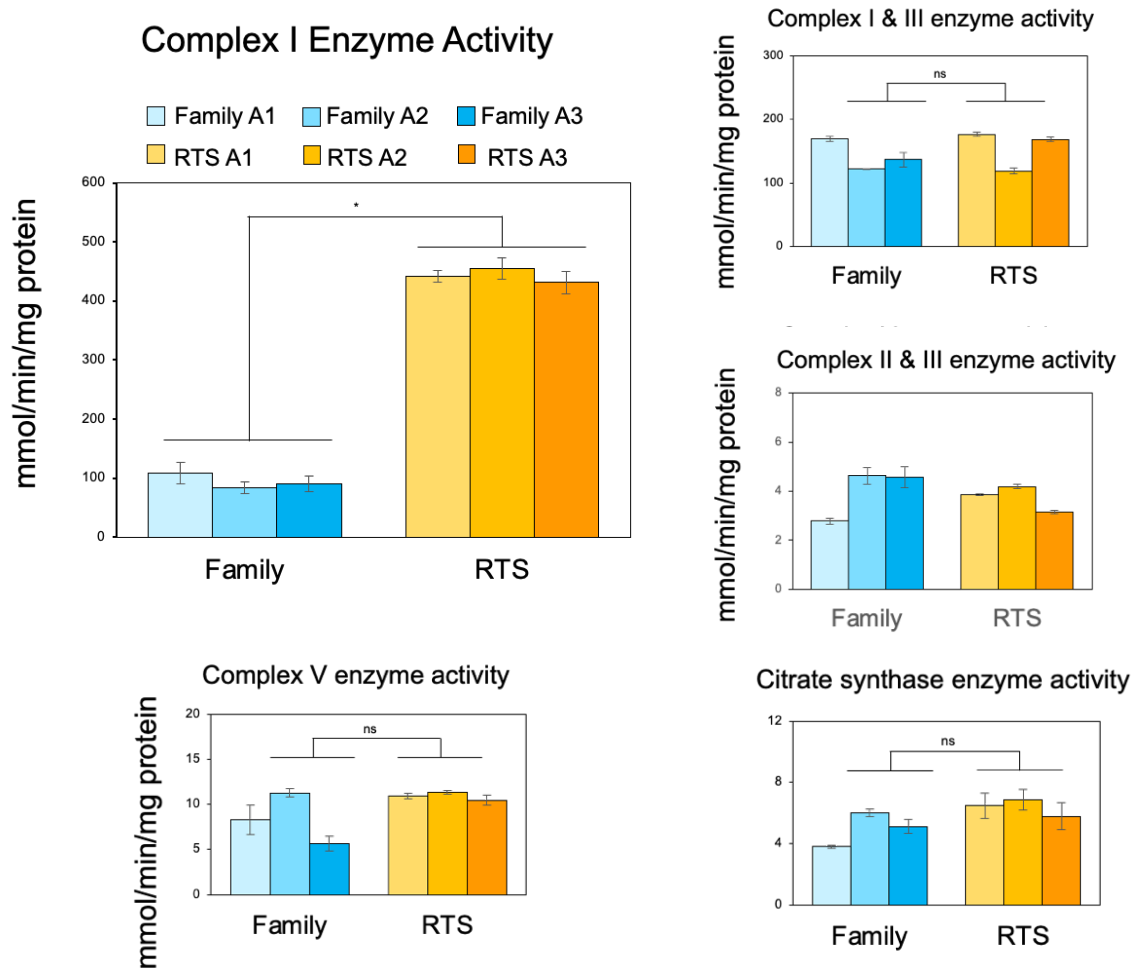


Figure 23: RTS patient osteoblasts have increased enzyme activity through complex I

Enzyme activity of complex I was increased in RTS osteoblasts. Enzyme activity of complexes I and III, complex II, complexes II and III, complex V, and citrate synthase showed no significant difference between Family and RTS osteoblasts, leaving complex I as the only component of the electron transport chain with upregulated activity. n=3 biological replicates; error bars represent \pm SEM; statistical significance was determined using one-way ANOVA following by Student's t test (Tukey's multiple comparison test); *p< 0.05.

3.4 Characterization of Oxidative Phosphorylation in RTS Osteoblasts

Seahorse assays are a robust and sensitive methodology to measure changes in oxidative phosphorylation and glycolysis via measurements of oxygen consumption rate (OCR) and extracellular acidification rate (ECAR) (Zhang and Zhang, 2019). Therefore, we applied Seahorse metabolic assays to explore oxidative phosphorylation and cellular metabolic flux of RTS osteoblasts. We found that RTS osteoblasts had increased OCR compared to Family cells (Figure 23). The basal respiration of RTS osteoblasts was increased significantly as compared to Family osteoblasts, indicating that RTS osteoblasts have an increased ability to produce ATP. In comparison with Family osteoblasts, RTS osteoblasts also had significantly increased proton leak under normal culture conditions. This indicated an increased ability to create the proton gradient across the mitochondrial inner matrix that is essential for ATP synthase activity. Indeed, RTS osteoblasts specifically increased all ATP linked respiration and maximal respiration. These findings led us to conclude that RTS osteoblasts produce significantly more ATP via oxidative phosphorylation.

RTS osteoblasts also retained significantly more spare respiratory capacity through increased activity in complex I. In contrast, both RTS and Family osteoblasts had similar non-mitochondrial respiration (Figure 24), suggesting that mitochondria associated oxidative phosphorylation was the only cause of increased oxygen consumption rate. We validated our findings in distinct RTS osteoblasts with different *RECQL4* mutations to test if the increased oxygen consumption rate was universal. We observed a similar trend in increases of OCR (Figure 23), maximal respiration, and spare respiratory capacity but no difference in non-mitochondrial respiration in RTS osteoblasts (Figure 25).

Osteoblasts are shown to be largely reliant on glycolysis for ATP production during bone morphogenesis (Lee et al., 2017). Therefore, we next compared extracellular acidification rates (ECAR) to assay for glycolysis function in RTS osteoblasts. We found that RTS osteoblasts shifted away from glycolysis toward oxidative phosphorylation as a means of ATP production (Figure 26). Also, RTS osteoblasts had significantly decreased maximal ECAR (Figure 26). Consistent with the OCR result, this finding indicated that RTS osteoblasts had little reliance on glycolytic metabolism. Taken together, these OCR and ECAR data demonstrated that RTS osteoblasts had increased ATP production, specifically through oxidative phosphorylation and had decreased glycolysis compared to Family osteoblasts.

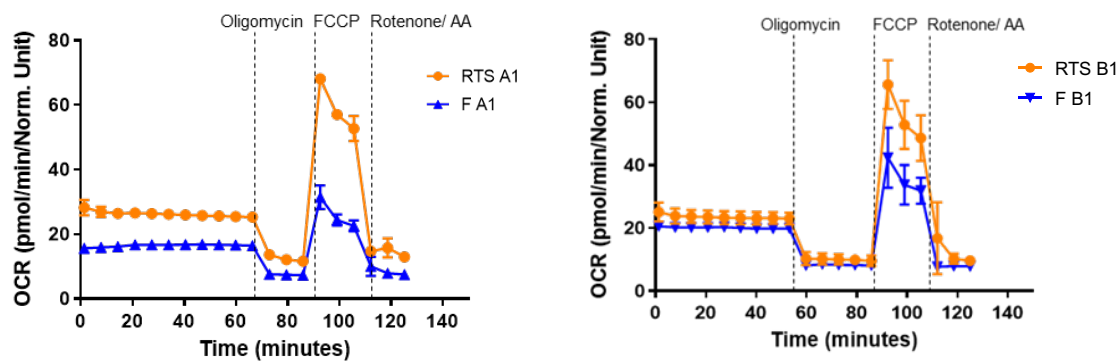


Figure 24: Seahorse assays show increased oxygen consumption rate in RTS Patients

Seahorse assays indicated increased oxygen consumption rate, which is a measure of oxidative phosphorylation, in RTS osteoblasts. n=3 biological replicates; error bars represent \pm SEM.

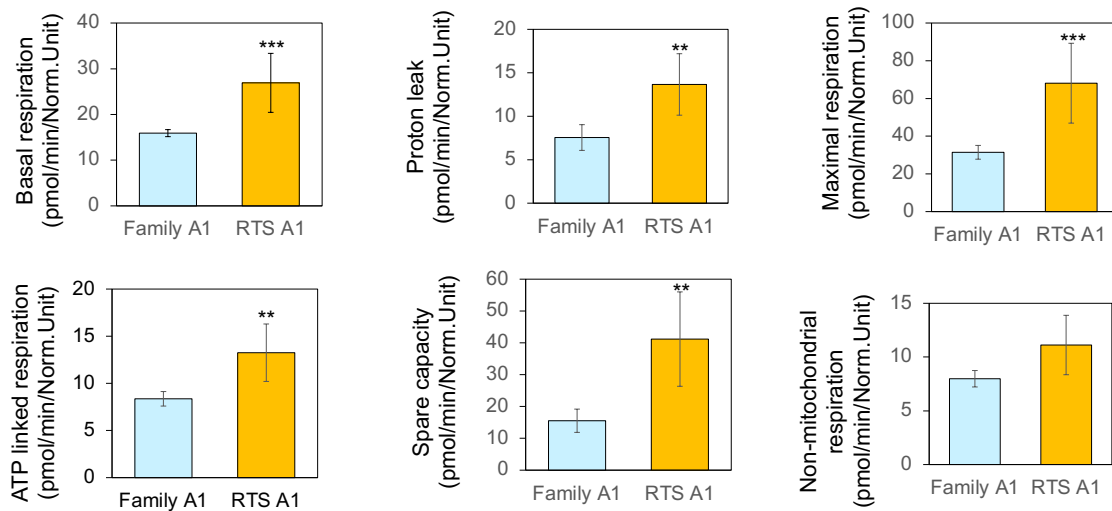


Figure 25: Seahorse assays revealed increase in mitochondrial respiration in RTS Patient A

Individual calculations of basal respiration, proton leak, ATP-linked respiration, maximal respiration, and spare capacity were significantly upregulated in RTS osteoblasts as measured by Seahorse assay. Non-mitochondrial respiration, which is not attributed to oxidative phosphorylation, showed no significant difference between Family and RTS osteoblasts. n=3 biological replicates; error bars represent \pm SEM; statistical significance is determined using one-way ANOVA followed by Student's t test (Tukey's multiple comparison test); **p< 0.01; ***p< 0.001

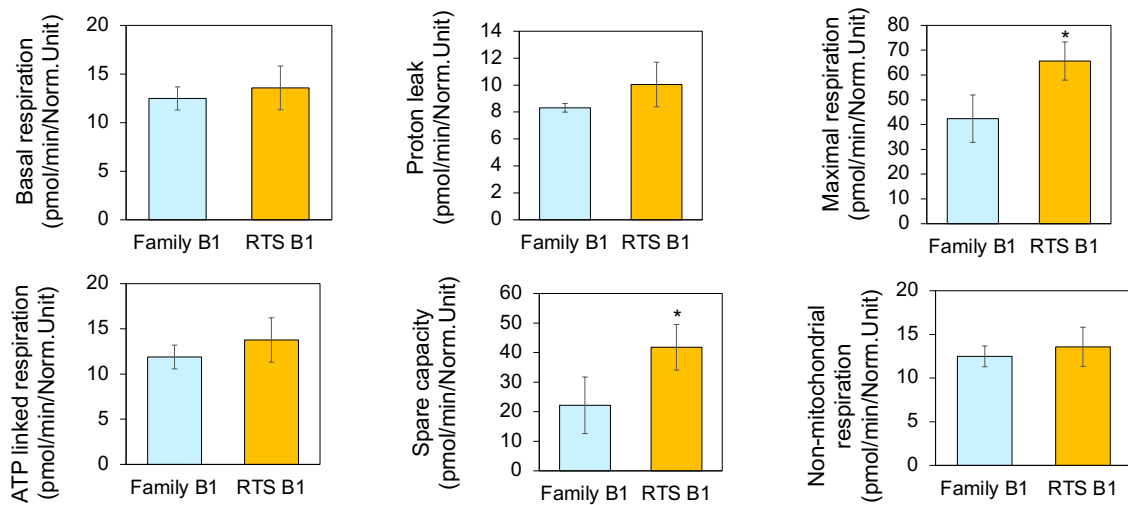


Figure 26: Seahorse assays revealed increase in mitochondrial respiration in RTS Patient B

Individual calculations of maximal respiration, and spare capacity were significantly upregulated in independent RTS osteoblasts as measured by Seahorse assay.

Basal respiration, proton leak, and ATP-linked respiration trend towards increased rates, consistent with set A. Non-mitochondrial respiration, which is not attributed to oxidative phosphorylation, was not significantly different between Family and RTS osteoblasts. n=3 biological replicates; error bars represent \pm SEM; statistical significance is determined using one-way ANOVA following by Student's t test (Tukey's multiple comparison test); *p< 0.05.

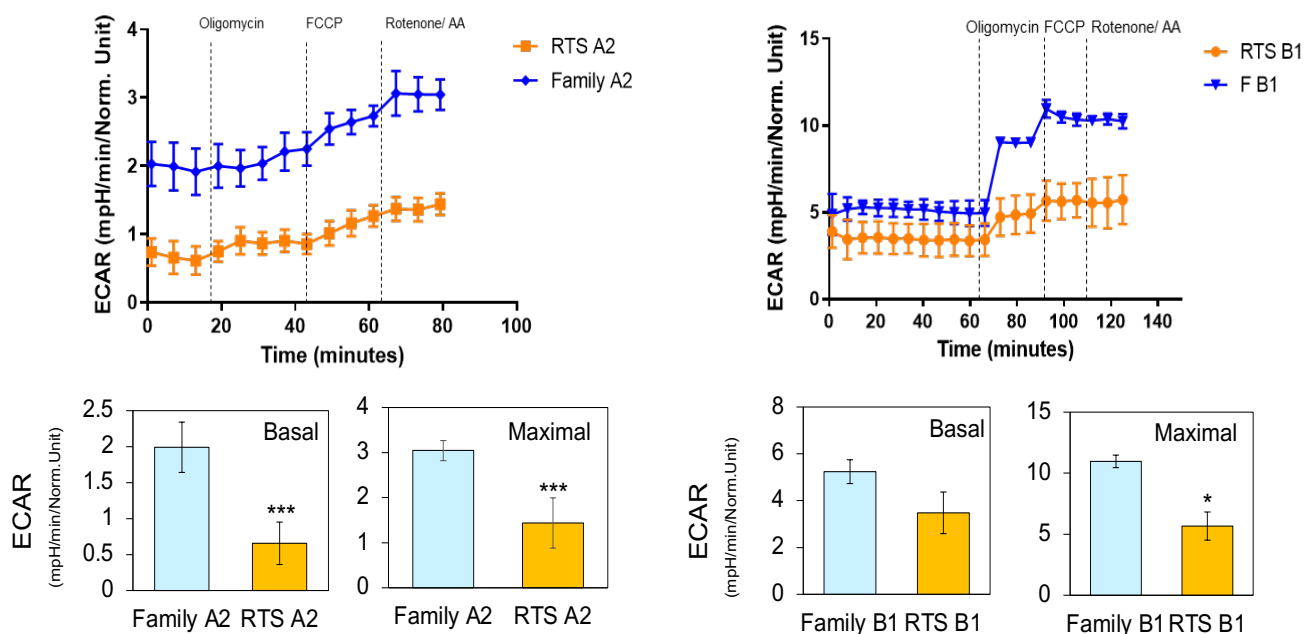


Figure 27: Seahorse assays demonstrate less reliance on glycolysis in RTS Patients than Family osteoblasts

Seahorse assays showed decreased extracellular acidification rate in RTS osteoblasts, which is a measure of glycolysis. Individual calculations of basal extracellular acidification rate and maximal acidification rate were decreased significantly in RTS A osteoblasts, indicating that RTS osteoblasts rely on oxidative phosphorylation for ATP production. Maximal acidification rate was decreased significantly in RTS B osteoblasts indicating RTS osteoblasts rely on oxidative phosphorylation for ATP production. Basal respiration was not different significantly, but trends toward decreased extracellular acidification rate in RTS osteoblasts. n=3 biological replicates; error bars represent \pm SEM; statistical significance was determined using one-way ANOVA followed by Student's t test (Tukey's multiple comparison test); * $p < 0.05$.

Chapter Four: Targeting Complex I to Reverse Increased Reliance on Oxidative Phosphorylation in Osteoblasts

4.1 Introduction

In this study, we utilized non-biased transcriptome analyses of Type II RTS iPSC-derived osteoblasts, determined the pathological pathways involved in Type II RTS-associated bone malignancies, and then set out to explore a treatment strategy for Type II RTS patients with osteosarcoma.

Oxidative phosphorylation inhibitor IACS-070759 shows a potential antineoplastic activity by binding to and inhibiting mitochondrial respiratory complex I of the electron transport chain, thereby selectively inhibiting cells relying on complex I function (Molina et al., 2018; Vangapandu et al., 2018). IACS-070759 robustly suppresses proliferation and induced cell death in tumor cells reliant on oxidative phosphorylation. It is currently being evaluated in phase I clinical trials in acute myeloid leukemia (AML) and solid tumors (Molina et al., 2018). As hyperactivated mitochondrial complex I function in RTS osteoblasts meets their increased demands for energy, we tested whether mitochondrial complex I is a cancer vulnerability for RTS osteoblasts, and whether IACS-070759 is capable of serving as a therapeutic drug for RTS patients with bone malignancies.

4.2 Inhibition of Oxidative Phosphorylation via Complex I

First, we examined the effect of IACS-010759 on ATP production via oxidative phosphorylation in RTS osteoblasts using the Seahorse assay. RTS osteoblasts showed decreased OCR, indicative of decreased oxidative phosphorylation upon IACS-010759 treatment (Figure 27). RTS osteoblasts had significantly decreased maximal respiration, ATP-linked respiration, and spare capacity to produce ATP (Figure 27). Similar results were validated using another RTS osteoblast line which showed decreased oxidative phosphorylation (Figure 27), with significantly reduced maximal respiration, ATP-linked respiration, and spare respiratory capacity (Figure 27). This indicated inhibition of complex I via specific inhibition by IACS-010759.

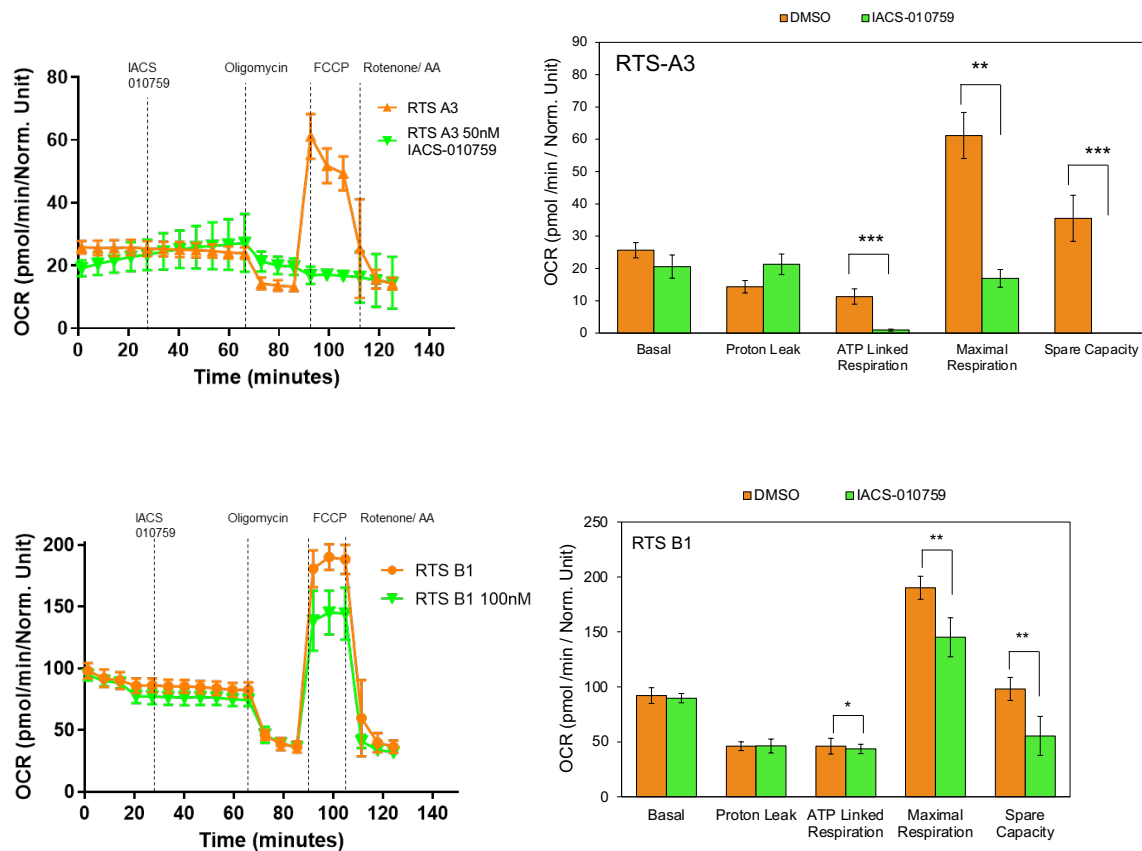


Figure 28: Treatment with Complex I Inhibitor IACS-010759 decreases oxidative phosphorylation in RTS Patients

Oxygen consumption rate showed reduced ATP lined respiration, maximal respiration, and spare capacity in RTS osteoblasts after 100 nM IACS-010759 treatment. Time course of the Seahorse experiment demonstrated that differences in OCR were most apparent after addition of FCCP, which measure the maximum potential of ATP production through the electron transport chain. n=3 biological replicates; error bars represent \pm SEM; statistical significance was determined using one-way ANOVA followed by Student's t test (Tukey's multiple

IACS-010759 is common to RTS treated osteoblasts, irrespective of the specific *RECQL4* mutation. Therefore, we asked if IACS inhibition selectively suppressed RTS osteoblast growth, as compared to Family controls. Cell proliferation assays demonstrated that IACS-010759 had a limited effect on Family osteoblast cell proliferation but strongly inhibited RTS osteoblast cell growth (Figure 28). Overall, these data demonstrated that oxidative phosphorylation in RTS osteoblasts was upregulated specifically through complex I. Furthermore, we showed that it was possible to directly target that upregulation in complex I activity by inhibition with IACS-010759 and this inhibition was specific for RTS osteoblasts, sparing healthy Family osteoblasts. These results not only demonstrated that the inhibition of complex I was sufficient to abrogate upregulated levels of maximal respiration in RTS osteoblasts, but also emphasized the specificity of IACS-010759 to treat the increased oxidative phosphorylation characteristic of RTS osteoblasts.

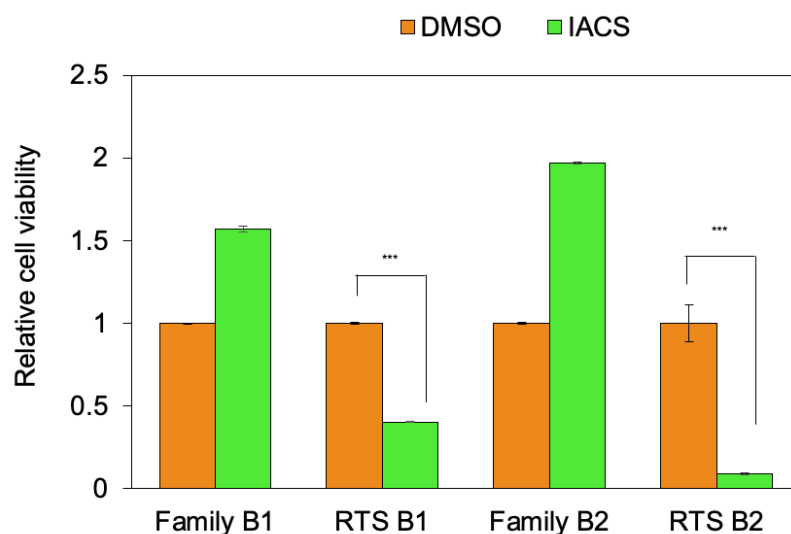


Figure 29: IACS-010759 specifically inhibits RTS Patient osteoblasts

IACS-010759 selectively inhibited RTS osteoblast proliferation. Cell proliferation assays after treatment with 100 nM IACS-010759, a specific complex I inhibitor, showed growth inhibition of RTS osteoblasts but little effect on Family osteoblasts. n=3 biological replicates; error bars represent \pm SEM; statistical significance was determined using one-way ANOVA followed by Student's t test (Tukey's multiple comparison test); ***p< 0.001.

4.3 Transcriptional Changes After Complex I Inhibition

We next examined the transcriptional changes in RTS osteoblasts upon IACS-010759 treatment in order to shed light on the effect of IACS-010759 in halting RTS osteoblast proliferation. A scatter plot gene expression comparison between IACS-010759 and DMSO treated RTS osteoblasts demonstrated upregulations of long non-coding RNA H19 and numerous ribosome proteins, including RSP27, RPL11, RPL32, RPL35A, and RPL11 (Figure 29). Interestingly, H19 was found to function as a tumor suppressor to promote osteogenesis and inhibit osteosarcomagenesis in LFS osteoblasts and osteosarcoma (Lee et al., 2015). This provides a potential pharmacological mechanism to explain IACS-010759-mediated growth suppression effects. It is important to note that ribosome protein gene mutations are commonly found in osteosarcoma-prone Diamond-Blackfan Anemia (DBA) patients (Lin et al., 2017b). Upregulation of ribosomal proteins and ribosome biogenesis by IACS-010759 could reverse RTS associated oncogenic properties by promoting translation of tumor suppressors and osteoblast differentiation programming. A KEGG pathway analysis of significantly upregulated genes IACS-010759-treated RTS osteoblasts further validated the importance of the upregulation of the ribosome pathway (Figure 30).

In contrast, the downregulation of cell cycle process (e.g., EPGN, EREG, GPSM2, etc.) and MAP kinase pathway (STK39, HGF, GHR, etc.) was observed in IACS-010759-treated RTS osteoblasts (Figure 30). Enrichr-based GO_BP analysis of differentially expressed genes (>1.5 fold changes) between DMSO and IACS-010759-treated RTS osteoblasts demonstrated an increase in protein targeting, T cell mediated cytotoxicity, and protein translation; whereas there was a decrease in cell cycle processes and MAP kinase activity in IACS-010759-treated RTS osteoblasts (Figure 30). It is important to note that the MAP kinase pathway is shown to upregulate cell lifespan and proliferation of RTS fibroblasts (Davis et al., 2013). In summary, our well-ordered transcriptome analyses provided the

potential pharmacological mechanisms of IACS- 010759-mediated cell growth inhibition in RTS osteoblasts.

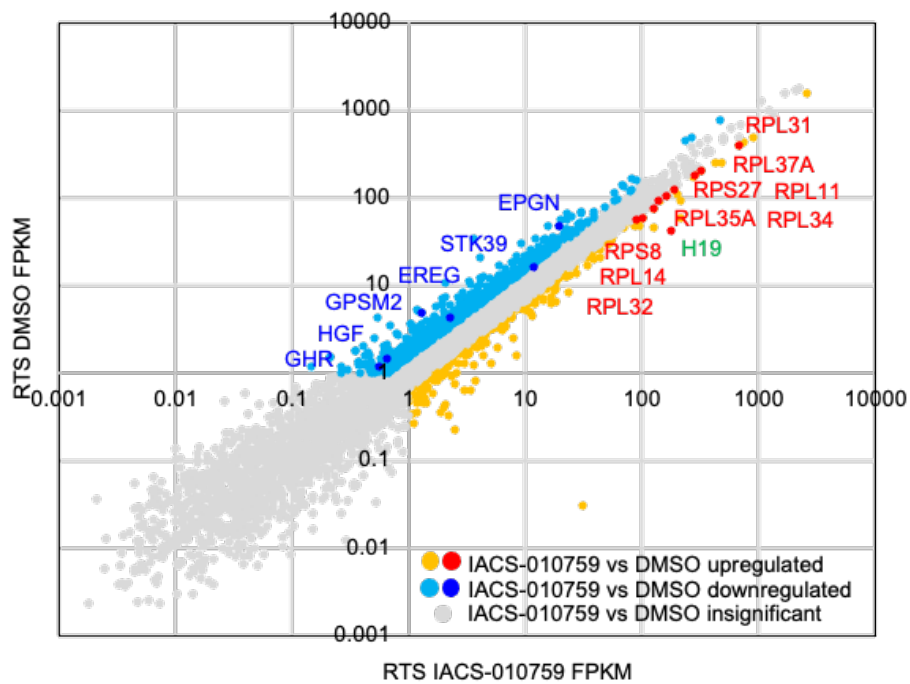


Figure 30: Transcriptional changes after IACS-010759 implicate important osteosarcoma-related genes

Scatter plot indicated the marked difference of transcripts between DMSO and 100 nM IACS-010759-treated RTS osteoblasts. H19 and numerous ribosomal protein genes were upregulated but MAP kinase pathway and cell cycle related genes were downregulated upon IACS-010759 treatment.

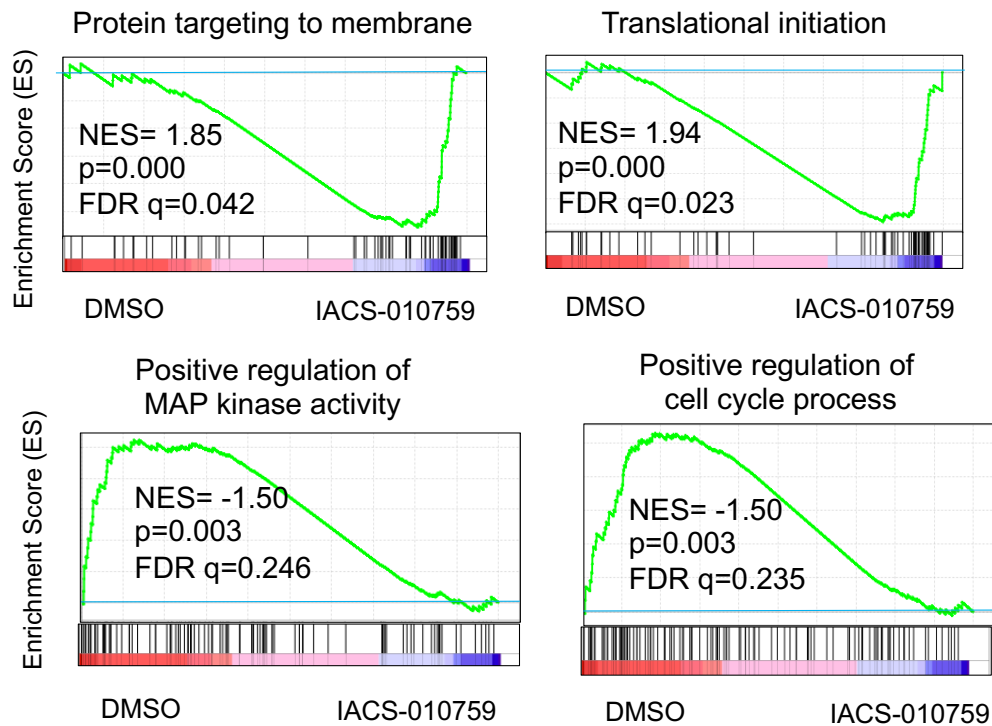


Figure 31: IACS-010759 causes transcriptional changes that promote healthy cellular function

Representative IACS-010759-influenced GO_BP, including protein targeting to membrane, translational initiation, positive regulation of MAP kinase activity, and positive regulation of cell cycle processes.

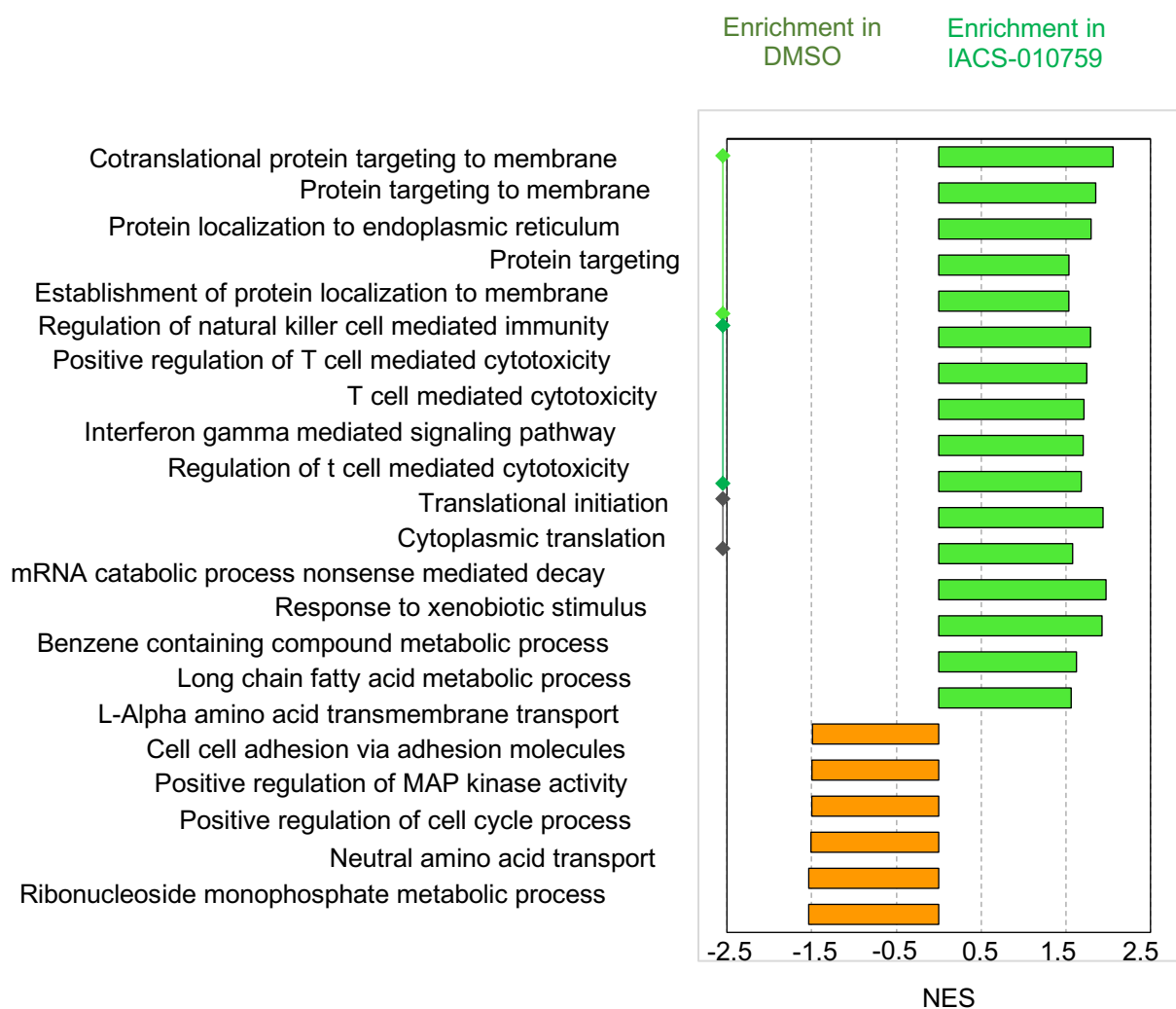


Figure 32: IACS-010759 causes transcriptional changes that indicate reversal of tumor promoting pathways associated with RTS osteoblasts

GO_BP analysis indicated dysregulated pathways in RTS osteoblasts upon IACS-010759 treatment. IACS-010759 activated protein targeting, T cell mediated toxicity, and protein translation related biological processes, but inhibited MAP kinase and cell cycle processes in RTS osteoblasts.

Chapter Five: Discussion

5.1 Modeling RTS associated bone malignancies using iPSC-derived osteoblasts

In this study, we established RTS iPSC disease models from RTS patients with compound heterozygous *RECQL4* mutations and their parental controls with a heterozygous *RECQL4* mutation. Thus far, studies of *RECQL4* mutations in murine models have not been shown to recapitulate the changes that promote osteosarcoma. Other models of sporadic osteosarcoma focus on fully developed tumors, which may be preselected for chemoresistance.

The advantages of this disease platform lie in the genetic specificity with which we dissect the impact of *RECQL4* mutation on RTS associated pathological consequences, such as defective osteogenesis and osteosarcomagenesis. Family-derived iPSCs share 50% genetic fidelity to their child, who are RTS patients. By utilizing these paired Family/RTS sets, we can specifically interrogate the question of *RECQL4* contribution to the processes that promote osteosarcomagenesis. In addition to the resources we established in MSCs and osteoblasts, RTS and Family iPSCs are capable of being differentiated into other germ layers. Differentiation of iPSCs to other tissues might allow for investigation of the role of *RECQL4* in other aspects of Rothmund-Thomson Syndrome, indicating their potential use to study other disease features of RTS including cataracts, poikiloderma, and abnormal dentition. Although our model does not recapitulate an osteosarcoma tumor, osteoblasts differentiated from RTS iPSCs provide a model of osteosarcomagenesis that is complementary to other models of osteosarcoma.

The iPSC-derived model of osteosarcomagenesis, and associated controls, provide an ideal model to test potential new therapeutics. In this work, we utilized the disease in a dish platform to test the efficacy of the complex I inhibitor, IACS-010759. In a similar way, we provide an ideal model for use in testing other potential therapeutics and show benefits in using the iPSC derived model for drug testing in general.

5.2 Increased ATP Production via Oxidative Phosphorylation

Previous studies found that increased rates of metabolic function caused the rate of bone formation to increase (Guntur et al., 2014). This is consistent with osteosarcoma, as it is a tumor of uncontrolled bone formation (Lindsey et al., 2017). In our study, we examined the dysregulated pathways using multiple gene set categories, including GO_BP, KEGG pathway, Reactome, oncogenic signature, and TFT. These system analyses pointed to the same culprit of increased metabolism: oxidative phosphorylation. Recent reports of other cancer types, such as leukemias and lymphomas, as well as for solid cancers like pancreatic ductal adenocarcinoma, oxidative phosphorylation subtype melanoma, and endometrial carcinoma, have established the importance of increased oxidative phosphorylation in tumor formation and progression (Ashton et al., 2018). Here, we demonstrated increased transcription of oxidative phosphorylation associated genes in RTS osteoblasts. For example, ATP synthesis coupled electron transport, electron transport chain, and the TCA cycle (Figure 16) were all indicative of reliance on oxidative phosphorylation. Electron transport pathways detail the upregulation of genes that are vital for the creation of the electrochemical gradient necessary for proton pumping through the inner mitochondrial membrane matrix that allows for conversion of ADP to ATP. In order to feed the electron transport chain with NADH, which is reduced to free H^+ in the first step of creating the electrochemical gradient, the TCA cycle may produce additional NADH. It would be interesting to explore the amount of NADH and other TCA cycle substrates, like FADH, that are produced in the RTS osteoblasts and other cell types, which could be derived from RTS iPSCs and are relevant to RTS pathology.

The maximal amount of ATP production in bone cells is consistent with increased osteoblast energy, necessary for tumor formation. It is important to note that in our study, increased ATP production did not result in upregulation in differentiation in the RTS osteoblast; in contrast, differentiation was downregulated in RTS cells, suggesting that

metabolic ATP production is not an osteogenic promoter. Additionally, increased production of NAD⁺ through complex I has been shown to immortalize neural tumor cells (Bonnay et al., 2020). Here, we showed this exact phenomenon in osteoblasts. The increased activity of complex I was a direct measure of reduction of NADH to NAD⁺ (Figure 22). Furthermore, it was shown that an increase of oxidative phosphorylation was essential for cell immortalization. Bonnay and colleagues speculated that NAD⁺, which is a PARP co-factor could play a role in genome stability and cell fate (Bonnay et al., 2020). Therefore, we would underscore the need for more exploration of these interactions, especially given that RECQL4 interacts with PARP-1 in the nucleus (Woo et al., 2006).

Bonnay and colleagues, also showed that this switch to oxidative phosphorylation was important for tumors at stages beyond initiation (Bonnay et al., 2020). Our study, comparing osteosarcoma tumors and healthy osteoblasts/ bone (Figure 21), showed that, at a transcriptional level, oxidative phosphorylation was upregulated in osteosarcoma tumors. This indicates that our findings with regards to osteosarcomagenesis may be important for osteosarcoma tumor metabolism, in general. It also underscores the appropriateness of RTS as a model of sporadic osteosarcoma (Lu et al., 2020).

It has been reported that an increase in RECQL4 protein leads to an accumulation of R-loops, thereby decreasing oxidative phosphorylation in HEK293 cells with a RECQL4 mutation lacking the p32 binding domain (Chang et al., 2020). In our study, RECQL4 mutations led to decreased mtDNA replication due to increased R-loop intermediates. While it will be necessary to undertake further studies to understand the role of *RECQL4* in RTS associated osteosarcoma, we provide, here, the basis for exploring the role of RECQL4 in mitochondrial processes. Taken together with the aforementioned studies, an exploration of RECQL4 in mitochondrial DNA replication in RTS derived osteoblasts is an important avenue for future study. Given these two findings and our own conclusions of increased oxidative phosphorylation, one might speculate that the mutant *RECQL4* found in RTS patient cells results in stalled R loop resolution, which is needed for translation of mtDNA. It

is of particular relevance to this study as seven of the 44 genes necessary to encode complex I are encoded in mitochondrial DNA (Vartak et al., 2015).

5.3 Targeting Complex I Upregulation with IACS-010759

We sought to explore if inhibition of mitochondrial complex I can be a therapeutic treatment for RTS osteosarcoma based on our thorough transcriptional and biochemical studies of oxidative phosphorylation in RTS osteoblasts. IACS-010759 is a complex I inhibitor specific for the ND1 subunit, blocking the intermembrane transport of H⁺ (Molina et al., 2018). It is currently in phase I clinical trial for the treatment of relapsed lymphoma and metastatic solid tumor cancers. In our study, we demonstrated its efficacy in specifically inhibiting oxidative phosphorylation and cell proliferation capability of RTS osteoblasts (Figure 28). We performed RNA-seq to analyze RTS osteoblasts' transcription upon IACS-010759 treatment in order to better understand the effects of IACS-010759 on gene expression in RTS osteoblasts. It is interesting that IACS-010759 upregulates the expression of ribosomal protein genes such as *RSP27*, *RPL11*, *RPL32*, *RPL35A*, and *RPL11*, which are known to be mutated in osteosarcoma-prone Diamond-Blackfan Anemia patients (Chae et al., 2014; Choesmel et al., 2008; Lin et al., 2017b). It is possible that the homeostasis of ribosomal biogenesis is essential to maintain the survival of RTS osteoblasts. Furthermore, H19 functioning as an osteogenic promoter and tumor suppressor was upregulated upon IACS-010759 treatment. This implies that IACS-010759 may indicate a shift from a tumorigenic, undifferentiated profile back towards normal osteoblast differentiation. Downregulation of the MAPK pathway and cell cycle were observed, which has been reported to increase cell life span and proliferation in RTS fibroblasts (Tivey et al., 2013).

5.4 Implications of this Study

We have shown that abnormal upregulation of oxidative phosphorylation was the dominant source of ATP necessary for osteosarcomagenesis in Type II RTS patients. Inhibition of complex I was sufficient to abrogate the increased oxidative phosphorylation and cell proliferation of Type II RTS osteoblasts. Taken together, our Type II RTS iPSC disease platform and targeting of complex I provided a therapeutic target for osteosarcoma treatment, addressing a great need for Type II RTS osteosarcoma patients, and sporadic osteosarcoma patients, as a whole.

In summary, our study utilized a RTS iPSC disease platform to dissect the pathological mechanisms involved in RTS associated bone malignancies. Transcriptome analysis revealed upregulation of genes involved in oxidative phosphorylation, especially mitochondrial complex I. Seahorse assays validated upregulation of oxidative phosphorylation in RTS osteoblasts. The upregulation was targetable in a specific and clinically relevant manner, using IACS-010759. This study demonstrated a targetable molecular pathogenesis of osteosarcoma and a clinically relevant treatment option for RTS patients.

Chapter Six: Methods

6.1 Culture of RTS and Family Fibroblasts

Fibroblasts were obtained from RTS patients and their biological parents via a punch biopsy of the arm (IRB #H-7207, Baylor College of Medicine). The primary fibroblasts were cultured in fibroblasts culture media (DMEM/F-12 supplemented with 10% FBS, 100 U/ml Penicillin/Streptomycin (P/S), and 1% GlutaMAX supplement). Fibroblasts were maintained in a CO₂ incubator (37°C, 5% CO₂, and 95% humidity). Fibroblasts used for cellular reprogramming were cultured less than 10 passages.

6.2 Reprogramming fibroblasts to iPSCs

Confluent fibroblasts in healthy condition were transduced with Sendai virus containing the Yamanaka four factors OCT4, SOX2, KLF4, and MYC using the CytoTune - iPS 2.0 Sendai Reprogramming Kit (Invitrogen). Cells were cultured in transduction media (4 ml reprogramming fibroblast media and 80µl each of OCT4, SOX2, KLF4, and MYC) for 24 hr. After, media were changed to reprogramming culture media (500ml DMEM, 10 ml FBS, 5ml non-essential amino acid solution (100X), and 3.5µl β-mercaptoethanol). Cells were cultured in this media for five days, then the media were changed to fresh reprogramming culture media. On Day 6, mouse embryonic fibroblasts (MEF) were seeded from frozen cells and cultured in DMEM, supplemented with 10% FBS and 1x P/S for one day. On day 7, media were removed from MEFs and transduced cells were seeded on MEFs in growth media after being dissociated using Accutase cell detachment solution for approximately 5 min at 37°C. On day 8, the media were changed to iPSC media (Knockout DMEM, 10% Knockout serum, 10ng/µL BFGF, 10ng/µL PDGFAB, 1% non-essential amino acids, and 0.000007% β mercaptoethanol). Cells were cultured for 28 days and the media were changed every other day. At day 28, individual iPSC clones were picked using a P200 pipette tip, then subcultured on fresh MEFs for 15 days. iPSCs were then dissociated with Accutase cell detachment solution and passaged onto 6-well plates coated with Matrigel for

30 min in iPSC media. After one day, the media were changed to BREW media with XF supplement. Clones that successfully formed colonies were passaged 10 times in the same manner described above to ensure removal of the Sendai virus.

6.3 Differentiating Mesenchymal Stem Cells

Cells were differentiated based on the protocol described (Lian et al., 2007). Passage 10 or later iPSCs that were verified by RT-PCR and immunofluorescent staining were plated on MEFs for two weeks until 80% confluent. At this point, cells were dissociated using Accutase, then centrifuged at 1,100 rpm for 5 min. Cells were resuspended in MSC induction media (DMEM with 10% Knockout Serum, 20ng/mL BFGF, 10ng/ μ L SB431542, 3.5 μ L β -mecaptoethanol, and 20ng/ mL), then plated at 1:3 dilution on plates coated with gelatin for 5 min. Media were changed every day for 14 days, then changed every two to three days for a total of two times per week, leaving about 500 μ L in the dish, each time. After cell morphology changed from clusters to elongated/ spindle-like, cells were split. Cells were dissociated with trypsin for 3-5 min, resuspended in DMEM, then centrifuged, as before. Cells then were incubated for several days to proliferate. Once cells reached 80% confluency, they were split again to 6-well plates for characterization and propagated in MSC media (DMEM with 10% FBS, 1% L-glutamine, and 1% Penicillin and Streptomycin).

6.4 Differentiating Osteoblasts

Osteogenic differentiation was carried out based on previously described protocols (Barberi et al., 2005; Lee et al., 2015). MSCs were split then passaged at a density of 3×10^5 cells/per well of a 6 -well dish in osteoblast differentiation media (α MEM supplemented with 10mM β glycerol phosphate, 2% Penicillin/ Streptomycin, 200 μ M ascorbic acid, and 10%

FBS). The media were changed every three days for 24 days, at which point cells were stained with Alazarin Red to verify calcium production.

6.5 Sendai Virus PCR

PCR was performed using isolated genomic DNA from iPSCs in order to verify Sendai virus removal. It was prepared using the Invitrogen Easy DNA Kit, according to the manufacturer's protocol. A 350µl solution A was added to a pellet of iPSCs from one 10cm dish in order to isolate genomic DNA. Cells were vortexed for 15 sec, then incubated at 65°C for 10 min (in an Eppendorf heat block). A 150µL solution B was added to each tube, then vortexed vigorously for approximately 20 sec until precipitate moved freely in the tube. Then, 500µl chloroform was added to each tube and it was vortexed for about 15 sec until the mixture was homogenous. Next, each tube was centrifuged at 1,200 x g for 20 min at 4°C. The supernatant was aspirated and discarded carefully to not disturb the DNA pellet. The pellet was washed once in 75% ethanol, then centrifuged at 1,200 x g for 5 min. The ethanol was removed, then the isolated genomic DNA was resuspended in 100µl of water.

PCR to detect Sendai virus removal was performed using the primers and following manufacturer's instructions. PCR was performed using the OneTaq master mix (New England Biosciences) along with 1µl forward primer (100µM), 1µl reverse primer (100µM), 4.2 µl water, 10 µl OneTaq, and 3.8µl genomic DNA per reaction. The reaction was carried out as follows: initially denatured at 94°C for 30 sec, 30 cycles of denaturing (94°C, 30 sec), annealing (52°C, 30 sec), elongation (68°C, 1 min), elongation at 68°C for 5 min, and then held at 4°C. PCR products were resolved in a 1% agarose gel.

6.6 qRT-PCR

Cells were scraped off a 10cm dish, then resuspended in 1ml 1xDPBS, and centrifuged at 21,000xg for 1 min. Cells were then resuspended in 1ml of Trizol (Life

Technologies) and incubated at room temperature for 5 min. Next, 200 μ L of chloroform were added, inverted to mix, and incubated for 10 min. The mixture was centrifuged at 1,200 x g for 20 min at 4°C. The aqueous phase was aspirated into a new tube, where RNA was precipitated using 500 μ l of isopropyl alcohol. The mixture was incubated for 10 min at room temperature and then centrifuged again. After washing with 1ml of 75% ethanol, the RNA pellet was resuspended in 40 μ l of DNase/RNase-free water. A 4 μ g of RNA was used to make cDNA, according to the reverse transcriptase protocol using iScript Reverse Transcription Supermix (BioRad). A qPCR was then performed using primers for OCT4, NANOG, SOX2, and GAPDH (Table 3), according to the protocol using iQ SYBR Green Supermix (Biorad) on a CFX96 machine (Bio-Rad). The RT-PCR reaction was performed as follows: 50 °C for 10 min, 95 °C for 5 min, 40 cycles of 95 °C for 10 sec and 60 °C for 30 sec, and 95 °C for 10 min. Results were calculated using the $\Delta\Delta$ CT method and were normalized to GAPDH expression and are displayed relative to hESC H1.

Table 3: Primers

Primers	Target	Forward/reverse primer(5'-3')
PCR/Sequencing	<i>RECQL4</i> Exons 11–12	CAGATTCGGGCAGCCCAGGTAC ACCCACCTGGTCTGTGTCCCTG
Pluripotency Marker (qPCR)	<i>NANOG</i>	TTTGTGGGCCTGAAGAAACT AGGGCTGTCCTGAATAAGCAG
Pluripotency Marker (qPCR)	<i>Oct-4</i>	AACCTGGAGTTTGTGCCAGGGTTT TGAACCTCACCTTCCCTCCAACCA AGAAGAGGAGAGAGAAAGAAAGGG AGAGA
Pluripotency Marker (qPCR)	<i>SOX2</i>	GAGAGAGGCCAACTGGAATCAGGA TCAA
Pluripotency Marker (qPCR)	<i>DPPA4</i>	GACCTCCACAGAGAAGTCGAG TGCCTTTTCTTAGGGCAGAG
Pluripotency Marker (qPCR)	<i>REX1</i>	GCCTTATGTGATGGCTATGTGT ACCCCTTATGACGCATTCTATGT
Pluripotency Marker (qPCR)	<i>TERT</i>	TGAAAGCCAAGAACGCAGGGATG TGTCGAGTCAGCTTGAGCAGGAAT G
Housekeeping Genes (qPCR)	<i>GAPDH</i>	CCACTCCTCCACCTTTGAC ACCCTGTTGCTGTAGCCA
Sendai Virus Removal (RT-PCR)	<i>SeV</i>	GGATCACTAGGTGATATCGAGC ACCAGACAAGAGTTTAAGAGATATG TATC
Pluripotency Marker (RT-PCR)	<i>KOS</i>	ATGCACCGCTACGACGTGAGCGC ACCTTGACAATCCTGATGTGG
Pluripotency Marker (RT-PCR)	<i>KLF4</i>	TTCCTGCATGCCAGAGGAGCCC AATGTATCGAAGGTGCTCAA
Pluripotency Marker (qPCR)	<i>MYC</i>	TAACTGACTAGCAGGCTTGTGCG TCCACATACAGTCCTGGATGATGAT G

6.7 Immunofluorescent Staining

iPSCs and iPSC-derived MSCs were fixed with 4% paraformaldehyde (Affymatrix) for 8 min. Cells were then washed with 500 μ l 1XDPBS twice, followed by blocking with 1XDPBS with 10% donkey serum (Jackson ImmunoResearch Labs) and 0.3% Triton X-100 (Sigma) for 1 hr. Then, cells were incubated with primary antibody NANOG (R and D Systems Cat# AF1997 RRID: AB_355097; 1:1000), TRA-1-81 (R and D Systems Cat# FAB3195A RRID:AB_663789; 1:500), SSEA4 (R and D Systems FA1435P-025; 1:600), CD73 (Thermo-Fisher, cat # 41-0200; 1:200), CD44 (Thermo-Fisher, cat # MA5-13890; 1:200), and CD105 antibody (R & D Systems, cat # MAB10971; 1:500) at 4 °C overnight with gentle rocking. Next, cells were washed twice and stained with secondary antibodies for 1 hr at room temperature in the dark. This was followed by 3 times 1xDPBS washes, then counterstained with DAPI (1:5000), then stored in 1XDPBS for imaging.

6.8 Alkaline Phosphatase Staining

iPSCs were grown to 80% confluence in 12-well plates, then fixed and stained using the Alkaline Phosphatase Staining Kit II (Stemgent), according to manufacturer's instructions.

6.9 Alizarin Red Staining

One gram of alizarin red was dissolved in 45ml deionized water. The pH was adjusted to 4.2, then deionized water was added up to 50ml. Fixed osteoblasts were rinsed 2 times with water, then stained for 30 min at room temperature. After staining, cells were washed twice with water and then ARS staining images were taken.

6.10 Karyotyping

Karyotyping was performed at either the Cancer Cytogenetics Core Laboratory at Texas Children's Hospital or at the Cytogenetics and Cell Authentication Core Facility at The University of Texas MD Anderson Cancer Center. iPSCs were harvested and G-banded using standard protocols. Clonal chromosomal changes identified by G-banding were described according to an International System for Human Cytogenetic Nomenclature ISCN. Twenty metaphase chromosome spreads at 400 band resolution were analyzed.

6.11 Teratoma

RTS and Family iPSCs were grown in 10 cm dishes to 80% confluence. Cells were dissociated from the dish, then resuspended in phenol red-free Matrigel (Corning cat#354262). Immunodeficient NOD SCID mice (Charles River Laboratories) were injected subcutaneously with 2×10^7 cells in each flank and observed for palpable teratoma formation. After approximately six weeks, teratomas were excised and then fixed in 10% formalin (Sigma). Histology was performed by Histowiz (Brooklyn, New York).

6.12 RNAseq

Cells were isolated for RNA-seq at three different time points: MSC, pre-osteoblasts (Day 15), and mature osteoblasts (Day 24). RNA samples were prepared by Trizol (Life Technologies), as described above. RNA sequencing was performed by BGI Genomics and UTHealth Cancer Genomics Core. DESeq2 analysis was performed, as described (Love et al., 2014), to normalize all data. GSEA Analysis (Subramanian et al., 2005) was utilized to identify significant pathways and biological processes between RTS and Family cells at distinct timepoints. Gene sets that were used were GO_BP, KEGG, as well as the MSigDB data sets oncogenic signature, TFT, and Reactome. Significant pathways were determined using a p-value < 0.05 and FDR q-value < 0.25 (Subramanian et al., 2005). Osteosarcoma

data sets (2) and osteoblast and bone data sets (4) were requisitioned from the NCBI Gene Expression Omnibus (accession number GSE36001). These were analyzed using Gene Set Enrichment Analysis using the GO_BP gene set. Network mapping was done using Cytoscape (Shannon et al., 2003) for visualization of the dysregulated GO biological pathways.

6.13 Cell Proliferation Assays

Three thousand osteoblasts per well were plated in a Falcon flat bottom 96-well plate in 200µl osteogenic differentiation medium with or without IACS-010759 (dissolved in DMSO, 50nM or 100nM) for three days. Next, 100µl Presto Blue (ThermoFisher), which had been diluted 1:20 in 1XDPBS, was added to each well and incubated at 37°C for 15 min. Then, the plates were read at 570 nm absorbance.

6.14 Enzymatic Assays

Electron transport chain (ETC) enzyme activity was performed using previously described procedures (Chen et al., 2019). Briefly, RTS and Family osteoblasts from a 10cm dish were dissociated and washed with cold 1XDPBS. Cell pellets were frozen at -80°C until the assay was run. Cells were lysed and the protein concentration was determined by the Bradford assay. ETC enzyme activity was analyzed in triplicate using Tecan Infinite M200, as previously described (Ma et al., 2010). The same protein concentration was used for ETC complexes and citrate synthase (CS) activity measurements in order to normalize activity.

6.15 Seahorse Assays

Seahorse assays were carried out according to the manufacturer's protocol, with the modifications and specifications described, here. Thirty thousand cells (Day 17 osteoblasts) were added to each well of a Seahorse cell culture plate in 200µl osteogenic differentiation

media (ODM), with the exception of a minimum of four blank wells per assay. Cells were incubated at 37°C for three days. The assay plate was prepared by incubating in water overnight, then in calibration media for a minimum of 4 hr before the assay began. Next, 180µL of assay media, prepared with 10mM pyruvate, 2mM glutamine, 25mM glucose, and 4mg/ml BSA, were added to each well. The tissue culture plate then was incubated at 37°C without CO₂ and humidity. Assay chemicals were prepared using the assay media without BSA. When testing IACS 010759, these were added to well A or to assay media as noted and incubated for the indicated duration at 37°C. The assay measurements were at baseline for 18 min (3 cycles of 3-min mix and 3-min measure), complex I inhibitor injection from port A for 30 min (immediate measurement, then 5 cycles of 3-min mix and 3-min measure), then 15µM Oligomycin (port B), 30µM FCCP, and 5µM Rotenone/ Antimycin A, each for 18 min.

Immediately following each assay, cells were fixed by removing assay media, gently washing with 200µl 1XDPBS, then adding 100µl 4% paraformaldehyde for 8 min. After fixation, cells were gently rinsed again twice with 200µl 1XDPBS, then stained immediately with DAPI diluted in 1XDPBS at 1:5000. Cell numbers were counted using a Biotek Lionheart automatic microscope with default settings for TPP 96-well TC flat bottom plates. Nuclei were counted by thresholding for a minimum size of 5µm and a maximum size of 50µm, including edge objects. OCAR and ECAR were calculated using the Wave software, normalized to total cell number.

Bibliography

- (2017). ZFIN Gene: recql4. In ZFIN ID: ZDB-GENE-091112-2 (Eugene, Oregon: University of Oregon), p. Zebrafish Information Network: RECQL4.
- Ajeawung, N.F., Nguyen, T.T.M., Lu, L., Kucharski, T.J., Rousseau, J., Molidperee, S., Atienza, J., Gamache, I., Jin, W., Plon, S.E., et al. (2019). Mutations in ANAPC1, Encoding a Scaffold Subunit of the Anaphase-Promoting Complex, Cause Rothmund-Thomson Syndrome Type 1. *Am J Hum Genet* 105, 625-630.
- Ashton, T.M., McKenna, W.G., Kunz-Schughart, L.A., and Higgins, G.S. (2018). Oxidative Phosphorylation as an Emerging Target in Cancer Therapy. *Clin Cancer Res* 24, 2482-2490.
- Barberi, T., Willis, L.M., Socci, N.D., and Studer, L. (2005). Derivation of multipotent mesenchymal precursors from human embryonic stem cells. *PLoS Med* 2, e161.
- Behjati, S., Tarpey, P.S., Haase, K., Ye, H., Young, M.D., Alexandrov, L.B., Farndon, S.J., Collord, G., Wedge, D.C., Martincorena, I., et al. (2017). Recurrent mutation of IGF signalling genes and distinct patterns of genomic rearrangement in osteosarcoma. *Nat Commun* 8, 15936.
- Blattmann, C., Thiemann, M., Stenzinger, A., Roth, E.K., Dittmar, A., Witt, H., Lehner, B., Renker, E., Jugold, M., Eichwald, V., et al. (2015). Establishment of a patient-derived orthotopic osteosarcoma mouse model. *J Transl Med* 13, 136.
- Bonnay, F., Veloso, A., Steinmann, V., Kocher, T., Abdusselamoglu, M.D., Bajaj, S., Rivelles, E., Landskron, L., Esterbauer, H., Zinzen, R.P., et al. (2020). Oxidative Metabolism Drives Immortalization of Neural Stem Cells during Tumorigenesis. *Cell* 182, 1490-1507 e1419.
- Brandt, U. (2006). Energy converting NADH:quinone oxidoreductase (complex I). *Annu Rev Biochem* 75, 69-92.

Brosh, R.M., Jr. (2013). DNA helicases involved in DNA repair and their roles in cancer. *Nat Rev Cancer* 13, 542-558.

Capulli, M., Paone, R., and Rucci, N. (2014). Osteoblast and osteocyte: games without frontiers. *Arch Biochem Biophys* 561, 3-12.

Chae, H., Park, J., Lee, S., Kim, M., Kim, Y., Lee, J.W., Chung, N.G., Cho, B., Jeong, D.C., Kim, J., et al. (2014). Ribosomal protein mutations in Korean patients with Diamond-Blackfan anemia. *Exp Mol Med* 46, e88.

Chang, C.W., Xu, X., Li, M., Xin, D., Ding, L., Wang, Y.T., and Liu, Y. (2020). Pathogenic mutations reveal a role of RECQ4 in mitochondrial RNA:DNA hybrid formation and resolution. *Sci Rep* 10, 17033.

Chen, C.J., Sgritta, M., Mays, J., Zhou, H., Lucero, R., Park, J., Wang, I.C., Park, J.H., Kaiparettu, B.A., Stoica, L., et al. (2019). Therapeutic inhibition of mTORC2 rescues the behavioral and neurophysiological abnormalities associated with Pten-deficiency. *Nat Med* 25, 1684-1690.

Chen, C.S., Chiou, C.T., Chen, G.S., Chen, S.C., Hu, C.Y., Chi, W.K., Chu, Y.D., Hwang, L.H., Chen, P.J., Chen, D.S., et al. (2009). Structure-based discovery of triphenylmethane derivatives as inhibitors of hepatitis C virus helicase. *J Med Chem* 52, 2716-2723.

Chen, D., Zhao, Z., Huang, Z., Chen, D.C., Zhu, X.X., Wang, Y.Z., Yan, Y.W., Tang, S., Madhavan, S., Ni, W., et al. (2018). Super enhancer inhibitors suppress MYC driven transcriptional amplification and tumor progression in osteosarcoma. *Bone Res* 6, 11.

Chen, X., Bahrami, A., Pappo, A., Easton, J., Dalton, J., Hedlund, E., Ellison, D., Shurtleff, S., Wu, G., Wei, L., et al. (2014). Recurrent somatic structural variations contribute to tumorigenesis in pediatric osteosarcoma. *Cell Rep* 7, 104-112.

Cheung, H.H., Liu, X., Canterel-Thouennon, L., Li, L., Edmonson, C., and Rennert, O.M. (2014). Telomerase protects werner syndrome lineage-specific stem cells from premature aging. *Stem Cell Reports* 2, 534-546.

Choesmel, V., Fribourg, S., Aguisa-Toure, A.H., Pinaud, N., Legrand, P., Gazda, H.T., and Gleizes, P.E. (2008). Mutation of ribosomal protein RPS24 in Diamond-Blackfan anemia results in a ribosome biogenesis disorder. *Hum Mol Genet* 17, 1253-1263.

Chu, W.K., and Hickson, I.D. (2009). RecQ helicases: multifunctional genome caretakers. *Nat Rev Cancer* 9, 644-654.

Colombo, E.A., Locatelli, A., Cubells Sanchez, L., Romeo, S., Elcioglu, N.H., Maystadt, I., Esteve Martinez, A., Sironi, A., Fontana, L., Finelli, P., et al. (2018). Rothmund-Thomson Syndrome: Insights from New Patients on the Genetic Variability Underpinning Clinical Presentation and Cancer Outcome. *Int J Mol Sci* 19.

Croteau, D.L., Popuri, V., Opresko, P.L., and Bohr, V.A. (2014). Human RecQ helicases in DNA repair, recombination, and replication. *Annu Rev Biochem* 83, 519-552.

Davis, T., Tivey, H.S., Brook, A.J., Grimstead, J.W., Rokicki, M.J., and Kipling, D. (2013). Activation of p38 MAP kinase and stress signalling in fibroblasts from the progeroid Rothmund-Thomson syndrome. *Age (Dordr)* 35, 1767-1783.

De, S., Kumari, J., Mudgal, R., Modi, P., Gupta, S., Futami, K., Goto, H., Lindor, N.M., Furuichi, Y., Mohanty, D., et al. (2012). RECQL4 is essential for the transport of p53 to mitochondria in normal human cells in the absence of exogenous stress. *J Cell Sci* 125, 2509-2522.

Doulatov, S., Vo, L.T., Macari, E.R., Wahlster, L., Kinney, M.A., Taylor, A.M., Barragan, J., Gupta, M., McGrath, K., Lee, H.Y., et al. (2017). Drug discovery for Diamond-Blackfan anemia using reprogrammed hematopoietic progenitors. *Sci Transl Med* 9.

Duan, S., Yuan, G., Liu, X., Ren, R., Li, J., Zhang, W., Wu, J., Xu, X., Fu, L., Li, Y., et al. (2015). PTEN deficiency reprogrammes human neural stem cells towards a glioblastoma stem cell-like phenotype. *Nat Commun* 6, 10068.

Fan, W., and Luo, J. (2008). RecQ4 facilitates UV light-induced DNA damage repair through interaction with nucleotide excision repair factor xeroderma pigmentosum group A (XPA). *J Biol Chem* 283, 29037-29044.

Formosa, L.E., Dibley, M.G., Stroud, D.A., and Ryan, M.T. (2018). Building a complex complex: Assembly of mitochondrial respiratory chain complex I. *Semin Cell Dev Biol* 76, 154-162.

Funato, K., Major, T., Lewis, P.W., Allis, C.D., and Tabar, V. (2014). Use of human embryonic stem cells to model pediatric gliomas with H3.3K27M histone mutation. *Science* 346, 1529-1533.

Fusaki, N., Ban, H., Nishiyama, A., Saeki, K., and Hasegawa, M. (2009). Efficient induction of transgene-free human pluripotent stem cells using a vector based on Sendai virus, an RNA virus that does not integrate into the host genome. *Proc Jpn Acad Ser B Phys Biol Sci* 85, 348-362.

Gambera, S., Abarategi, A., Gonzalez-Camacho, F., Morales-Molina, A., Roma, J., Alfranca, A., and Garcia-Castro, J. (2018). Clonal dynamics in osteosarcoma defined by RGB marking. *Nat Commun* 9, 3994.

Garcon, L., Ge, J., Manjunath, S.H., Mills, J.A., Apicella, M., Parikh, S., Sullivan, L.M., Podsakoff, G.M., Gadue, P., French, D.L., et al. (2013). Ribosomal and hematopoietic defects in induced pluripotent stem cells derived from Diamond Blackfan anemia patients. *Blood* 122, 912-921.

Gross, D.N., van den Heuvel, A.P., and Birnbaum, M.J. (2008). The role of FoxO in the regulation of metabolism. *Oncogene* 27, 2320-2336.

Guijarro, M.V., Ghivizzani, S.C., and Gibbs, C.P. (2014). Animal models in osteosarcoma. *Front Oncol* 4, 189.

Guntur, A.R., Le, P.T., Farber, C.R., and Rosen, C.J. (2014). Bioenergetics during calvarial osteoblast differentiation reflect strain differences in bone mass. *Endocrinology* 155, 1589-1595.

Gupta, S., De, S., Srivastava, V., Hussain, M., Kumari, J., Muniyappa, K., and Sengupta, S. (2014). RECQL4 and p53 potentiate the activity of polymerase gamma and maintain the integrity of the human mitochondrial genome. *Carcinogenesis* 35, 34-45.

Gupta, S.V., and Schmidt, K.H. (2020). Maintenance of Yeast Genome Integrity by RecQ Family DNA Helicases. *Genes (Basel)* **11**.

Hanahan, D., and Weinberg, R.A. (2000). The hallmarks of cancer. *Cell* **100**, 57-70.

Haydon, R.C., Deyrup, A., Ishikawa, A., Heck, R., Jiang, W., Zhou, L., Feng, T., King, D., Cheng, H., Breyer, B., et al. (2002). Cytoplasmic and/or nuclear accumulation of the beta-catenin protein is a frequent event in human osteosarcoma. *Int J Cancer* **102**, 338-342.

Hicks, M.J., Roth, J.R., Kozinetz, C.A., and Wang, L.L. (2007). Clinicopathologic features of osteosarcoma in patients with Rothmund-Thomson syndrome. *J Clin Oncol* **25**, 370-375.

Hoki, Y., Araki, R., Fujimori, A., Ohhata, T., Koseki, H., Fukumura, R., Nakamura, M., Takahashi, H., Noda, Y., Kito, S., et al. (2003). Growth retardation and skin abnormalities of the Recql4-deficient mouse. *Hum Mol Genet* **12**, 2293-2299.

Ichikawa, K., Noda, T., and Furuichi, Y. (2002). [Preparation of the gene targeted knockout mice for human premature aging diseases, Werner syndrome, and Rothmund-Thomson syndrome caused by the mutation of DNA helicases]. *Nihon Yakurigaku Zasshi* **119**, 219-226.

Im, J.S., Ki, S.H., Farina, A., Jung, D.S., Hurwitz, J., and Lee, J.K. (2009). Assembly of the Cdc45-Mcm2-7-GINS complex in human cells requires the Ctf4/And-1, RecQL4, and Mcm10 proteins. *Proc Natl Acad Sci U S A* **106**, 15628-15632.

Kansara, M., Teng, M.W., Smyth, M.J., and Thomas, D.M. (2014). Translational biology of osteosarcoma. *Nat Rev Cancer* **14**, 722-735.

Kim, H., Yoo, S., Zhou, R., Xu, A., Bernitz, J.M., Yuan, Y., Gomes, A.M., Daniel, M.G., Su, J., Demicco, E.G., et al. (2018). Oncogenic role of SFRP2 in p53-mutant osteosarcoma development via autocrine and paracrine mechanism. *Proc Natl Acad Sci U S A* **115**, E11128-E11137.

Kliszczak, M., Sedlackova, H., Pitchai, G.P., Streicher, W.W., Krejci, L., and Hickson, I.D. (2015). Interaction of RECQ4 and MCM10 is important for efficient DNA replication origin firing in human cells. *Oncotarget* **6**, 40464-40479.

Kumari, J., Hussain, M., De, S., Chandra, S., Modi, P., Tikoo, S., Singh, A., Sagar, C., Sepuri, N.B., and Sengupta, S. (2016). Mitochondrial functions of RECQL4 are required for the prevention of aerobic glycolysis-dependent cell invasion. *J Cell Sci* 129, 1312-1318.

L. Van Maldergem, J.P., L. Larizza, L.L. Wang (2016). RECQL4-Related Recessive Conditions. In *Epstein's Inborn Errors of Development*. A.J.W.-B. Robert P. Erickson, ed. (Oxford, England: Oxford University Press), pp. 1137-1144.

Lamm, N., Ben-David, U., Golan-Lev, T., Storchova, Z., Benvenisty, N., and Kerem, B. (2016). Genomic Instability in Human Pluripotent Stem Cells Arises from Replicative Stress and Chromosome Condensation Defects. *Cell Stem Cell* 18, 253-261.

Lee, D.F., Su, J., Kim, H.S., Chang, B., Papatsenko, D., Zhao, R., Yuan, Y., Gingold, J., Xia, W., Darr, H., et al. (2015). Modeling familial cancer with induced pluripotent stem cells. *Cell* 161, 240-254.

Lee, W.C., Guntur, A.R., Long, F., and Rosen, C.J. (2017). Energy Metabolism of the Osteoblast: Implications for Osteoporosis. *Endocr Rev* 38, 255-266.

Leyendecker Junior, A. (2018). TGF-beta Inhibitor SB431542 Promotes the Differentiation of Induced Pluripotent Stem Cells and Embryonic Stem Cells into Mesenchymal-Like Cells. *Stem Cells Int* 2018, 7878201.

Li, Z., Wang, L., Luo, N., Zhao, Y., Li, J., Chen, Q., and Tian, Y. (2018). Metformin inhibits the proliferation and metastasis of osteosarcoma cells by suppressing the phosphorylation of Akt. *Oncol Lett* 15, 7948-7954.

Lian, Q., Lye, E., Suan Yeo, K., Khia Way Tan, E., Salto-Tellez, M., Liu, T.M., Palanisamy, N., El Oakley, R.M., Lee, E.H., Lim, B., et al. (2007). Derivation of clinically compliant MSCs from CD105+, CD24- differentiated human ESCs. *Stem Cells* 25, 425-436.

Lin, Y.H., Jewell, B.E., Gingold, J., Lu, L., Zhao, R., Wang, L.L., and Lee, D.F. (2017a). Osteosarcoma: Molecular Pathogenesis and iPSC Modeling. *Trends Mol Med* 23, 737-755.

Lin, Y.H., Jewell, B.E., Gingold, J., Lu, L., Zhao, R., Wang, L.L., and Lee, D.F. (2017b). Osteosarcoma: Molecular Pathogenesis and iPSC Modeling. *Trends Mol Med*.

Lindsey, B.A., Markel, J.E., and Kleinerman, E.S. (2017). Osteosarcoma Overview. *Rheumatol Ther* 4, 25-43.

Love, M.I., Huber, W., and Anders, S. (2014). Moderated estimation of fold change and dispersion for RNA-seq data with DESeq2. *Genome Biol* 15, 550.

Lu, H., Shamanna, R.A., Keijzers, G., Anand, R., Rasmussen, L.J., Cejka, P., Croteau, D.L., and Bohr, V.A. (2016). RECQL4 Promotes DNA End Resection in Repair of DNA Double-Strand Breaks. *Cell Rep* 16, 161-173.

Lu, L., Harutyunyan, K., Jin, W., Wu, J., Yang, T., Chen, Y., Joeng, K.S., Bae, Y., Tao, J., Dawson, B.C., et al. (2015). RECQL4 Regulates p53 Function In Vivo During Skeletogenesis. *J Bone Miner Res* 30, 1077-1089.

Lu, L., Jin, W., Liu, H., and Wang, L.L. (2014). RECQ DNA helicases and osteosarcoma. *Adv Exp Med Biol* 804, 129-145.

Lu, L., Jin, W., and Wang, L.L. (2017). Aging in Rothmund-Thomson syndrome and related RECQL4 genetic disorders. *Ageing Res Rev* 33, 30-35.

Lu, L., Jin, W., and Wang, L.L. (2020). RECQ DNA Helicases and Osteosarcoma. *Adv Exp Med Biol* 1258, 37-54.

Ma, Y., Bai, R.K., Trieu, R., and Wong, L.J. (2010). Mitochondrial dysfunction in human breast cancer cells and their transmitochondrial cybrids. *Biochim Biophys Acta* 1797, 29-37.

Mann, M.B., Hodges, C.A., Barnes, E., Vogel, H., Hassold, T.J., and Luo, G. (2005). Defective sister-chromatid cohesion, aneuploidy and cancer predisposition in a mouse model of type II Rothmund-Thomson syndrome. *Hum Mol Genet* 14, 813-825.

Matsuno, K., Kumano, M., Kubota, Y., Hashimoto, Y., and Takisawa, H. (2006). The N-terminal noncatalytic region of *Xenopus* RecQ4 is required for chromatin binding of DNA polymerase alpha in the initiation of DNA replication. *Mol Cell Biol* 26, 4843-4852.

Mirabello, L., Troisi, R.J., and Savage, S.A. (2009a). International osteosarcoma incidence patterns in children and adolescents, middle ages and elderly persons. *Int J Cancer* 125, 229-234.

Mirabello, L., Troisi, R.J., and Savage, S.A. (2009b). Osteosarcoma incidence and survival rates from 1973 to 2004: data from the Surveillance, Epidemiology, and End Results Program. *Cancer* *115*, 1531-1543.

Mohaghegh, P., and Hickson, I.D. (2002). Premature aging in RecQ helicase-deficient human syndromes. *Int J Biochem Cell Biol* *34*, 1496-1501.

Molina, J.R., Sun, Y., Protopopova, M., Gera, S., Bandi, M., Bristow, C., McAfoos, T., Morlacchi, P., Ackroyd, J., Agip, A.A., et al. (2018). An inhibitor of oxidative phosphorylation exploits cancer vulnerability. *Nat Med* *24*, 1036-1046.

Mulero-Navarro, S., Sevilla, A., Roman, A.C., Lee, D.F., D'Souza, S.L., Pardo, S., Riess, I., Su, J., Cohen, N., Schaniel, C., et al. (2015). Myeloid Dysregulation in a Human Induced Pluripotent Stem Cell Model of PTPN11-Associated Juvenile Myelomonocytic Leukemia. *Cell Rep* *13*, 504-515.

Ng, A.J., Walia, M.K., Smeets, M.F., Mutsaers, A.J., Sims, N.A., Purton, L.E., Walsh, N.C., Martin, T.J., and Walkley, C.R. (2015). The DNA helicase recql4 is required for normal osteoblast expansion and osteosarcoma formation. *PLoS Genet* *11*, e1005160.

Pardy, L., Rosati, R., Soave, C., Huang, Y., Kim, S., and Ratnam, M. (2020). The ternary complex factor protein ELK1 is an independent prognosticator of disease recurrence in prostate cancer. *Prostate* *80*, 198-208.

Peng, J., Tang, L., Cai, M., Chen, H., Wong, J., and Zhang, P. (2019). RECQL5 plays an essential role in maintaining genome stability and viability of triple-negative breast cancer cells. *Cancer Med*.

Perry, J.A., Kiezun, A., Tonzi, P., Van Allen, E.M., Carter, S.L., Baca, S.C., Cowley, G.S., Bhatt, A.S., Rheinbay, E., Pedamallu, C.S., et al. (2014). Complementary genomic approaches highlight the PI3K/mTOR pathway as a common vulnerability in osteosarcoma. *Proc Natl Acad Sci U S A* *111*, E5564-5573.

Petkovic, M., Dietschy, T., Freire, R., Jiao, R., and Stagljar, I. (2005). The human Rothmund-Thomson syndrome gene product, RECQL4, localizes to distinct nuclear foci that

coincide with proteins involved in the maintenance of genome stability. *J Cell Sci* 118, 4261-4269.

Qi, N.N., Tian, S., Li, X., Wang, F.L., and Liu, B. (2019). Up-regulation of microRNA-496 suppresses proliferation, invasion, migration and in vivo tumorigenicity of human osteosarcoma cells by targeting eIF4E. *Biochimie* 163, 1-11.

Quist, T., Jin, H., Zhu, J.F., Smith-Fry, K., Capecchi, M.R., and Jones, K.B. (2015). The impact of osteoblastic differentiation on osteosarcomagenesis in the mouse. *Oncogene* 34, 4278-4284.

Roberts, R.D., Lizardo, M.M., Reed, D.R., Hingorani, P., Glover, J., Allen-Rhoades, W., Fan, T., Khanna, C., Sweet-Cordero, E.A., Cash, T., et al. (2019). Provocative questions in osteosarcoma basic and translational biology: A report from the Children's Oncology Group. *Cancer* 125, 3514-3525.

Rodriguez, R., Rubio, R., and Menendez, P. (2012). Modeling sarcomagenesis using multipotent mesenchymal stem cells. *Cell Res* 22, 62-77.

Rubio, R., Gutierrez-Aranda, I., Saez-Castillo, A.I., Labarga, A., Rosu-Myles, M., Gonzalez-Garcia, S., Toribio, M.L., Menendez, P., and Rodriguez, R. (2013). The differentiation stage of p53-Rb-deficient bone marrow mesenchymal stem cells imposes the phenotype of in vivo sarcoma development. *Oncogene* 32, 4970-4980.

Sangrithi, M.N., Bernal, J.A., Madine, M., Philpott, A., Lee, J., Dunphy, W.G., and Venkitaraman, A.R. (2005). Initiation of DNA replication requires the RECQL4 protein mutated in Rothmund-Thomson syndrome. *Cell* 121, 887-898.

Schott, C., Shah, A.T., and Sweet-Cordero, E.A. (2020). Genomic Complexity of Osteosarcoma and Its Implication for Preclinical and Clinical Targeted Therapies. *Adv Exp Med Biol* 1258, 1-19.

Schurman, S.H., Hedayati, M., Wang, Z., Singh, D.K., Speina, E., Zhang, Y., Becker, K., Macris, M., Sung, P., Wilson, D.M., 3rd, et al. (2009). Direct and indirect roles of RECQL4 in modulating base excision repair capacity. *Hum Mol Genet* 18, 3470-3483.

Shamanna, R.A., Singh, D.K., Lu, H., Mirey, G., Keijzers, G., Salles, B., Croteau, D.L., and Bohr, V.A. (2014). RECQ helicase RECQL4 participates in non-homologous end joining and interacts with the Ku complex. *Carcinogenesis* 35, 2415-2424.

Shannon, P., Markiel, A., Ozier, O., Baliga, N.S., Wang, J.T., Ramage, D., Amin, N., Schwikowski, B., and Ideker, T. (2003). Cytoscape: a software environment for integrated models of biomolecular interaction networks. *Genome Res* 13, 2498-2504.

Shimamoto, A., Kagawa, H., Zensho, K., Sera, Y., Kazuki, Y., Osaki, M., Oshimura, M., Ishigaki, Y., Hamasaki, K., Kodama, Y., et al. (2014). Reprogramming suppresses premature senescence phenotypes of Werner syndrome cells and maintains chromosomal stability over long-term culture. *PLoS One* 9, e112900.

Sottnik, J.L., Campbell, B., Mehra, R., Behbahani-Nejad, O., Hall, C.L., and Keller, E.T. (2014). Osteocytes serve as a progenitor cell of osteosarcoma. *J Cell Biochem* 115, 1420-1429.

Subramanian, A., Tamayo, P., Mootha, V.K., Mukherjee, S., Ebert, B.L., Gillette, M.A., Paulovich, A., Pomeroy, S.L., Golub, T.R., Lander, E.S., et al. (2005). Gene set enrichment analysis: a knowledge-based approach for interpreting genome-wide expression profiles. *Proc Natl Acad Sci U S A* 102, 15545-15550.

Takahashi, K., Tanabe, K., Ohnuki, M., Narita, M., Ichisaka, T., Tomoda, K., and Yamanaka, S. (2007). Induction of pluripotent stem cells from adult human fibroblasts by defined factors. *Cell* 131, 861-872.

Takahashi, K., and Yamanaka, S. (2006). Induction of pluripotent stem cells from mouse embryonic and adult fibroblast cultures by defined factors. *Cell* 126, 663-676.

Tao, J., Jiang, M.M., Jiang, L., Salvo, J.S., Zeng, H.C., Dawson, B., Bertin, T.K., Rao, P.H., Chen, R., Donehower, L.A., et al. (2014). Notch activation as a driver of osteogenic sarcoma. *Cancer Cell* 26, 390-401.

Tataria, M., Quarto, N., Longaker, M.T., and Sylvester, K.G. (2006). Absence of the p53 tumor suppressor gene promotes osteogenesis in mesenchymal stem cells. *J Pediatr Surg* 41, 624-632; discussion 624-632.

Taylor, W.B. (1957). Rothmund's syndrome; Thomson's syndrome; congenital poikiloderma with or without juvenile cataracts. *AMA Arch Derm* 75, 236-244.

Thangavel, S., Mendoza-Maldonado, R., Tissino, E., Sidorova, J.M., Yin, J., Wang, W., Monnat, R.J., Jr., Falaschi, A., and Vindigni, A. (2010). Human RECQ1 and RECQ4 helicases play distinct roles in DNA replication initiation. *Mol Cell Biol* 30, 1382-1396.

Thomas, D.M., Johnson, S.A., Sims, N.A., Trivett, M.K., Slavin, J.L., Rubin, B.P., Waring, P., McArthur, G.A., Walkley, C.R., Holloway, A.J., et al. (2004). Terminal osteoblast differentiation, mediated by runx2 and p27KIP1, is disrupted in osteosarcoma. *J Cell Biol* 167, 925-934.

Tivey, H.S., Brook, A.J., Rokicki, M.J., Kipling, D., and Davis, T. (2013). p38 (MAPK) stress signalling in replicative senescence in fibroblasts from progeroid and genomic instability syndromes. *Biogerontology* 14, 47-62.

Vangapandu, H.V., Alston, B., Morse, J., Ayres, M.L., Wierda, W.G., Keating, M.J., Marszalek, J.R., and Gandhi, V. (2018). Biological and metabolic effects of IACS-010759, an OxPhos inhibitor, on chronic lymphocytic leukemia cells. *Oncotarget* 9, 24980-24991.

Vartak, R., Deng, J., Fang, H., and Bai, Y. (2015). Redefining the roles of mitochondrial DNA-encoded subunits in respiratory Complex I assembly. *Biochim Biophys Acta* 1852, 1531-1539.

Walkley, C.R., Qudsi, R., Sankaran, V.G., Perry, J.A., Gostissa, M., Roth, S.I., Rodda, S.J., Snay, E., Dunning, P., Fahey, F.H., et al. (2008). Conditional mouse osteosarcoma, dependent on p53 loss and potentiated by loss of Rb, mimics the human disease. *Genes Dev* 22, 1662-1676.

Wang, J.Y., Wu, P.K., Chen, P.C., Lee, C.W., Chen, W.M., and Hung, S.C. (2017). Generation of Osteosarcomas from a Combination of Rb Silencing and c-Myc Overexpression in Human Mesenchymal Stem Cells. *Stem Cells Transl Med* 6, 512-526.

Wang, L.L., Gannavarapu, A., Kozinetz, C.A., Levy, M.L., Lewis, R.A., Chintagumpala, M.M., Ruiz-Maldonado, R., Contreras-Ruiz, J., Cunniff, C., Erickson, R.P., et al. (2003). Association between osteosarcoma and deleterious mutations in the RECQL4 gene in Rothmund-Thomson syndrome. *J Natl Cancer Inst* 95, 669-674.

Wang, L.L., and Plon, S.E. (1993). Rothmund-Thomson Syndrome. In *GeneReviews*(R). R.A. Pagon, M.P. Adam, H.H. Ardinger, S.E. Wallace, A. Amemiya, L.J.H. Bean, T.D. Bird, C.T. Fong, H.C. Mefford, R.J.H. Smith, et al., eds. (Seattle (WA)).

Wang, L.L., Worley, K., Gannavarapu, A., Chintagumpala, M.M., Levy, M.L., and Plon, S.E. (2002). Intron-size constraint as a mutational mechanism in Rothmund-Thomson syndrome. *Am J Hum Genet* 71, 165-167.

Wang, W., Chen, D., and Zhu, K. (2018). SOX2OT variant 7 contributes to the synergistic interaction between EGCG and Doxorubicin to kill osteosarcoma via autophagy and stemness inhibition. *J Exp Clin Cancer Res* 37, 37.

Woo, L.L., Futami, K., Shimamoto, A., Furuichi, Y., and Frank, K.M. (2006). The Rothmund-Thomson gene product RECQL4 localizes to the nucleolus in response to oxidative stress. *Exp Cell Res* 312, 3443-3457.

Wu, J., Capp, C., Feng, L., and Hsieh, T.S. (2008). Drosophila homologue of the Rothmund-Thomson syndrome gene: essential function in DNA replication during development. *Dev Biol* 323, 130-142.

Xiao, W., Mohseny, A.B., Hogendoorn, P.C., and Cleton-Jansen, A.M. (2013). Mesenchymal stem cell transformation and sarcoma genesis. *Clin Sarcoma Res* 3, 10.

Xu, X., Rochette, P.J., Feyissa, E.A., Su, T.V., and Liu, Y. (2009). MCM10 mediates RECQ4 association with MCM2-7 helicase complex during DNA replication. *EMBO J* 28, 3005-3014.

Zeng, S., Liu, L., Ouyang, Q., Zhao, Y., Lin, G., Hu, L., and Li, W. (2016). Generation of induced pluripotent stem cells (iPSCs) from a retinoblastoma patient carrying a c.2663G>A mutation in RB1 gene. *Stem Cell Res* 17, 208-211.

Zhang, J., and Zhang, Q. (2019). Using Seahorse Machine to Measure OCR and ECAR in Cancer Cells. *Methods Mol Biol* 1928, 353-363.

Zhao, J., Dean, D.C., Hornicek, F.J., Yu, X., and Duan, Z. (2020). Emerging next-generation sequencing-based discoveries for targeted osteosarcoma therapy. *Cancer Lett* 474, 158-167.

Zhou, R., Xu, A., Gingold, J., Strong, L.C., Zhao, R., and Lee, D.F. (2017). Li-Fraumeni Syndrome Disease Model: A Platform to Develop Precision Cancer Therapy Targeting Oncogenic p53. *Trends Pharmacol Sci* 38, 908-927.

Zhu, K., Yuan, Y., Wen, J., Chen, D., Zhu, W., Ouyang, Z., and Wang, W. (2020). LncRNA Sox2OT-V7 promotes doxorubicin-induced autophagy and chemoresistance in osteosarcoma via tumor-suppressive miR-142/miR-22. *Aging (Albany NY)* 12, 6644-6666.

Zu, X.L., and Guppy, M. (2004). Cancer metabolism: facts, fantasy, and fiction. *Biochem Biophys Res Commun* 313, 459-465.

Vita

Brittany Ellis Jewell was born in Houston, Texas, the daughter of Henry Brian Ellis and Alice Rodriguez Ellis. After completing her primary education at Clear Lake High School, Houston, Texas, she attended Baylor University, Waco, Texas, earning a Bachelor of Science in Biology with minors in Chemistry and Medical Humanities. Following her graduation, she began her research career at Baylor College of Medicine assisting in the laboratory of Dr. Robert B. Couch in the Department of Molecular Virology and Microbiology and later in the laboratory of Dr. Anthony Flores in the Department of Pediatric Infectious Diseases. In January 2016, Brittany began her doctoral studies at the University of Texas MD Anderson UT Health Graduate School of Biomedical Sciences.